INTERCELLULAR DIHYDROCAMALEXIC ACID CONTRIBUTES TO ARR

NON-TARGETED METABOLITE PROFILING OF LEAF INTERCELLULAR WASHING FLUIDS REVEALS A NOVEL ROLE FOR DIHYDROCAMALEXIC ACID IN THE *ARABIDOPSIS* AGE-RELATED RESISTANCE RESPONSE AGAINST *PSEUDOMONAS SYRINGAE*

By CHRISTINE JANINE KEMPTHORNE, B.Sc.

A Thesis Submitted to the School of Graduate Studies in Partial Fulfillment of the Requirements for the Degree Master of Science

McMaster University MASTER OF SCIENCE (2018) Hamilton, Ontario (Biology)

TITLE: Non-targeted metabolite profiling of leaf intercellular washing fluids reveals a novel role for dihydrocamalexic acid in *Arabidopsis* Age-Related Resistance to *Pseudomonas syringae*

AUTHOR: Christine J Kempthorne, B.Sc. (McMaster University)

SUPERVISOR: Dr. Robin K. Cameron

NUMBER OF PAGES: xix, 115

LAY ABSTRACT

During Age-Related Resistance (ARR), mature plants including some crop plants become resistant to pathogens they were susceptible to when younger. How ARR works is poorly understood. My objective was to identify potential antimicrobial metabolites contributing to ARR in *Arabidopsis* against the bacterial pathogen *Pseudomonas syringae*. Genetic analyses combined with mass-spectrometry based metabolite profiling demonstrates that two cytochromes P450, *CYP71A12* and *CYP71A13* contribute to ARR. My research provides evidence that DHCA accumulates in the leaf intercellular space in ARR-competent plants, where it may act to inhibit the bacterial infection process. DHCA has low antimicrobial activity against *P. syringae* suggesting its mechanism of action is not directly antimicrobial. Importantly, application of DHCA to the leaf intercellular space of *cyp71a12/cyp71a13* restored ARR, confirming that DHCA contributes to ARR in *Arabidopsis*. Understanding ARR will provide useful information for future crop breeding and genetic modification that will mitigate agricultural losses due to disease.

ABSTRACT

Many economically important crop systems exhibit an Age-Related Resistance (ARR) response whereby mature plants become resistant to pathogens they were susceptible to when younger. The signaling pathways and mechanisms of ARR have not been well studied. *Arabidopsis* displays ARR in response to *P. syringae* pv *tomato* (*Pst*). Several studies provide evidence that intercellular salicylic acid (SA) accumulation is required for ARR and SA acts as a direct antimicrobial agent to limit bacterial growth and biofilm-like aggregate formation. SA accumulation mutants are ARR defective; however, a modest level of resistance is occasionally observed leading to the hypothesis that other compounds contribute to ARR as antimicrobial agents. Previous studies demonstrated that *CYP71A13* (a key enzyme in indolic biosynthesis) is expressed during the ARR response. I demonstrated that CYP71A12 functionally compensated for CYP71A13 during ARR, as *cyp71a12/cyp71a13-1* mutants were consistently ARR-defective compared to their respective single mutants. I demonstrated that dihydrocamalexic acid (DHCA) accumulated in intercellular washing fluids (IWFs) collected from plants during the ARR response using high resolution mass spectrometry-based profiling. DHCA was detected in IWFs collected from wild-type ARR-competent plants and, was absent in IWFs from ARR-incompetent *cyp71a12/cyp71a13* mutants. *In vitro* DHCA antimicrobial activity against *P. syringae* was not observed, but exogenous infiltration of DHCA into the leaf intercellular space restored ARR in *cyp71a12/cyp71a13* mutants Unlike SA which exhibits direct antimicrobial activity against *P. syringae*, DHCA does not and instead may affect pathogen virulence in other ways. My research provides evidence that

intercellular DHCA contributes to ARR in response to *P. syringae* in *Arabidopsis*. Understanding the genes and metabolites contributing to ARR will provide useful information for future crop breeding/genetic modification that will mitigate agricultural losses due to disease.

ACKNOWLEDGEMENTS

I would like to thank my supervisor, Dr. Robin Cameron for challenging me -- I'm stronger because of her. I wish to express my gratitude to Dr. Elizabeth Weretilnyk for changing the direction of my research career by introducing me to the amazing world of plant biochemistry, and for wisdom I'll always remember: the plants don't read the textbooks! Thank you to Dr. David Liscombe for instilling in me the spirit of collaboration, for mentorship on this project (and our next!), and nerding out with me over technology and biochemistry. I wish to thank Dr. Brian Golding for introducing me to VIM (the gift of time!) and the power of bioinformatics; I'll carry these skills with me throughout my research career. A sincere thank you to my academic big brother Dr. Dan Wilson, for his friendship, wisdom, and endless encouragement (can we reset my backgammon score soon though?). I would like to express my gratitude to Dr. Jim McNulty for DHCA and analogues, and for sharing his expertise and passion for plant natural products with me. Thank you to Dr. Erich Glawischnig for generously providing me with *cyp71a12/cyp71a13-1* and DHCA. To the members of the Cameron lab past and present: thank you for your often-thankless work keeping things running smoothly; I look forward to hearing about all the wonderful adventures life takes you on! A special thank you to Angela Fufeng for her patience, creativity, and for making the Cameron lab a brighter place. I do have to thank my loyal little terrier, Alex, for waiting so patiently by my side. Finally, thank you so much to my family, especially my Grandparents, Dad, Mom, and my brother, Dave, for their endless support, understanding, and love.

TABLE OF CONTENTS

LIST OF FIGURES

LIST OF TABLES

LIST OF ABBREVIATION AND SYMBOLS

AgNO3: silver nitrate

ANOVA: analysis of variance

ARR: age-related resistance

BAK1: BRASSINOSTEROID INSENSITIVE 1-ASSOCIATED RECEPTOR KINASE 1

Bsa: β-substituted alanine synthase

BTH: benzothiadiazole

c Log*P*: calculated Log*P*

CFU: colony-forming unit

CYP: cytochrome P450

DAMP: damage-associated molecular pattern

DHCA: dihydrocamalexic acid

DIR1: DEFECTIVE IN INDUCED RESISTANCE 1

dpi: days post-inoculation

ESI-MS: electrospray ionization-mass spectrometry

ETI: effector-triggered immunity

ETS: effector-triggered susceptibility

FAH1: FERULIC ACID 5-HYDROXYLASE 1

FIC: Fractional Inhibitory Concentration

FLS2: FLAGELLIN INSENSITIVE 2

FW: fresh weight

GGP: gamma-glutamyl peptidase

GGT: gamma-glutamyl transpeptidase

GSH: glutathione

HIM: *hrp*-inducing minimal media

hpi: hours post-inoculation

HR: hypersensitive response

I3M: indole-3-methyl glucosinolate

IAA: indole-3-acetic acid

IAN: indole-3-acetonitrile

IAOx: indole-3-acetaldoxime

ICHO: indole-3-carbaldeyhde

ICN: indole-3-carbonylnitrile

ICOOH: indole-3-carboxylic acid

ICS1: isochorismate synthase 1

Ile: isoleucine

IWF: intercellular washing fluid

JA: jasmonic acid

KB: King's B

MAMP: microbial-associated molecular pattern

MAPK: mitogen-activated protein kinase

MATE: multi-drug and toxin extrusion

MBC: minimal bactericidal concentration

MIC: minimal inhibitory concentration

MS: Murashige and Skoog

NPR1: NONEXPRESSOR OF PR GENES 1

OD: optical density

PAD: phytoalexin deficient

PAL: phenylalanine ammonia lyase

PAMP: pathogen-associated molecular pattern

PCA: principal component analysis

ppm: parts per million

PRR: pathogen recognition receptor

Psl: Pseudomonas syringae pv. lachrymans

Psp: Pseudomonas syringae pv. phaseolicola

Pss: Pseudomonas syringae pv. syringae

Pst: Pseudomonas syringae pv. tomato

PTI: pattern-triggered immunity

R-protein: resistance-protein

SA: salicylic acid

SAR: systemic acquired resistance

SVP: SHORT VEGETATIVE PHASE

T-DNA: Transfer-DNA

T3SS: type III secretion system

TAIR: The Arabidopsis Information Resource

TALENs: transcription activator-like effector nuclease

TOF: time-of-flight

UPLC: ultra-performance liquid chromatography

wpg: weeks post-germination

DECLARATION OF ACADEMIC ACHEIVEMENT

I declare this thesis to be an original report of my research, except where indicated by referencing, and that I am the sole author of this document. No part of this work has been submitted, in whole or in part, in any previous applications or publications for a degree at another institution.

This work represents original research conducted by myself in collaboration with Dr. David Liscombe and Dr. Jim McNulty. Through the advice and guidance of Dr. Liscombe I conducted metabolomics analyses, optimization of intercellular washing fluid collection, and completed UPLC-MS experiments at The Vineland Research and Innovation Centre (Lincoln, Ontario). Dr. McNulty (McMaster University; Chemistry and Chemical Biology Department) and myself designed structure-activity relationships experiments for antimicrobial activity of DHCA. Peter Wojnicki and Alex Neilsen (McNulty Lab, McMaster University; Chemistry and Chemical Biology Department) synthesized and confirmed DHCA and four DHCA analogues for use in this work.

All literature reviews, experimental designs, data analyses and interpretations are entirely my own work. A portion of the research conducted in this thesis will be prepared as a manuscript for submission to a peer-reviewed publication.

CHAPTER 1 - INTRODUCTION

1.1 Plant immunity and disease outcomes

Plants have evolved in diverse environments to be highly attuned to their surroundings with a sophisticated immune system to protect against microbial pathogens. Plants do not possess adaptive immune mechanisms, so they rely on innate immunity consisting of complex signaling networks and remarkably diverse antimicrobial specialized metabolites and proteins (Arbrecht and Argueso, 2016; Dixon R., 2001). Constitutive defenses protect against pathogens and herbivores and are composed of physical barriers like the cell wall, phytoanticipins (constitutively produced or stored metabolites) and specialized structures like anti-herbivory calcium oxalate crystal idioblasts in the vacuole and glandular trichomes (Vorwerk et al., 2004; Hématy et al., 2009; VanEtten et al., 1994; Franceschi and Nakata, 2005; Clauss et al., 2006). If microbes by-pass constitutive defenses, the first line of defense they encounter is pathogen-associated molecular pattern-triggered immunity (PTI). PTI is activated when plasma membrane-localized pathogen recognition receptors (PRRs) bind to conserved regions of microbes (Dixon R., 2001; Pieterse et al., 2009; Passardi et al., 2004). Pathogenic microbes can interfere with PTI signaling cascades by introducing virulence effector proteins into the plant cell. The second line of defense, known as effector-triggered immunity (ETI), is initiated by host detection of these virulence effector proteins. ETI restores PTI responses and initiates other defense responses that contribute to enhanced resistance (Qi et al., 2011; Hatsugai et al., 2017; Tsuda and Katagiri, 2010; Birkenbihl et al., 2017). Pathogens that have evolved the ability to suppress host defense mechanisms via effector proteins cause disease unless the

host has a corresponding method for detection and response. These branches of plant immunity reflect the molecular "arms race" that continues to occur between plants and pathogens (Boller and He 2009). The presence of pathogens on or near a plant does not necessarily lead to disease; the outcome of plant-pathogen interactions is dependent on environment (e.g., temperature, humidity), host genetics (e.g., resistance genes, biochemical activity), and pathogen genetics (e.g., toxins, effector proteins). This combination of factors is referred to as the disease triangle model of pathogenicity (Franci, L., 2001). Variations on this model have been proposed to include the developmental stage of the host and the effect of humans on plant disease through cultivation practices (Dodds and Rathjen 2010; Scholthof K., 2007). An estimated 20% to 40% of agricultural productivity is lost to pathogens, pests, and weeds, with losses even higher if post-harvest losses to disease are included (Savary et al., 2012). Agricultural and horticultural ecosystems are especially susceptible to devastating pathogen outbreaks because they often consist of high-density monocultures with little to no genetic diversity and slight variation in crop composition over time (McDonald and Stukenbrock, 2016). Research on plant defense improves our understanding of how plants respond to pathogens. This knowledge allows for the development of resistant varieties and better disease management systems and ultimately contributes to increased global food security (Savary et al., 2012).

1.1.1 PAMP and DAMP-triggered immunity (PTI and DTI)

As in animal innate immunity, plants perceive pathogens via microbial or pathogen-associated molecular patterns (MAMPs or PAMPs) and damage-associated molecular patterns (DAMPs) via immune receptors associated with the plasma membrane along the plant cell surface (Choi and Klessig, 2016). Conserved bacterial components function as MAMPs; for example, amino acids in flagellin, lipoglycans, and peptidoglycans along the surface of the outer membrane, and bacterial surfactants (Gómez-Gómez and Boller, 2000; Beets et al., 2012; Gust et al., 2007; Sanchez et al., 2012). Pathogens damage plant cells and tissues, resulting in the release of conserved DAMPs (reviewed in Choi and Klessig, 2016). Pathogen-secreted hydrolytic enzymes release fragments of the plant cell wall, also known as DAMPs. These DAMPS can induce DAMP-TI responses such as mitogen-activated protein kinase (MAPK) signaling, oxidative burst, Ca^{2+} influx, and expression of defense genes (Denoux et al., 2008; Chandra and Low, 1997). Collectively, plant immune receptors that detect MAMPs or DAMPS are referred to as pattern recognition receptors. MAMP or DAMP binding causes PRRs to associate with co-receptors, triggering signaling cascades resulting in modified gene expression, ultimately inducing broad-spectrum defense responses. A well-studied example is FLAGELLIN INSENSITIVE 2 (FLS2). Specific epitopes or peptides from bacterial flagellin activate FLS2 to associate with BRASSINOSTEROID INSENSITIVE 1-ASSOCIATED RECEPTOR KINASE 1 (BAK1), which leads to a signaling cascade for PTI (Roux et al., 2011). Many plants appear to detect and respond to fatty acids involved in quorum sensing and bacterial DNA, potentially as a component of biofilms, but little is currently

known of the receptors and mechanisms involved (Kakkar et al., 2015; Whitechurch et al., 2002). Activation of PTI signaling mechanisms leads to a complex of responses to produce inhospitable conditions for microbes. PTI responses include production of antimicrobial specialized metabolites and defense-related proteins, limitation of nutrient transfer, oxidative burst producing toxic reaction oxygen species, and an influx of Ca^{2+} into the cell opening anion channels along the plasma membrane to alkalinize the intercellular space where bacterial pathogens thrive (Ahuja et al., 2012; Bednarek P., 2012; van Loon et al., 2006; Chen et al., 2011; Wang et al., 2012; O'Brien et al., 2012; Jeworutzki et al., 2010). PTI is non-specific, generally induced by microbes rather than by specific strains or subsets of pathogens (Gust et al., 2007; Aslam et al., 2009). Activation of immune responses requires substantial regulation to prevent inappropriate induction, as there are high fitness costs associated with defense (growth-defense trade-off) (Arbrecht and Argueso, 2016). For instance, research using SA biosynthesis mutants has shown that SA has a negative regulatory effect on cytokinin signaling (Argueso et al., 2012). Therefore, as SA accumulates to high levels during defense, cytokinin-regulated processes like cell division and development are negatively affected (Arbrecht and Argueso, 2016; Argueso et al., 2009). Mutant lines constitutively expressing defense genes tend to display dwarfed phenotypes and reduced seed production (Bowling et al., 1994, 1997; Heil and Baldwin, 2002).

1.1.2 Effector-Triggered Susceptibility (ETS) and Immunity (ETI)

Virulent pathogens such as *P. syringae* introduce effector proteins directly into the cytosol of plant cells via a Type III secretion system (T3SS) to suppress defense responses and alter metabolism to favour nutrient release for the bacteria (Khan et al., 2016). Effectors from *P. syringae* can directly disrupt PRR phosphorylation and co-receptor recruitment, perturbing the ability of the plant to sense and response to MAMPs (Macho et al., 2015), or indirectly by acting downstream of these kinases (Bi and Zhou, 2017). By disrupting PRR activation and PTI responses, virulent *P. syringae* effectively inhibits many downstream defense responses, resulting in effector-triggered susceptibility (ETS). If a plant possesses the immune receptors (known as resistance (*R*)-proteins) capable of detecting pathogen-derived effector proteins, these effectors are considered avirulence proteins and the interaction is termed incompatible or avirulent. As a result, ETI is initiated, including the hypersensitive response (HR) (Belkhadir et al., 2004; Thomma et al., 2011). During the HR, cells undergo a form of programmed cell death which is thought to limit pathogen spread by cutting off access to nutrients to biotrophic pathogens (Tsuda and Katagiri, 2010). ETI provides plants with effective defense to specific strains of a pathogen. When a pathogen produces effector proteins that remain undetected, the pathogen successfully suppresses PTI and thrives. These pathogens are termed virulent and the interaction is considered compatible. ETI activation may be an energy-intensive process as demonstrated in *Arabidopsis* lines that constitutively express R-proteins and have lower biomass, produce fewer seeds, and often accumulate high levels of SA relative to wild-type plants (Tian et al., 2003; Glazebrook et al., 2003).

1.1.3 *Arabidopsis thaliana – Pseudomonas syringae* pathosystem

The *Arabidopsis-Pseudomonas* pathosystem has been instrumental in furthering our understanding of host-pathogen interactions and plant immunity. *Arabidopsis thaliana* is a small plant in the mustard (Brassicaceae*)* family that grows in a wide range of soil compositions and habitats, with more than 750 naturally occurring wild-type accessions from around the world (Alonso-Blanco and Koornneef 2000). *Arabidopsis* is an ideal model plant due to its small size, short lifespan (full lifecycle in ~ 6 to 8 weeks), and self-pollination. It has one of the smallest genomes in the plant kingdom (approximately 135 Mbp, diploid, 5 chromosomes), which was sequenced in 2000 by the *Arabidopsis* Genome Initiative (2000). The Columbia (Col-0) accession (used in this work) is widely used in plant research. *Arabidopsis* is amenable to transformation by *Agrobacterium*, and transfer DNA (T-DNA) insertion mutants are readily available for most genes, with stocks maintained by several organizations including the *Arabidopsis* Information Resource (TAIR) (Rosso et al., 2003). Additionally, higher-order mutants and transgenic lines developed by individual researchers are often submitted to TAIR where they are maintained and made available to others. As well as PTI and ETI, *Arabidopsis* displays both systemic acquired resistance (SAR) and a developmentally regulated resistance response (termed Age-Related Resistance [ARR]) against *P. syringae*, making this an ideal system for the study of complex defense responses (Cameron et al., 2004; Kus et al., 2002). *Arabidopsis* has been used to clarify the genetic and molecular basis of plant-pathogen interactions with *Hyaloperonospora arabidopsis* (Ghanmi et al., 2004) and the

necrotrophic fungus *Alternaria brassicicola* (Pochon et al., 2012), but one of the best-studied plant-pathogen interactions is that of *Arabidopsis* and the bacterial pathogen *Pseudomonas syringae* (Katagiri et al., 2002).

P. syringae is a global agricultural pathogen, causing blight (necrosis) and spotting diseases in the leaves and fruit of several economically important crop species including tomato, bean, fruit trees, and cruciferous vegetables (Brassicaceae sp.) (Mansfield et al., 2012; Takikawa and Takahashi, 2014). As a hemibiotrophic pathogen, this gram-negative bacterium requires living host tissue and modifies host metabolism to promote its survival at early colonization stages, transitioning to a late necrotrophic stage resulting in necrotic tissue, which contributes to release of bacteria from tissues into the environment and spread of the bacterium via water droplets (e.g. from rain) (Laluk and Mengiste, 2010; Glazebrook J, 2005; Soylu et al., 2005). *P. syringae* has a wide host range, with approximately 50 pathovars, each specialized to infect a handful of hosts. *P. syringae* survives non-pathogenically in natural settings in soil and on leaves, often forming biofilms to survive in harsh environments exposed to temperature fluctuations and phytochemicals until the opportunity arises for pathogenic invasion of plant tissues (Morris et al., 2007). *P. syringae* are spread via seeds, water, and as aerosols, infecting crops in wet or humid weather by accessing the intercellular space via wounds or through open stomata (O'Brien and Lindow 1989; Melotto et al., 2006).

The strain used in this work, *P. syringae* pv. *tomato* DC3000 (*Pst*), infects tomato and *Arabidopsis* (Xin et al., 2013). The genome of *Pst* DC3000 was sequenced in 2003; it has one circular chromosome and two plasmids, with an estimated 5% of the genome

consisting of genes related to pathogenesis (Buell et al., 2003). *Pst* produces the phytotoxin coronatine, an analog of jasmonic acid conjugated to isoleucine, (JA-Ile; the bioactive form of JA), which activates JA signalling pathways to antagonize SA-mediated defense signalling. Coronatine also plays a role in producing the characteristic chlorosis observed in infected tissue (Moore et al., 1989; reviewed in Mittal and Davis, 1995). *Pst* DC3000 is less epiphytic than other pathovars of *P.syringae,* as demonstrated by the death of inoculum sprayed onto tomato leaves after 48 hours, while other pathovars remain alive on leaf surfaces for up to 96 hours post-spray inoculation (Hirano and Upper, 2000). Boreau et al. (2002) hypothesized that this strain is highly specialized for endophytic colonization of the intercellular space of leaf tissue relative to other pathovars, quickly colonizing leaves and causing disease symptoms upon access to the intercellular space (Boreau et al., 2002). Biofilms consist of aggregates of bacterial cells along a surface, embedded in an extracellular matrix consisting of polysaccharides, proteins, and extracellular DNA (reviewed in Mann and Wozniak, 2012; Whitechurch et al., 2002). *Pst* forms biofilm-like aggregates in the intercellular space perhaps creating a protective environment for bacteria against plant-produced antimicrobials (Wilson et al., 2017) and the water-limited environment of the intercellular space (Chang et al., 2007; Renzi et al., 2012).

1.1.4 Host-Pathogen Interactions in the Intercellular Space

The air-filled leaf intercellular space (apoplast) is composed of the area between adjacent plant cells (including the cell wall) and fluids that accumulate along the plant cell wall (O'Leary et al., 2014). This dynamic environment is the site of many plant-microbe interactions. Transcriptome studies of the bean pathovar, *P. syringae* pv. *syringae* (*Pss*), during infection of beans provided evidence of enhanced expression of osmotic stress-related genes in the pathogen during intercellular compared to epiphytic growth, suggesting that water limitation is a factor in colonization of the intercellular space (Yu et al., 2013). Alkalinisation of intercellular fluids collected from barley resistant to *Blumeria graminis* (powdery mildew) was observed (Felle et al., 2005), as well as in bean responding to *P. syringae* pv. *phaseolicola (Psp).* The pH of the intercellular space is estimated to be between 4.5 to 6.5 based on apoplastic pH measurements in several plant species (maize, sunflower, tomato, bean, *Arabidopsis* roots, rapeseed, pea, barley, spinach, sugar beet leaves) (Felle et al., 1998; Dannel et al., 1995; Jia and Davies, 2007; O'Leary et al., 2016; Cramer and Jones, 1996; Husted and Schjoerring, 1995; Lohaus et al., 2001). Slightly acidic conditions are generally favoured across plant species during healthy conditions to facilitate transportation of sugars and amino acids from the apoplast into the cell (Felle H, 2006; O'Leary et al., 2014, 2016). Intercellular alkalinisation (pH increases) was observed during incompatible interactions and acidification (pH decreases) was observed during compatible interactions (O'Leary et al., 2016). Upon pathogen detection, conditions in the intercellular space of bean responding to *Psp* change within 4 to 6 hours including changes to pH and Mg^{2+} and Ca^{2+} flux (O'Leary et al., 2016).

Evidence also shows that plants may sequester nutrients into intracellular areas to limit their availability to pathogenic bacteria (O'Leary et al., 2016; Naseem et al., 2017). The intercellular space also contains proteins as demonstrated in several proteomics studies in which IWFs collected from *Arabidopsis*, bean, and other plants were examined. Several proteins were identified including LRR domain proteins, RLKs, cysteine-rich motifs, peroxidases and other antioxidant proteins, galactosidases, xylanases, glucosidases, cell-wall remodelling proteins, and SA-dependent PR proteins that are involved in defense (reviewed in Delaunois et al., 2014). In addition to proteins, specialized metabolites with antimicrobial activity (phytoalexins) are released into the intercellular space and may be incorporated into the plant cell wall (O'Leary et al., 2014, 2016; Wilson et al., 2017; Forcat et al. 2010; Soylu et al., 2005; Garcia et al., 2013; Agrawal et al., 2010). Virulence mechanisms in *P. syringae* provide protection from the harsh intercellular environment and alter plant defense and metabolism. Virulent *Pst* may thrive in the intercellular space by increasing sugar transport into the bacterial cell, producing biofilm-like aggregations along the plant cell wall, degrading host cell walls, synthesizing phytotoxic metabolites and phytohormone analogues, producing siderophores for iron acquisition, and assembly of a type III secretion system pilus for translocation of effector proteins into the host cell (Buell et al., 2003; reviewed in Büttner and He, 2009; Kloek et al., 2001; Wilson et al., 2017).

1.2 Age-Related Resistance

Age-related resistance (ARR) refers to developmentally-regulated resistance observed in several economically important plants against herbivores and a variety of pathogens (reviewed in Develey-Rivière and Galiana, 2007; Whalen M., 2005; Table 1). During ARR, plants become more resistant to a pathogen that they were susceptible to when younger, and this can occur throughout all vegetative tissue or in a specific part of the plant such as the fruit (reviewed in Develey-Rivière and Galiana, 2007). ARR may occur suddenly at a specific stage of development or develop gradually over time (reviewed in Whalen M., 2005) and occurs without previous pathogen exposure.

Table 1. Examples of ARR observed in agricultural systems

Crop	Pathogen	Observed in
Pepper	Powdery mildew (*Phytophthora capsici*)	Leaves (Jeun and Hwang, 1991)
Grape	Oomycetes and fungi (*Guignardia bidwellii*, *Uncinula necator*)	Berries (Hoffman et al., 2002; Gadoury et al., 2003)
Apple	Scab (*Venturia inaequalis*)	Leaves and fruit (Schwa W., 1979; Li and Xu, 2002)
Hops	Powdery mildew (*Podosphaera macularis*)	Flowers (Twomey et al., 2015)
Soybean	*Phytophtora*	Leaves (Lazarovits et al., 1981)
Rice	*Xanthomonas campestris*	Whole plant (Koch M., 1991)
Wheat	*Puccinia recondite*	Whole plant (Pretorius et al., 1988)
Strawberry	Powdery mildew (*Podosphaera aphanis*)	Leaves and berries (Asalf et al., 2014, 2016; Carisse and Bouchard, 2010)
Tobacco	*Phytophthora infestans*, tobacco mosaic virus	Leaves (Shibata et al., 2010; Hugot et al., 1999; Yalpani et al., 1993)
Maize	Common rust (*Puccinia sorghi*) European corn borer (*Ostrinia nubilalis*)	Leaves (Abedon et al., 1996)
Legumes, cabbage, broccoli	Downy mildew	Whole plants, leaves (Coelho et al., 1997; Farinhó et al., 2004)
Cucumber	*Phytophthora capsica*	Fruit (Mansfield et al., 2017)
Pumpkin, squash	*Phytophthora capsica*	Fruit (Ando et al., 2009)

Arabidopsis displays ARR in response to *P. syringae,* with mature plants supporting 10- to 100-fold lower bacterial levels and fewer disease symptoms relative to young plants (Kus et al., 2002). *Arabidopsis* also displays ARR to the biotrophic oomycete that causes downy mildew, *Hyaloperonospora arabidopsis* (Rusterucci et al., 2005; Carviel et al., 2009), and cabbage looper larvae (*Trichoplusia ni*) (Tucker and Avila-Sakar, 2010). Although ARR in *Arabidopsis* occurs at the same time as the switch from vegetative to reproductive phase, late-flowering mutants are ARR-competent and early flowering does not induce early ARR in wild-type plants (Wilson et al., 2013, 2017). Furthermore, mutants for the *SHORT VEGETATIVE PHASE* (*SVP*) transcription factor are ARR-defective despite their early-flowering phenotype, suggesting that ARR and flowering are not directly related (Wilson et al., 2017). Senescence causing re-allocation of resources from older leaves to younger leaves does not appear to be involved in the ARR response in *Arabidopsis* (Kus et al., 2002, Carella et al., 2015). Additionally, *Arabidopsis* ARR does not involve the hypersensitive response, suggesting that ARR is not a form of ETI (Kus et al., 2002, Carviel et al., 2014).

ARR may involve changes in specialized metabolites known as phytoalexins. Phytoalexins are synthesized *de novo* in response to stressors, which can include heavy metals, salt, UV radiation, and fungal and bacterial pathogens. Generally, a phytoalexin is considered a specialized metabolite induced by stress (not constitutively produced) and displaying biological activity (e.g., inhibiting growth, virulence, or biofilm formation of microbes, acting as a toxin to herbivores or insect pests) (Pedras et al., 2011; VanEtten et al., 1994). In contrast, phytoanticipins are constitutively produced antimicrobial or

deterrent compounds that are found in healthy plants, although their levels may increase upon exposure to stress. Specialized metabolites contributing to defense accumulate within hours to days after pathogen exposure (Pedras et al., 2011; Darvill and Albersheim, 1984) and have been implicated in ARR responses (Mansfield et al., 2017; Shibata et al., 2010; Carviel et al., 2009; Kus et al., 2002; Wilson et al., 2017). In cucumber, the fruit of the 'Vlaspik' hybrid cultivar displays ARR, such that mature fruit at 10 to 12 days post pollination display resistance to the oomycete *Phytophthora capsici*. Mansfield et al. (2017) used non-targeted metabolomics to show that terpenoids and flavonoids in fruit peels are a major contributor to cucumber ARR. Similarly, Datura species produce tropane alkaloids as they age, which are thought to contribute to developmental resistance against herbivores. (Kariñho-Betancourt et al., 2015). In *Arabidopsis*, intercellular washing fluids from mature ARR-competent plants exhibit antimicrobial activity against *Pst in vitro* (this activity is not present in IWFs from young plants) and evidence strongly suggests that intercellular salicylic acid (SA) is largely responsible for this antimicrobial activity during ARR (Kus et al., 2002; Cameron and Zaton 2004, Wilson et al., 2017). Tryptophan-derived indolic compounds may have an important role to play as well (Carviel et al., 2009).

1.2.1 Salicylic acid and ARR

Salicylic acid (SA; 2-hydroxybenzoic acid) is a phenolic metabolite produced in plants and animals. In plants, SA acts as a phytohormone regulating growth and cellular homeostasis, a signaling molecule in immunity and abiotic stress responses, and evidence suggest it also acts as a phytoalexin during ARR against *Pst* in *Arabidopsis* (Rivas-San Vicente and Plasencia 2011; Klessig D., 2017; Cameron and Zaton, 2004; Wilson et al., 2017). Basal SA levels in healthy, uninfected, unstressed plants differs between species; in *Arabidopsis*, leaf intercellular SA levels range from ~10 to 500 ng/ml while SA levels in whole leaves range from ~ 50 to 500 ng/g FW (Cameron and Zaton, 2004; Wilson et al., 2017). SA is synthesized from chorismate via isochorismate synthase 1 (ICS1) or phenyalanine ammonia-lyase (PAL) (Figure 1). The isochorismate synthase (ICS) pathway appears to be the main contributor to SA accumulation from defense-initiated responses in *Arabidopsis* (Dempsey et al., 2011). SA originating from ICS1-mediated biosynthesis occurs in the chloroplasts and is transported out via EDS5 (a multi-drug and toxin extrusion (MATE)-family transporter) (Fragnière et al., 2011; Serrano et al., 2013). The *ics1* mutant (also known as *sid2* or *eds16)* accumulates significantly less SA than wild-type plants in response to bacterial infection, is highly susceptible to *P. syringae*, and is ARR-defective (Wildermuth et al., 2001; Kus et al., 2002). *NahG* is a transgenic line of *Arabidopsis* that expresses a bacterial salicylate hydroxylase (converts SA to catechol), and therefore can synthesize but not accumulate SA in response to pathogens (Delaney et al., 1994). *NahG* mutants are also more susceptible to *Pst* and are ARR-defective due to the inability to accumulate SA (Wildermuth et al., 2001, Kus et al., 2002). Interestingly,

mutants that accumulate SA but are defective for SA-mediated signaling pathways display a wild-type ARR phenotype (e.g., *npr1*), suggesting that ARR may occur independently of SA-mediated defense signalling (Carella et al., 2015, Kus et al., 2002). Rather, evidence strongly suggests that intercellular SA contributes to ARR by directly inhibiting growth and biofilm-like aggregation of *Pst.* Wilson et al. (2017) showed that ≥ 2 μM (~276 ng/ml) SA reduces biofilm formation and ≥ 100 μM (~ 14 μg/ml) inhibits the growth of *Pst in vitro*, with 1 mM (14 mg/ml) having a bactericidal effect. Furthermore, exogenous application of 100 μM (~14 μg/ml) SA four hours prior to inoculation with *Pst* restores ARR in *sid2-2* (defective in SA biosynthesis) and *svp* (defective in intercellular SA accumulation) mutants (Cameron and Zaton, 2004; Wilson et al., 2017). Although SA is required for ARR, the *sid2* mutant occasionally displays an ARR-like response (small but significant difference in bacterial levels between young and mature plants; see Figure S3), which may indicate a role for other compounds in the *Arabidopsis* ARR response.

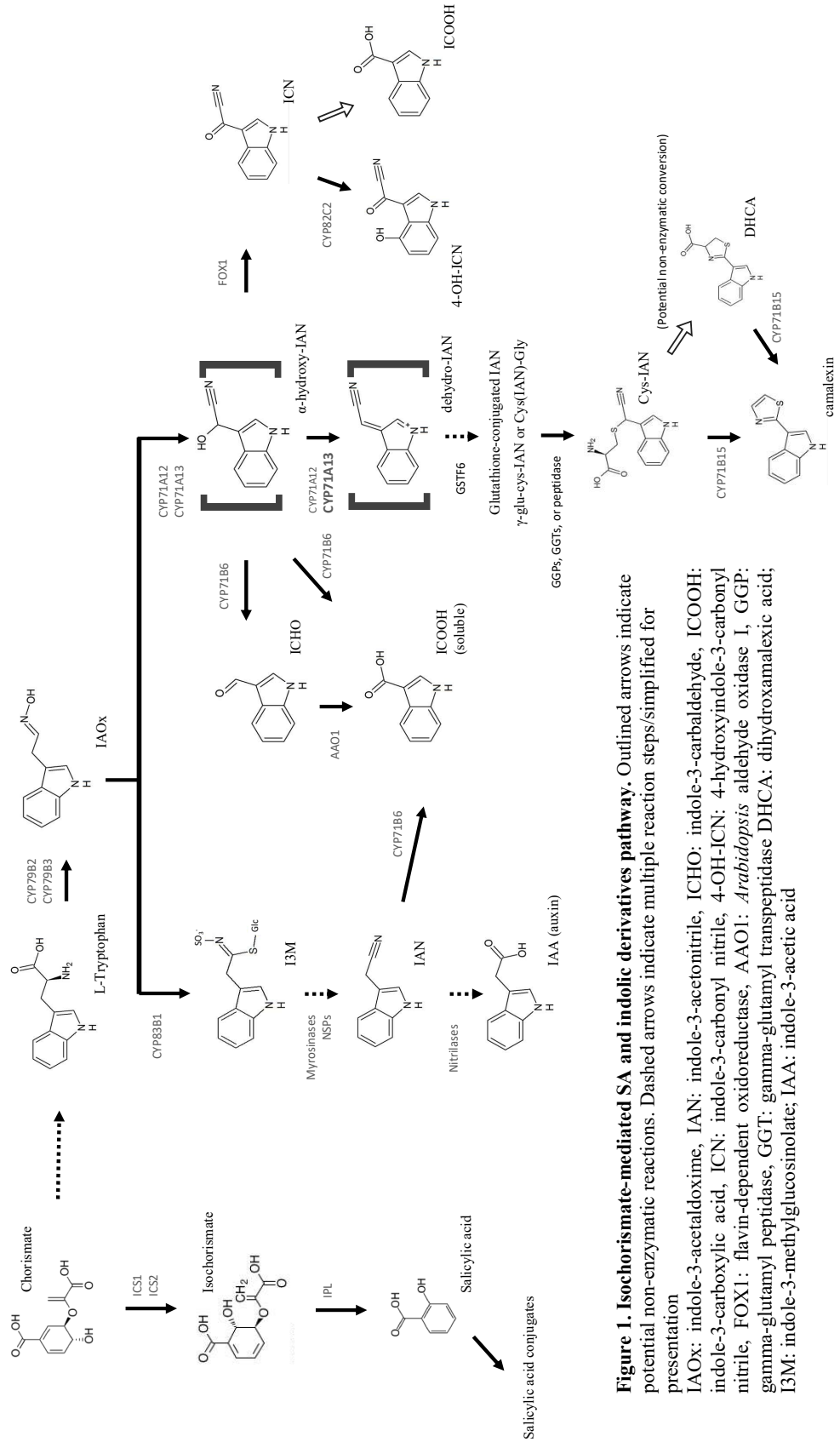

Figure 1. Isochorismate-mediated SA and indolic derivatives pathway. Outlined arrows indicate potential non-enzymatic reactions. Dashed arrows indicate multiple reaction steps/simplified for presentation
IAOx: indole-3-acetaldoxime, IAN: indole-3-acetonitrile, ICHO: indole-3-carbaldehyde, ICOOH: indole-3-carboxylic acid, ICN: indole-3-carbonyl nitrile, 4-OH-ICN: 4-hydroxyindole-3-carbonyl nitrile, FOX1: flavin-dependent oxidoreductase, AAO1: *Arabidopsis* aldehyde oxidase I, GGP: gamma-glutamyl peptidase, GGT: gamma-glutamyl transpeptidase DHCA: dihydroxamalexic acid; I3M: indole-3-methylglucosinolate; IAA: indole-3-acetic acid

1.2.2 Indolic metabolite biosynthesis and role in plant defense

Tryptophan-derived indolic metabolites accumulate in *Arabidopsis* during infection with *P. syringae* (Forcat et al., 2010; Zhou et al., 1999; Rajniak et al., 2015) and contribute to defense as indole glucosinolates (Bednarek et al., 2011). The indolic pathway in *Arabidopsis* was implicated in ARR in a study by Carviel et al. (2009) using significance analysis of microarrays to identify genes that were differentially expressed between mature wild-type Col-0 12 hours after *Pst* or mock inoculation. The indolic biosynthesis gene *CYP71A13* was the most highly upregulated (3.5-fold compared to the mock-inoculated control). *CYP71A13* is an oxidative dehydrogenase that produces a reactive form of indole-3-acetonitrile from indole-3-acetaldoxime (Figure 1). Carviel et al. (2009) hypothesized that a specialized metabolite produced by, or downstream of, *CYP71A13* was contributing to ARR. *CYP71A13* is at a metabolic branchpoint, producing indole-3-acetonitrile (IAN) from indole-3-acetaldoxime (IAOx) which is shuttled into indolic carboxylic acid, camalexin, indolic cyanonitrile, and indirectly affects auxin and indole glucosinolate pathways. These pathways are still being elucidated, with a new indole cyanonitrile pathway recently discovered by Rajniak et al (2015). A brief introduction to the indolic alkaloid pathways of *Arabidopsis* is outlined below.

Camalexin: *CYP71A13* has been extensively studied for its role in camalexin (3-thiazol-2'-yl-indole) production, a well-studied phytoalexin in *Arabidopsis* induced by stressors such as heavy metal salts (AgNO3, CuCl2), reactive oxygen species, UV, severe mechanical wounding, and in response to bacterial and fungal pathogens (Glawischnig et

al., 2004; Müller et al., 2015; Saga et al., 2012; Frerigmann et al., 2015; Zhou et al., 1999). Camalexin and indole glucosinolates share a common precursor (Figure 1), with both pathways branching from IAOx produced by CYP79B2/CYP79B3. For camalexin biosynthesis, IAN is conjugated to glutathione (Nafisi et al., 2007; Böttcher et al., 2009) and a cysteine-conjugate of IAN is formed through γ-glutamyl peptidase and/or γ-glutamyl transpeptidase activity (Geu-Flores et al., 2011; Su et al., 2011; Møldrup et al., 2013). Cys(IAN) cyclizes non-enzymatically to form dihydrocamalexic acid (DHCA) and is also the substrate for the multifunctional enzyme *CYP71B15/PAD3* that sequentially converts Cys(IAN) to DHCA and then to camalexin (Zhou et al., 1999; Shuhegger et al., 2006; Böttcher et al., 2009).

Indole-3-carboxylic acid (ICOOH) and indole-3-carbaldehyde (ICHO): IAN produced by *CYP71A12* and *CYP71A13* or from indole glucosinolate breakdown is a precursor to ICHO and ICOOH. Böttcher et al. (2014) identified *CYP71B6* and *AAO1* as having a role in biosynthesis of ICHO and ICOOH through non-targeted metabolite profiling of silver nitrate ($AgNO_3$)-treated leaves of knock-out and overexpression lines for these genes. Labelling experiments demonstrated that ICOOH and ICHO can be synthesized via IAN (Böttcher et al., 2009), *in vitro* CYP71B6 can utilize IAN as a substrate to produce both ICOOH and ICHO, and AAO1 oxidizes ICHO to ICOOH (Böttcher et al., 2014). *CYP71A12* is likely more effective at producing the IAN intermediate channeled to ICOOH derivatives (Figure 1), as *cyp71a12* produces less indole-3-carboxylic acid (including glycosylated derivatives and the methyl esters) but

these levels are not further reduced in the *cyp71a12 cyp71a13* double mutant (Böttcher et al., 2014; Müller et al., 2015).

Indole cyanonitriles: Rajniak et al. (2015) examined publicly available NASCArrays for cytochrome P450 genes upregulated during biotic stress and identified *CYP82C2* as a gene of interest. Metabolite profiling of *cyp82c2* T-DNA insertion mutants compared to wild-type seedlings responding to *Pst,* revealed a new indolic compound, indole-3-carbonylnitrile (ICN) in *cyp82c2*. This compound was not present in wild-type plants or *cyp79b2/cyp79b3* mutants, indicating IAOx is a precursor. ICN is unstable, so it rapidly degrades to ICOOH in aqueous solutions. CYP82C2 converts ICN to 4-hydroxy-ICN (also degraded to 4-OH-ICOOH in aqueous solutions). Upstream of CYP82C2, the flavin-dependent oxidoreductase, FOX1, produces the ICN substrate for CYP82C2 from a reactive IAN intermediate preferentially made by CYP71A12 and also thought to be shuttled to ICOOH production via CYP71B6 (Böttcher et al., 2014).

Indole glucosinolates: Indole glucosinolates are precursors to antiherbivory and antimicrobial defense compounds produced in *Brassicaceae*. They contain a thioglucose group, sulfonated oxime, and tryptophan-derived indole side-chain. 1-methoxy and 4-methoxy indole-3-methyl glucosinolates are phytoanticipins in *Arabidopsis* (Sønderby et al., 2010; Pedras et al., 2011). Indole-3-methylglucosinolates are stored in the vacuole and specialized cells; they are released by cellular damage and hydrolyzed to indole-3-methylisothiocyanates. Tissue damage may also result in indolic glucosinolates coming into contact with thioglucosidases (myrosinases stored in specialized idioblast cells) and

nitrile specifier proteins, resulting in cleavage of the thio-linked glucose and formation of IAN (Wittstock and Burow, 2010; Andréasson et al., 2001).

Indole-3-acetic acid (IAA): Auxin (IAA; indole-3-acetic acid) is a phytohormone involved in regulation of plant growth. Recent evidence shows that IAA-produced by *Pst* interferes with SA-mediated defense signaling (McClerklin et al., 2018). Microbes synthesize IAA via several biosynthetic pathways and precursors, but as in plants, these pathways originate from L-tryptophan (Spaepen and Vanderleyden, 2011). CYP79B2/CYP79B3 were initially thought to contribute to IAA biosynthesis via IAN produced by CYP71A13 (Kutz et al., 2002; Park et al., 2003). CYP79B2/CYP79B3 is also a branching point for biosynthesis of the same compounds as CYP71A12/CYP171A13; the main difference is IAOx is also a precursor for the biosynthesis of indole glucosinolates (Glawischnig et al., 2004; Zhao et al., 2002). High-auxin phenotypes observed in indole glucosinolate mutants and sulfur-starved plants were initially hypothesized to involve IAN. However, recent evidence suggests high-auxin phenotypes in these plants are caused by blocks in indole glucosinolate biosynthesis resulting in IAOx overflow to IAA biosynthesis, or from the breakdown of indole glucosinolates during stress to produce IAN (Halkier and Gershenzon, 2006; Nafisi et al., 2006). IAN-derived IAA likely originates from IAN produced during the breakdown of indole-3-methyl glucosinolates (I3M) (Malka et al., 2017).

1.2.3 *CYP71A12* and *CYP71A13*

CYP71A12 and *CYP71A13* (Carviel et al., 2009) are upregulated in response to pathogens and stressors like heavy metal salts (Glawischnig et al., 2004). *CYP71A12* and *CYP71A13* are in tandem location on chromosome 2 and are 89% identical at the amino acid level (Nafisi et al., 2007). Both contribute to camalexin biosynthesis, although CYP71A13 preferentially produces the IAN derivative that is shuttled into camalexin biosynthesis (Klein et al., 2013). CYP71A12 can compensate for the loss of CYP71A13 and vice versa (Klein et al., 2013; Müller et al., 2015). The *cyp71a13* mutant produces significantly less camalexin when induced with silver nitrate, and fungal pathogens (Nafisi et al., 2007). In heterologous systems, CYP71A12 has been shown to functionally compensate for CYP71A13 (Klein et al., 2013; Møldrup et al., 2013). Klein et al. (2013) showed that *in vitro* the primary product of CYP71A13 is IAN along with ~ 3 % ICHO and the primary product of CYP71A12 is ICHO along with 3% IAN. They hypothesized that oxidation of IAN results in the loss of the hydrogen cyanide moiety and formation of an aldehyde (ICHO). Based on *in vitro* results and metabolic profiling of *cyp71a12* and *cyp71a13* mutants, CYP71A12 is more efficient that CYP71A13 at oxidizing IAN. The CYP71A13 product is a reactive form of IAN (dehydro-IAN; Figure 1) that is conjugated with glutathione, an intermediate in camalexin biosynthesis. These results are supported by *in vitro* studies measuring Cys(IAN) when either enzyme is incubated with L-cysteine (Klein et al., 2013). Multifunctional sequential reactions such as those hypothesized to produce IAN derivatives are prevalent in cytochrome P450 enzymes of indolic pathways. For example, CYP79B2/CYP79B3 likely catalyzes two oxidation reactions, and

CYP71B15 cyclizes Cys(IAN) to DHCA resulting in hydrogen cyanide loss, then an oxidative decarboxylation reaction to produce camalexin. To study the contribution of *CYP71A12* to camalexin biosynthesis, Müller et al. (2015) developed a double mutant through transcription activator-like effector nuclease (TALENs) resulting in a five base pair deletion in *CYP71A12* in the *cyp71a13-1* (T-DNA insertion) background. The five base pair deletion results in loss of the Asp-488 residue, which is a conserved feature of *CYP71A12* hypothesized to be required for protein function (Müller et al., 2015). The *cyp71a12 cyp71a13* mutant produces trace amounts of camalexin, and ICOOH derivative accumulation matches that of *cyp71a12*. Interestingly *cyp71a12*/*cyp71a13*-1 produces wild-type levels of ICHO, suggesting other enzymes contribute to the production of ICOOH/ICHO (Müller et al., 2015, Agerbirk et al., 2008). Initially we hypothesized that indole-3-acetonitrile produced by CYP71A13 was contributing to ARR; however, IAN was not detected in rosette leaves of *Arabidopsis* treated with silver nitrate, UV irradiation, *Phytophthora capsici*, or *P. syringae* (Böttcher et al., 2009, Böttcher et al., 2004, Shuhegger et al., 2006; Müller et al., 2015; Table S2). If *CYP71A13* is contributing to ARR resistance in mature plants, it may be through one or more downstream indolic pathways (Figure 1).

1.3 Non-targeted metabolomics

Non-targeted metabolomics integrates high resolution mass spectrometry-based metabolite profiling with ‘omics’ bioinformatics tools to interrogate changes in biological systems (Sawada and Hirai, 2013). Metabolites are a direct readout of gene expression

and gene product activity; by using a non-targeted approach insight is gained into how metabolism is contributing to a biological question (e.g., which metabolites differentially accumulate in an ARR-defective mutant). Samples containing complex mixtures of metabolites can be extracted in solvent, separated by polarity, and ionized. Ionization is essential for forming charged molecules (losing or gaining an electron) for detection by mass spectrometry. Samples can be subjected to positive electrospray ionization (ESI+) or negative (ESI-); some compounds only ionize in one mode, therefore analyzing samples with ESI+ and ESI- gives wider metabolic coverage. In the mass spectrometer, ions collide with argon gas and the energy from this process breaks bonds in each molecular ion to produce smaller fragments called product (or daughter) ions. Fragmentation information for each molecular ion can then be used to elucidate structural components for identification. The instrument used in this work is a quadrupole time-of-flight (QTof) mass spectrometer capable of filtering and detecting exact mass of each ion within 5 parts-per-million (ppm) of its actual mass. Exact mass is essential for downstream identification in non-targeted approaches, as these values are used to estimate the elemental composition of parent and product ions. Collectively, mass spectral features provide information on hundreds to thousands of metabolites in each sample.

The cheminformatics tools used to find metabolic features of interest are analogous to bioinformatics tools used in transcriptomics, employing multivariate statistics to putatively identify differentially accumulating metabolites (mass features) instead of genes (Figure 2). Exact mass measurement and fragmentation information are used to estimate the elemental composition and structural components of a metabolite of interest

identified through multivariate statistics. Chemical databases are useful for identifying metabolites of interest; however, it is important to remember that "identifications" are based on mass and the database entries screened. For example, pharmaceuticals with a similar mass as a natural product in plant extracts will come up as an identification in most database searches. Additionally, if a compound expected in a model system is not a database entry, it will not be returned as an identification, so it is important to use caution when relying on database searches.

Non-targeted metabolomics in this work was used to test the hypothesis that a CYP71A12/CYP71A13-derived indolic metabolite is involved in ARR. These datasets are also hypothesis generating since all detectable metabolites differentially accumulating in *cyp71a12/cyp71a13-1* compared to wild-type plants can be observed, potentially identifying new pathways of interest in ARR. For example, downstream indolic compounds are likely to be affected by the loss of CYP71A12 and CYP71A13, but it is not known whether they contribute to the ARR-defect in a *cyp71a12/cyp71a13-1* mutant. A non-targeted approach makes it possible to profile indolic compounds in samples, as well as all other detectable semi-polar compounds that may be affected by loss of *CYP71A12* and *CYP71A13*. These metabolites can then be linked back to pathways and genes of interest. Since this study has identified a biosynthetic pathway producing indolic metabolites as potentially contributing to ARR, metabolite profiling is ideal as some aspect of metabolism is involved. All analyses and mass feature identifications in this work were completed within recommended guidelines set by the Metabolomics Standards Initiative (Kind and Fiehn 2006; Fiehn et al. 2007) and all metabolite identifications

remain putative unless confirmed with a known reference standard matching retention time, exact mass, and fragmentation experiments.

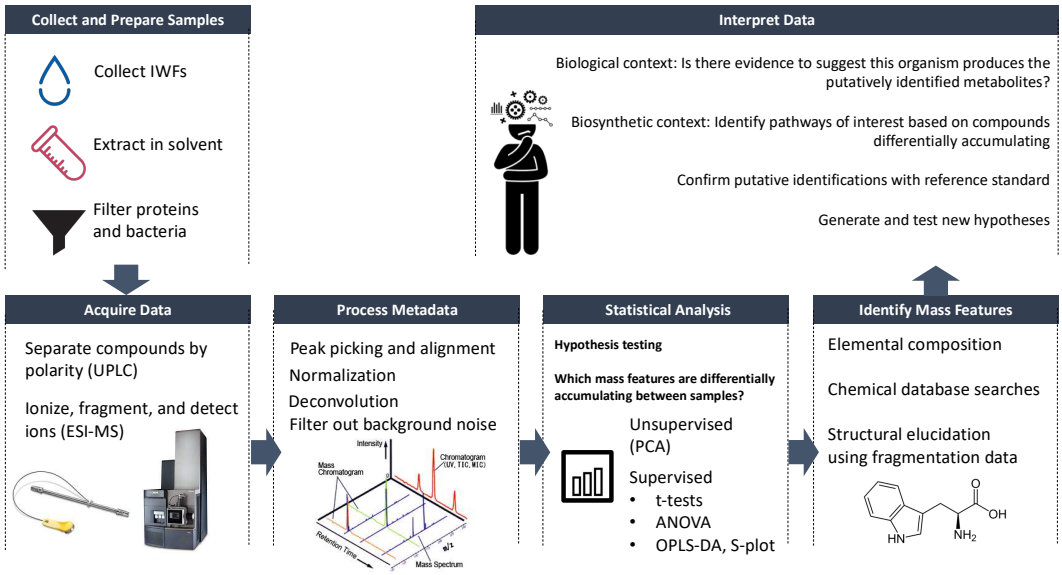

Figure 2. Workflow for non-targeted metabolomics experiments. See Materials and Methods for details on workflow. Intercellular washing fluids (IWFs); ultra-performance liquid chromatography (UPLC); electrospray ionization mass spectrometry (ESI-MS); Principal component analysis (PCA); Orthogonal projections to latent structures discriminant analysis (OPLS-DA). Images of UPLC BEH C18 column and Xevo G2-XS qTOF from Waters Corporation. Diagram of chromatogram and mass spectra from Shimadzu Corporation.

1.4 Hypotheses and objectives

Hypothesis 1: Indolic compounds derived from CYP71A12 and CYP71A13 accumulate in the intercellular space and inhibit growth and biofilm formation of virulent *Pseudomonas syringae.*

Objectives:

- Determine the ARR phenotype of the *cyp71a12/cyp71a13* double mutant
- Identify indolic compounds that may contribute to ARR by profiling semi-polar compounds in intercellular washing fluids of *cyp71a12/cyp71a13-1* and *cyp71b15* using non-targeted mass spectrometry-based profiling.

- Test the antimicrobial activity of indolics accumulating in mature plants during ARR by testing their ability to limit *P. syringae* growth and biofilm formation.

Hypothesis 2: Antimicrobial compounds or levels in the intercellular space or leaf tissue of mature plants differ from those in young plants and are important for Age-Related Resistance in *Arabidopsis*.

Objectives:

- Identify small molecules important for ARR using non-targeted metabolite profiling by comparing young ARR-incompetent with mature ARR-competent intercellular washing fluids and whole leaf tissue.

Hypothesis 3: An indolic compound or indolic compounds derived from *CYP71A12* and *CYP71A13* contributes to the small but significant ARR-like response occasionally observed in *sid2* and together these compounds act additively or synergistically to inhibit growth of *P. syringae*

Objectives:

- Assess the contribution of indolic pathways to the ARR-like response observed in the *sid2* SA biosynthesis mutant by crossing *cyp71a12/a13* with *sid2-2* to create a triple mutant
- Test the ARR phenotype of the *cyp71a12/a13 sid2-2* triple mutant compared to the *sid2-2* single mutant
- Assay for synergistic or additive interactions of indolics and SA by testing the antimicrobial activity against *P. syringae in vitro*

1.5 Research contributions not otherwise discussed

In addition to the work outlined in this thesis, I contributed to a number of other projects in the Cameron lab.

Enhancing resistance in Cucumber & Tomato (collaboration with Drs. Liscombe & Poleatwich, Vineland Research and Innovation Centre)

I completed high-resolution mass spectrometry metabolite profiling of cucumber and tomato leaves responding to powdery mildew to i) identify compounds that accumulate in resistant plants during early stages of the infection and ii) identify metabolites affected by chemical inducers of defense to protect against powdery mildew. Resistance was only observed in cucumber and tomato plants pre-treated with the salicylic acid analog, benzothiadiazole (BTH), so I analyzed these samples and putatively identified a few metabolic compounds associated with metabolism of BTH. I also performed preliminary experiments with young cucumber plants to determine optimal timing for pipecolinic acid root drench prior to inoculation with *Pseudomonas syringae* pv. *lachrymans* (*Psl*) and observed cucumber cultivar-dependent differences in induction of resistance to *Psl*.

SAR Experiments

I worked with Dr. Phil Carella to understand the contribution of LTP1 and LTP2 during SAR by examining the SAR phenotype of mutant lines, collecting petiole exudates, and performing protein immunoblots to assess potential effects of LTP1 or LTP2 on movement of the LTP Defective in Induced Resistance 1 (DIR1) (published in Carella et al., 2016). I contributed to understanding the importance of DIR1 functional domains for SAR, by transiently expressing DIR1 domain variants in the SAR-defective *dir1-1* mutant

to determine if the variants restored SAR. I contributed to creating a stable *dir1-1 dir1-like* double mutant line by performing Agrobacterium-mediated transformation using the floral dip method with an estrogen-inducible DIR1-Like RNAi construct (developed by Dr. Marissa Isaacs) in the *dir1-2* (Col-0 background). Seeds were screened to the T2 generation.

Salicylic acid during ARR

I also worked with Dr. Dan Wilson and contributed to a publication in Molecular Plant-Microbe Interactions on the direct antimicrobial activity of SA against *P. syringae* and the role of *SVP* in ARR (Wilson et al., 2017). I assisted with imaging of *Pst* in the intercellular space with epifluorescence microscopy by preparing epidermal peels and assessing bacterial aggregation, *in vitro* biofilm and growth assays with SA and *Pst*, disease resistance assays and intercellular washing fluid collection of the *sid2* and *svp* mutant. SA quantification by UPLC-MS in an estrogen-inducible SVP line showed this line was not the best to use for gene expression analysis due to variability in SA accumulation.

ARR Metabolomics

Three additional non-targeted metabolomics studies were completed during my graduate work: whole leaf tissue of mature *cyp71a12/cyp71a13-1* compared to wild-type and profiling of young and mature wild-type IWFs and whole leaf tissue. Somewhat lower bacterial densities supported by young plants and high levels of SA in *Pst*-inoculated young IWFs and whole leaf tissue indicated potential defense priming of plants used in these experiments. Results from these experiments are not discussed here due to possible

priming hypothesized to be from unintended exposure to resistance-inducing volatiles from other studies occuring at the time. As ARR was observed, but was not as robust as in other experiments (~ 15-fold), analyses were completed but require follow-up studies (e.g., using mutant lines) to examine the role of putatively identified compounds in ARR vs. as induced/primed defense compounds. Analyses are outlined in a separate document provided with raw data.

CHAPTER 2 – MATERIALS AND METHODS

Plant Growth Conditions: Seeds were surface sterilized (70% ethanol for 1 min followed by seed sterilization solution of 30% bleach and 0.1% Tween 20 in sterile water with shaking for 10 min), rinsed with ddH_2O five times, and suspended in 0.1% phytoblend. Seeds stratified for 2-3 days at 4°C and then plated on Murashige and Skoog (MS) basal salt medium (Murashige and Skoog, 1962). Seedlings germinated under continuous light (22°C, light intensity ~90 µmol/m^2/s, ~45% humidity). At 6 to 7 days, seedlings were transplanted in soil (Sunshine Mix No. 1 – JUIC Ltd.) prepared with 2 L of 1g/L of 20-20-20 fertilizer. To maintain high humidity, seedlings were covered with a plastic transparent dome for 48 hours and grown at 22°C – 24° C at ~80% relative humidity under a nine-hour photoperiod (long-night conditions, average light intensity ~150 µmol/m^2/s). Plants were fertilized with 1g/l of 20-20-20 fertilizer at 3 weeks post-germination (wpg) and 5 wpg. *Arabidopsis thaliana* ecotypes and mutant lines are summarized in Table S1. All mutant lines are in the Col-0 accession background. Sequence data for these genes can be found using the following *Arabidopsis* Genome Initiative Identifiers: Sequence data for these genes can be found using the following *Arabidopsis* Genome Initiative Identifiers: *AAO1* (At5g20960), *CYP71A12* (At2g30750), *CYP71A13* (At2g30770), *CYP71B15* (At3g26830), *CYP71B6* (At2g24180), *CYP79B2* (At4g39950), *CYP79B3* (At2g22330), *CYP82C2* (At4g31970), *FOX1* (At1g26380), *ICS1* (At1g74710).

Pathogen Culture and Inoculation: Bacterial inoculations for all ARR and *in vitro* assays utilized virulent *Pseudomonas syringae* pv. *tomato* (*Pst*) DC3000 (pVSP61)

(Whalen et al., 1991). Cultures were prepared in King's B (KB) media supplemented with 50 µg/ml kanamycin (plasmid resistance) and grown overnight with agitation at 200 rpm for ~16 hours at 22-25°C to mid-log phase (OD_{600} = 0.2 to 0.6). Cultures were re-suspended and diluted to 10^6 colony forming units (cfu) per ml of 10mM $MgCl_2$. Diluted culture was pressure infiltrated into the abaxial (underside) of leaf tissue using a needless 1 ml syringe.

***In planta* bacterial density quantification:** Leaf discs were removed at 3 days post-inoculation (dpi) using a cork-borer (6 mm diameter) for a total of three replicates of eight leaf discs each (maximum two leaf discs per leaf). *Pst* was isolated from tissue by submersing leaf discs in sterile 0.1% Silwet L-77 in 10 mM $MgCl_2$ on an orbital shaker (Lab-Line) at 200 rpm for 1 hour. *In planta* bacterial levels were quantified by plating 10 µl of dilution series on King's B with kanamycin (50µg/ml) and rifampicin (100 µg/ml).

Antibacterial growth assays (*in vitro*): Virulent *Pst* overnight cultures (OD_{600} = 0.2 to 0.6) were centrifuged (Beckman GS-15R) and the bacterial pellet was washed twice by centrifugation in *Hrp*-inducing minimal (HIM) liquid media (Huynh et al. 1989) to remove nutrient-rich KB media, then resuspended in HIM. Serial dilutions of compounds were prepared in 95% ethanol (IAN, ICOOH, ICHO, SA, camalexin) or DMSO (SA, DHCA). Sterile non tissue-culture treated 96-well plates were used under aseptic conditions. For antibacterial growth assays, each well contained a total of 163 µl: 160 µl of media/bacterial culture, 3 µl of compound, for a total of three wells per concentration. For checkerboard synergy antibacterial growth assays, each well contained a total of 163 uL: 160 uL of media/bacterial culture and 1.5 uL of each respective compound for a total

of 3 uL compounds in DMSO. HIM media with equal percentage solvent (EtOH or DMSO) was used as a blank and the average of three wells at each time point subtracted from absorbance (OD600) values of experimental wells for analysis. Solvent was added to HIM with *Pst* as a control for solvent contributing to growth inhibition in the absence of either compound. Plates were taped at edges to prevent contamination and spillage and incubated at room temperature in a plate reader with shaker (Tecan Sunrise). Optical density (OD_{600}) was measured every 15 minutes for 72 hours. After 72 hours, three wells per concentration were pooled, centrifuged at 1000 x g for 7 min, resuspended in 10 mM $MgCl_2$ and plated on non-selective KB plates. Blank controls were plated to check for bacterial/fungal contamination. Minimal bactericidal concentration (MBC) was determined by the lowest concentration that killed all bacteria (no lawn after pooling and plating). Minimal inhibitory concentration (MIC) was determined as the lowest concentration that inhibited exponential growth during log phase (relative to control) at approximately 24 to 48 hours but did not kill bacteria (lawn present after pooling and plating).

DHCA metabolism bacterial growth assays (*in vitro*): To test for the ability of *Pst* to utilize dihydrocamalexic acid (DHCA) as a carbon source or as a nitrogen and sulfur source, bacteria were grown in *Hrp*-inducing minimal media with DHCA as outlined in "Antibacterial growth quantification (*in vitro*)" with the following alterations. To test for ability of *Pst* to use DHCA as a carbon source, bacteria were incubated with DHCA in HIM without a carbon source (lacking fructose). To test for ability of *Pst* to use DHCA as

a nitrogen and/or sulfur source, bacteria were incubated with DHCA in HIM without a nitrogen and sulfur source (lacking ammonium sulfate).

Biofilm quantification (*in vitro*): Biofilm formation of surface-adherent *Pst* cells was quantified using the method developed by O'Toole (2011). Virulent *Pst* overnight cultures (OD_{600} = 0.2 to 0.6) were centrifuged (Beckman GS-15R). The bacterial pellet was washed twice in Hrp-inducing minimal media (HIM) liquid media. Sterile non-tissue-culture treated 96-well plates were prepared under aseptic conditions; non-tissue-culture-treated plates were used to prevent bacteria from having a pre-formed matrix that could encourage biofilm formation. Each well contained a total of 183 µl of solution: 180 µl of media/bacterial culture, 3 µl of compound (SA or DHCA), for a total of six wells per concentration. Plates were left stationary at room temperature to allow for biofilm formation. At 24, 36, 48, 60 and 72 hours, plates were rinsed thoroughly in water to remove planktonic bacteria, then incubated with 0.1% crystal violet for 10 minutes for staining of biofilm, rinsed to remove extra strain and any planktonic bacteria remaining and left overnight to dry. To de-stain for biofilm quantification, plates were incubated with 30% acetic acid (200 µl) for 15 minutes. Optical density (OD_{570}) was recorded on a plate reader (Biotek Synergy 2).

Exogenous chemical rescue assays: Mature (7 wpg) *Arabidopsis* rosette leaves were inoculated with *Pst* (see "*In planta* bacterial density quantification"). At 4 hours post-inoculation (hpi), DHCA (30 ug/ml, 100 mM or 70 ng/ml, 0.2 mM) or IAN (39 ug/ml, 100 mM) and 24 hpi (DHCA concentrations previously listed) was infiltrated into inoculated leaves. Mock control inoculum consisted of 10 mM $MgCl_2$ with equivalent

amount of 95% ethanol (IAN) or DMSO (DHCA) added. Once thoroughly dried (~ 1 hour), plants were returned to chambers. Bacterial growth was quantified as outlined in "*In planta* bacterial density quantification".

Intercellular washing fluid extraction: The infiltration-centrifugation method in Wilson et al. 2017 and developed by O'Leary et al 2014 was used with slight modifications. Plants were watered approximately 1 hr before collecting leaves to ensure similar turgor pressure in all plants (O'Leary et al., 2014). Detached fully expanded rosette leaves at the petiole with a razor blade. Leaves were weighed to 2 g fresh weight (FW) total (~ 24 young leaves or ~12 mature leaves). Leaves were separated into three sets of approximately 667 mg and rinsed for 5 seconds in chilled, distilled water to remove surface contamination. Leaves were placed in 60 ml syringe filled with 30 ml of chilled, distilled water. Using a gloved finger, negative pressure was created in the syringe by pulling the plunger out to the 60 ml mark and slowly releasing. This was repeated approximately three times per set until leaves were thoroughly infiltrated (darkened transparent colour, no light patches, sink in water). Leaves were blotted dry with a Kimwipe and weighed to calculated infiltration volumes. Infiltrated leaves were sandwiched between two – three pieces of Parafilm and rolled around a 1000 µl pipette tip. The parafilm sandwiched leaf roll was secured around the tip with a plastic twist tie gently so as not to leave any marks in the Parafilm/leaves. The pipette tip with rolled leaves was placed in a cut 20 ml syringe bottom with the tip placed in a 1.5 ml microfuge tube (petioles facing upward) and centrifuged for 6 minute at 600 *x g* in a swinging rotor bucket at 4°C, resulting in 150 to 200 µl of IWF collected. IWFs were weighed and stored

in ice until all samples collected. Leaves were visually examined after collection to ensure intercellular washing fluids were removed from all leaves (dark patches indicate intercellular washing fluids are uncollected and still present in leaves). For some experiments, 150 mg (approx. 6 to 3 leaves) were rolled in to a 2 ml microfuge tube with 3 to 5 glass beads and flash frozen in liquid nitrogen (represents the intracellular contents). Cytoplasmic contamination was assayed by measuring chlorophyll and turbidity. IWFs were spun at 21 000 *x g* for 5 min at 4°C. Supernatant was transferred to a new tube, and chlorophyll pellet (if present) were resuspended in 1 ml anhydrous ethanol.

Chemical standards: Indole-3-acetonitrile (IAN), indole-3-carboxylic acid (ICOOH), indole-3-carbaldeyhde (ICHO), indole-3-acetic acid (IAA), camalexin, salicylic acid (SA), L-tryptophan, L-phenylalanine, L-tyrosine, camalexin were purchased from Sigma-Aldrich, all > 95% purity. Indole-3-carbonitrile and D-Cysteine were purchased from Toronto Research Chemicals.

Synthesis of dihydrothiazole carboxylic acids: (-)-(4*S*)-dihydrocamalexic acid was synthesized according to the method outlined in Shuhegger et al. (2006) with slight modifications; all other enantiomers and structural analogues were synthesized and confirmed by the McNulty Lab (McMaster University, Dept Chem and Chem Bio).

IWF preparation for UPLC-mass spectrometry: IWFs were diluted (100 µl IWF) in 60 µl of 5% acetonitrile in water (w/ 0.1% formic acid). Samples were sonicated with ice for 15 minutes and vortexed twice then centrifuged at 20 000 *x g* for 3 minutes. The supernatant was filtered with 0.2 micron GHP filters (Acrodisc) and transferred to LC vials (Waters) with 250 uL glass insert (Chromatography Specialty Inc). A quality control

pool consisting of equal amounts of individual extracted samples was prepared for column equilibration and injected every six runs to assess for unusual variation over time (e.g., shifts in retention time, analytical equipment malfunction) that could affect downstream analyses. The quality control chromatograms are homogenous mixture of all samples, so variation between the 10 – 15 quality control injections may indicate equipment malfunction.

Whole leaf tissue preparation for UPLC-mass spectrometry: Flash frozen whole rosette leaves were ground with glass beads using Geno/Grinder tissue homogenizer (SPEX). Ground tissue was extracted in 1 ml of acidified 50:50 acetonitrile/water (0.1% formic acid), sonicated with ice for 15 minutes and vortexed twice then centrifuged at 20 000 *x g* for 3 minutes. The supernatant was filtered with 0.2 micron GHP filters (Acrodisc) and transferred to LC vials (Waters). A quality control pool consisting of equal amounts of individual extracted samples was prepared for column equilibration and to assess for unusual variation over time between runs (e.g., every 2 hrs from first to last run) that could affect downstream analyses. The quality control chromatograms are homogenous mixture of all samples, so variation between the 10 – 15 quality control injections may indicate equipment malfunction.

UPLC-qTOF MS^{E} and MS/MS: Chromatographic separation was performed on an Acquity UPLC Class I (Waters, Manchester, UK) equipped with an Acquity UPLC BEH C18 1.7 µm column (Waters) using a binary solvent mixture consisting of solvent A (5% acetonitrile in water with 0.1% formic acid) and solvent B (acetonitrile with 0.1% formic acid), with 1 ul (leaf) or 5 µl (IWFs) sample injection at infusion flow rate of 0.3 ml/min.

Gradient was set for solvent B at 0-40% for 0.0-22.5 min, 100% over 23.0-24.5 min, decreasing to 0% over 25.0-26.0 min. Analytic data were acquired on a Xevo G2-XS QTOF (Waters) with a capillary voltage of 3 kV (ESI+) or 2.5 kV (ESI-) and sample cone voltage of 40 eV. MS^E data were acquired in positive and negative electrospray ionization (ESI) modes, in ESI+ for dihydrocamalexic acid MS/MS. A survey scan time of 0.25 sec in continuum data format with an acquisition mass range of 50 to 1200 Da was used for MS^E was 100°C, desolvation temperature 500°C, cone gas flow of 50 L/hr and desolvation gas flow 800 L/hr. For MS^E low energy collision energy was 6 eV and high energy ramp collision energy 15-35 eV. Leucine enkephelin (200 pg/µl in 50:50 acetonitrile/water with 0.1 % formic acid) was used as a reference calibrant with LockSpray ion source (Waters; infusion flow rate 10 µl/min) for exact mass measurement. MS/MS data for DHCA was acquired over 5-10 min at a mass range of 50-250 Da and set mass of 247.0537 Da [M+H] using a scan time of 0.25 sec in continuum format at 25 eV collision energy.

Non-targeted metabolomics data analysis: High resolution UPLC-qTOF-MS data was analyzed with multivariate statistics and cheminformatics software (Progenesis QI and Metaboanalyst 3.1; Xia et al., 2015). Peak alignment, quality control (pooled runs of each sample), peak picking, pseudomolecular ion (adduct) composition, and normalization to all mass features was performed in Progenesis QI (Non-Linear Dynamics). Suitability of data for downstream analysis was assessed by ensuring tight clustering of quality control pooled samples in principal component analysis considering all samples. Mass features were filtered based on manual examination of each dataset to remove low

abundance/background features and datasets saved as .csv files for further analysis. Putative metabolite identification was completed by: establishing fragmentation patterns (fragmentation in mass spectra for low and high energy (first and second function), adducts, neutral loss); estimating elemental composition (Range C0-100, H0-100, N0-5, O0-30, S0-3, unsaturation, 5 ppm ≥ m/z 300, 8 ppm < m/z 300, 15 ppm ≤ 200); putative identification from publicly available and in-house customized natural products databases. Principal component analysis, mass feature abundance plots, T-tests ($P < 0.05$), and ANOVA ($P < 0.05$, Tukey's HSD) statistical analyses performed in and figures generated with Metaboanalyst 3.1 (Xia et al., 2016). Mass error calculated by (observed *m/z* – theoretical *m/z*)/(theoretical *m/z* * 10^6). Theoretical *m/z* calculated in Mass Lynx 3.1.

Production of *Arabidopsis* double and single mutants: The *sid2-2* mutant was crossed with *cyp71a12*/*cyp71a13-1* from the main bolt. The first few flowers (usually sterile) were cut. Under dissection microscope, all siliques and flowers (all stages) were cut. Using fine tweezers, the pollen (stamen) and sepals were gently peeled away from the stigma, being careful not to get pollen on stigma. The detached stamen with pollen of *cyp71a12/cyp71a13-1* was thoroughly applied to the stigma of *sid2-2* for approximately 3-4 stigmas per plant. Plastic stakes and a balloon holder covered in plastic wrap were tied around crossed bolts to create a high humidity environment and placed in growth chambers set to long day (12 hr light) photoperiod. Yellow siliques were removed and dried in microfuge tubes with labels. After one week, seeds were collected from siliques and planted for F2 generation. Twenty-two F3 lines were screened for homozygous *sid2-*

2 cyp71a12/cyp71a13-1 and two putative homozygous lines found. The line labelled AJ8 was used for this work and confirmed with PCR and sequencing.

DNA Extraction and Amplification by PCR: Leaf tissue was harvested from the T2 generation of *cyp71a12/cyp71a13-1 sid2-2* crosses and immediately flash frozen in liquid nitrogen and stored at -80°C. After grinding frozen tissue over liquid nitrogen, DNA extraction buffer (200 mM tris-HCl pH 7.5, 250 mM NaCl, 25 mM EDTA, 0.5% SDS) was added and samples were homogenized by vortex. DNA was purified using phenol-chloroform extraction and precipitated with isopropanol (1:1 v/v). After centrifugation and ethanol wash (70%), the DNA pellet was re-suspended in 50 µl of nuclease-free water and stored at -20°C. Individual T2 plants homozygous for the *cyp71a13-1* T-DNA insertion were identified using PCR as described in Nafisi et al. (2007). Gene-specific primers designed to identify absence of wild-type *CYP71A13* in *cyp71a13-1*: 5'-GTAAGAGAAGACGAGGTAAATGC-3' (forward) and 5'-CTTCTGATCAGTTCCGTCATCG-3' (reverse). The primer used to identify the T-DNA left border was 5'-GGAACAACACTCAACCCTATCTCG-3' (LBe). The deletion in exon 9 in *sid2-2* was confirmed using primers designed to expand the deleted area in *ICS1* 5;- GACATACATCTTTGTGAAACAGCC-3' (forward) and 5'-GCCCCAAGACCCTGTAAATC-3' (reverse). The TALENs-mediated 5 base pair deletion in *CYP71A12* was confirmed with sequencing using primers 5'-TGACATTCCGCAATCTGAAAACC-3' (forward) and 5'-GGGAGAAGGATTTGTCCAGGG-3'.

RNA isolation, cDNA synthesis, and RT-PCR analyses: Whole rosette leaves (4 and 7 wpg) were flash frozen in liquid nitrogen and stored at -80 °C. Total RNA was isolated from frozen tissue using Sigma TRI-reagent (Sigma, St Louis, MI, USA). Turbo DNA-free (Life Technologies, Carlsbad, CA, USA) was used to degrade DNA following manufacturer's instructions. cDNA synthesis was performed with Sigma M-MLV reverse transcriptase (Sigma) using 2 µg of RNA and following the manufacturer protocol. *CYP71A13* expression was confirmed using the following primers:

5'- TGATCAGTTCCGTCATCGTCC-3' (forward) and

5'- AGGCGAGTAACGATAAAGCGG-3' (reverse).

Statistical Analyses: ANOVA was used to determine statistically significant differences in bacterial densities for *in vivo* assays. Means for cfu/leaf disc with unequal variances were log-transformed prior to analysis. Tukey's HSD post hoc test was used for comparisons ($p < 0.05$). All non-metabolomic statistical tests were completed in R or Prism 6.0 and 7.0 (GraphPad).

CHAPTER 3 – RESULTS

3.1 The *cyp71a12/cyp71a13-1* double mutant is ARR-defective

As mentioned (see Introduction), *CYP71A12* can compensate for the loss of *CYP71A13* (Klein et al., 2013; Müller et al., 2015). Results from my undergraduate work demonstrated that the ARR phenotype of the *cyp71a13-1* mutant varied between a partial ARR-defect and wild-type ARR to *Pst* (Figure S1). Similar variability in ARR was observed for the single *cyp71a12* mutant (Figure S2). A double mutant for both *CYP71A12* and *CYP71A13* was obtained from Müller et al. (2015) to test the contribution of *CYP71A13* to ARR. The ARR phenotype of this mutant was compared to the wild-type (Col-0) accession by measuring bacterial levels in plants at three days post-inoculation (dpi) with virulent *P.syringae* pv. *tomato* DC3000 (*Pst*; the strain used throughout this work). The *cyp71a12*/*cyp71a13-1* double mutant consistently displayed a partial ARR defect (Figure 3), with *cyp71a12*/*cyp71a13-1* supporting higher bacterial levels compared to wild-type Col-0 (~ 7 weeks post-germination; wpg). The *cyp71a12*/*cyp71a13-1* line did not exhibit enhanced susceptibility when young, with both wild-type and the double mutant supporting similar levels of bacterial growth (Figure 3). These results suggest that *CYP71A12* and *CYP71A13* contribute to ARR.

Indole-3-acetaldoxime (IAOx) is the substrate for CYP71A12 and CYP71A13, and IAOx is synthesized by CYP79B2 and CYP79B3. A *cyp79b2/cyp79b3* double mutant was generated by Zhao et al. (2002) by crossing *cyp79b2* and *cyp79b3* T-DNA insertion lines. The insertion occured upstream of the heme-binding site in both mutants, therefore, they

are likely to be null mutants (Zhao et al., 2002). As expected if *CYP71A12* and *CYP71A13* are contributing to ARR, the *cyp79b2/cyp79b3* double mutant displayed a partial ARR-defect (similar to *cyp71a12*/*cyp71a13-1*) (Figure 3).

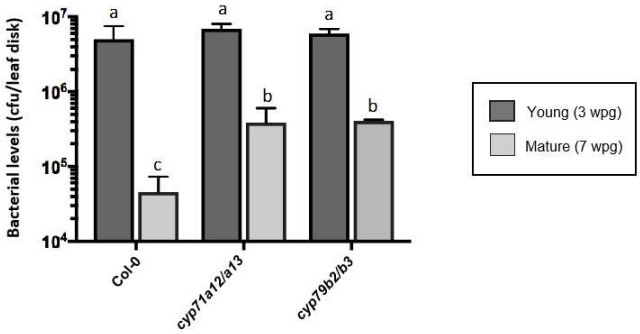

Figure 3. *CYP71A12* and *CYP71A13* contribute to ARR in *Arabidopsis*. ARR assays were performed by quantifying bacterial levels of *Pst* (3 dpi) in young (3 wpg) and mature (7 wpg) Col-0 and indolic biosynthesis mutants *cyp79b2/cyp79b3* and *cyp71a12/cyp71a13-1*. Values represent the mean +/- standard deviation of three sample replicates. Each genotype was tested at least 5 times with similar results. Different letters indicate statistically significant differences (ANOVA, Tukey's honestly significant difference [HSD], $P < 0.05$, n=9 plants / treatment).

3.2 The *cyp71b15 (pad3-1)* camalexin biosynthesis mutant is ARR-competent

CYP71A13 is an upstream component of the camalexin biosynthesis pathway, so a *cyp71b15* camalexin biosynthesis mutant (downstream of CYP71A12 and CYP71A13) was examined to confirm previous studies demonstrating that it is ARR competent (Kus et al., 2002). The *cyp71b15* mutant used in this work (*pad3-1*) is an ethyl methane sulfonate-mutagenesis line in the Col-0 background with a nucleotide deletion in *CYP71B15* that results in a frameshift (early stop codon) and produces trace amounts of camalexin (Zhou et al., 1999; Glazebrook and Ausubel, 1994). If *cyp71b15* shows a similar ARR-defect to *cyp71a12*/*cyp71a13-1*, this would suggest a role for camalexin in ARR. However, the *cyp71b15* (*pad3-1*) mutant consistently displayed a wild-type ARR phenotype (Figure 4), confirming previous work by Kus et al., (2002). The wild-type

ARR phenotype of camalexin-deficient *cyp71b15* suggests that camalexin is not required for ARR.

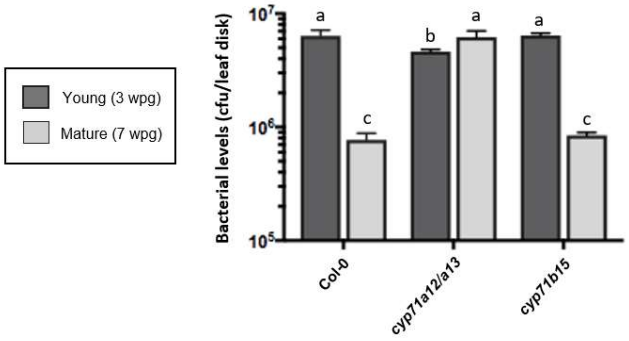

Figure 4. The *cyp71b15 (pad3-1)* mutant has a wild-type ARR phenotype. ARR assays were performed by quantifying bacterial density of virulent *Pst* DC3000 (3 dpi) in young (3 wpg) and mature (7 wpg) Col-0 and indolic biosynthesis mutants *cyp71a12/cyp71a13-1* and *cyp71b15* (*pad3-1*). Values represent the mean +/- standard deviation of three sample replicates. All experiments were performed at least 3 times with similar results. Different letters indicate statistically significant differences (ANOVA, Tukey's honestly significant difference [HSD], $P < 0.05$, n=9 plants / treatment).

3.3 The *cyp71b6* and *aao1* indolic biosynthesis mutants are ARR-competent

The understanding of indole metabolism in *Arabidopsis* is still evolving, and recent evidence has shown that CYP71A12 and CYP71A13 form a metabolic branch-point for several indolic pathways implicated in plant defense (Rajniak et al. 2015, Müller et al. 2015, Böttcher et al. 2014). As a camalexin biosynthesis mutant was not defective for ARR and did not exhibit enhanced susceptibility to *P. syringae* when young, CYP71A12 and CYP71A13 were initially hypothesized to contribute to ARR via an indole-3-carboxylic acid-dependent pathway rather than a camalexin-dependent pathway (Figure 1). To test this hypothesis, homozygous T-DNA insertion mutants were obtained from the *Arabidopsis* Biological Resource Centre (Ohio State University) in genes identified by Böttcher et al. (2014) to be involved in indole-3-carboxylic acid biosynthesis. The ARR phenotypes of these mutants were examined to test the hypothesis that indole-3-

carboxylic acid derivatives contribute to ARR.

Both *cyp71b6* and *aao1* were tested as Böttcher et al. (2009) showed a partial reduction in ICOOH and ICHO derivatives in these mutants. ARR assays of these mutants demonstrated that loss of *CYP71B6* or *AAO1* did not negatively affect ARR (Figure 5), however as discussed above, it is not possible to rule out a role for indole carboxylic acid derivatives in ARR since ICOOH and ICHO derivatives were only partially reduced in both mutants (Böttcher et al., 2009).

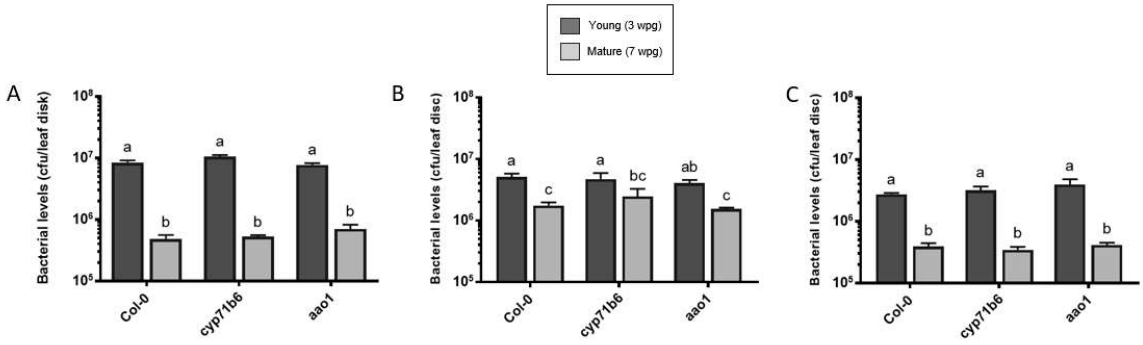

Figure 5. Indole carboxylic acid pathway mutants display wild-type ARR responses. ARR assays were performed by quantifying *Pst* levels (72 hpi) in young (3 wpg) and mature (7 wpg) plants. Values represent the mean +/- standard deviation of three sample replicates. Different letters indicate statistically significant differences (ANOVA, Tukey's honestly significant difference [HSD], $P < 0.05$, n=9 plants / treatment).

3.4 Indolic and SA pathway interaction *in planta*

Salicylic acid (SA) is required for ARR and has antimicrobial activity against *Pst* (Kus et al., 2002; Cameron and Zaton, 2004; Wilson et al., 2017). However, the SA biosynthesis mutant *sid2-2* occasionally has a residual ARR-like response, in which a small, but significant reduction (2- to 5-fold) in bacterial populations was observed in mature compared to young leaves (Figure S3). Therefore, it is possible that this ARR-like

response in *sid2* may be due to the activity of other antimicrobial compounds in the intercellular space during ARR, and these compounds may interact synergistically or additively with SA. The indolic biosynthesis mutant *cyp71a12*/*cyp71a13-1* has been observed to be partially ARR-defective (this work), thus an indolic compound or indolic compounds derived from CYP71A12 and CYP71A13 may contribute to the *sid2-2* ARR-like response. To test for potential synergistic or additive effects between SA and indolic pathways during ARR, the double *cyp71a12*/*cyp71a13-1* mutant was crossed with *sid2-2* and homozygous *cyp71a12*/*cyp71a13-1 sid2-2* triple mutants were identified (see Methods; Figure S4). If CYP71A12/CYP71A13-mediated pathways are involved in the residual ARR-like response observed in *sid2*, then the triple mutant should display a full ARR-defect consistently across experiments. In three assays performed to date, the partial ARR-like response was not observed in *sid2-2* or the triple mutant and instead both mutant lines were fully ARR-defective making it impossible to answer this question (Figure 6).

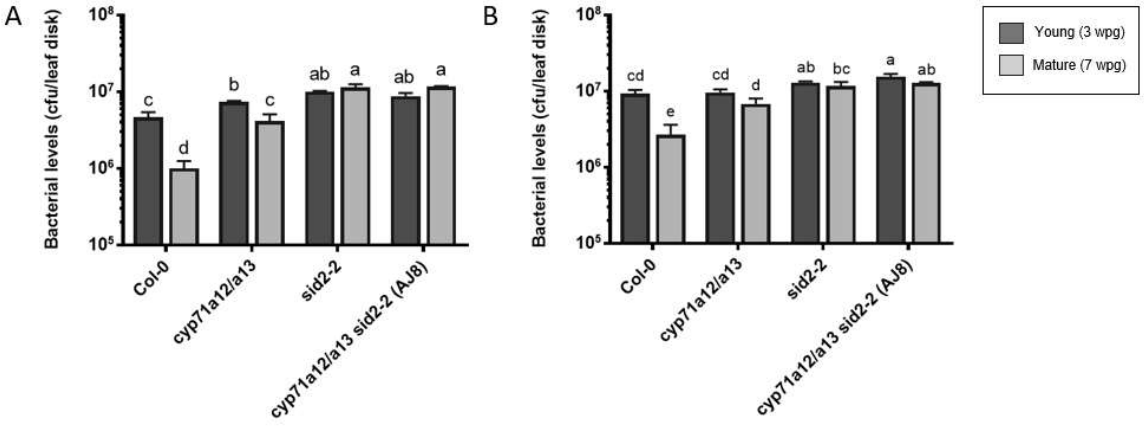

Figure 6. The SA and indolic biosynthesis triple mutant *cyp71a12/cyp71a13-1 sid2-2* is fully ARR-defective. ARR assays were performed by quantifying *Pst* levels (72 hpi) in young (3 wpg) and mature (7 wpg) plants. Values represent the mean +/- standard deviation of three sample replicates. All experiments were performed at least 3 times with similar results. Different letters indicate statistically significant differences (ANOVA, Tukey's honestly significant difference [HSD], $P < 0.05$, n=9 plants / treatment).

3.5 Identification of CYP71A12 and CYP71A13-derived compounds contributing to ARR

CYP71A12 and CYP71A13 are involved in several indolic biosynthesis pathways, therefore, to identify which compound(s) may contribute to ARR in addition to SA, a non-targeted mass spectrometry-based approach was used to profile metabolites affected by the *cyp71a12*/*cyp71a13-1* mutation. Differentially accumulating metabolites identified using this approach may be relevant for ARR and these techniques make it possible to probe overall indolic metabolism to see which CYP71A12/CYP71A13-derived compounds are affected by the mutation in the corresponding genes. All metabolomic studies in this work were completed in collaboration with Dr. David Liscombe (Biochemistry, Vineland Research and Innovation Centre).

3.5.1 Non-targeted metabolomics of intercellular washing fluids during ARR

Ultra-performance liquid chromatography-mass spectrometry (UPLC-MS) was used to profile semi-polar metabolites of the intercellular space where *Pst* thrives and where compounds of interest are hypothesized to accumulate during ARR. Intercellular washing fluids (IWFs) were collected from *Pst*-inoculated leaves at 24 hpi. The 24 hpi time-point was chosen based on expression of *CYP71A12*, *CYP71A13*, and *CYP71B15* in response to *Pst* (Figure S5) or silver nitrate (AgNO3) (Rajniak et al., 2015; Nafisi et al., 2007). The contents of IWFs represent the intercellular fluid (which contains plant and bacterial metabolites), and components of the exterior of the plant cell wall (for example, esterified indole-3-carboxylic acids) (O'Leary et al., 2014, 2016; Soylu et al., 2005). Since the inoculation procedure could result in accumulation of wound-induced compounds, IWFs were collected from mock-inoculated leaves to prevent erroneous identification of wound-induced compounds as contributing to ARR. Cytosolic contents may appear to accumulate in the intercellular space if cellular damage occurred during IWF collection. Therefore, chlorophyll and turbidity (indicators of contamination from organelles and sub-cellular structures) was measured by absorbance (OD664 and OD700 respectively) to assay for intracellular contamination in IWFs (Figure S6). The *cyp71b15* mutant was included in the IWF metabolite profiling since it is an indole biosynthesis mutant impaired downstream of CYP71A12/CYP71A13, but it is not ARR-defective. As *cyp71a12*/*cyp71a13-1* has a block in biosynthesis for several indolic compounds, the *cyp71b15* mutant should aide in elucidating which indolic compounds contribute to ARR. For example, compounds absent or reduced in both *cyp71a12*/*cyp71a13-1* and *cyp71b15*

are less likely to be involved in ARR and interest in compounds absent or reduced in *cyp71a12*/*cyp71a13-1* only would be of greater interest. ARR assays of plants grown with and inoculated at the same time as those used in IWF metabolomics assays showed that at three dpi *cyp71a12*/*cyp71a13-1* supported 4.7- and 7.6-fold higher bacterial density compared to mature wild-type and *cyp71b15* respectively and were ARR defective (Figure 7).

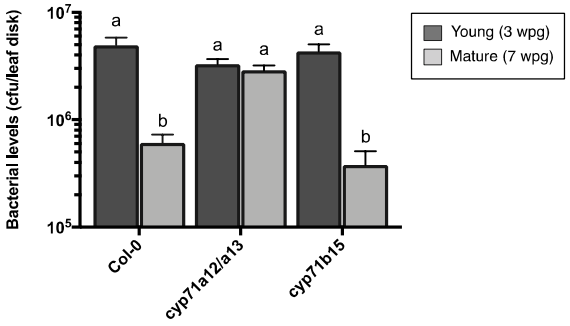

Figure 7. Bacterial quantification assays of young and mature of plants during IWFs metabolomics studies. Bacterial quantification assays of young and mature (ARR assays) of Col-0 and indolic biosynthesis mutants *cyp71a12/cyp71a13-1* and *cyp71b15* (*pad3-1*). ARR assays were performed by quantifying *Pst* levels (3dpi) in young (3 wpg) and mature (7 wpg) plants. Values represent the mean +/- standard deviation of three sample replicates. Different letters indicate statistically significant differences (ANOVA, Tukey's honestly significant difference [HSD], $P < 0.05$, n=9 plants / treatment).

Principal component analysis (PCA) is a multivariate statistical method used to visualize variance in samples based on clustering and separation of groups while considering hundreds of mass spectral features. It is an unsupervised method, meaning variation between samples is identified without knowledge of sample identity; PCA is useful for identifying anomalies in large datasets (e.g., outliers, potentially mislabeled samples). PCA score plots for mass spectral features measured in IWFs showed clustering of QC samples (Figure 8). The QC is a homogenous mix of all samples injected approximately

every six runs during data acquisition to check for variance between runs and analytical instrument performance. Low variation between QC runs (clustering) indicates high reproducibility (Fiehn et al., 2008). Since IWFs from two biosynthetic mutants compared to wild-type plants were profiled, only a subset of metabolites is expected to be affected intracellularly, and only those compounds that are transported to or synthesized in the intercellular space would be detected in these experiments. Minimal separation of all samples was observed for all detectable semi-polar compounds for both positive (Figure 8A) and negative (Figure 8B) ionization modes (947 and 737 normalized mass spectral features respectively). Genotypic variation in IWFs was minimal as the scores for IWFs cluster by genotype. Low variance (minimal separation) was observed between mock- and *Pst*-inoculated plants of the same genotype, or between IWFs from ARR-defective and ARR-competent plants. Biologically these results tell us only a small subset of metabolites (e.g., CYP71A12/CYP71A13-derived indolics) were observed to be significantly different between the genotypes and treatments, so perhaps minor changes in metabolite composition in the intercellular space affect disease outcomes during ARR.

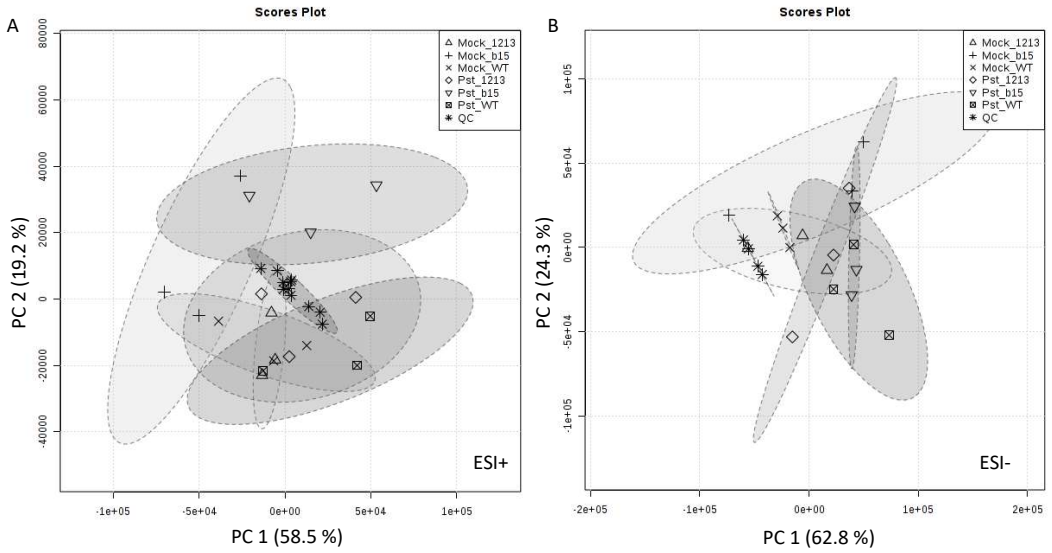

Figure 8. Principal component analysis scores plots for all mass spectral features for intercellular washing fluids from *Pst*- and mock-inoculated plants. Treatment and genotype represented by symbol with (A) representing IWFs run in positive electrospray ionization mode and (B) representing IWFs run in negative electrospray ionization mode. QC (quality control); WT (wild type Col-0); 1213 (*cyp71a12/cyp71a13-1*); b15 (*cyp71b15*). Percentage in brackets shows explained PCs. Analyzed with Metaboanalyst using prcomp package in R.

Unsupervised PCA is useful for exploring the global changes in IWF metabolites, but to answer the question of which compounds may be contributing to ARR, mass spectral features that were statistically different between an ARR-defective (*cyp71a12/cyp71a13-1*) compared to ARR-competent plants (Col-0 and *cyp71b15*) needed to be identified. Analysis of variance (ANOVA) testing of normalized abundance values was used to identify which of the hundreds of features detected were significantly changing between treatment groups and genotypes. In positive ESI mode, the most significantly different feature was a peak at 7.34 minutes with a nominal mass of 247 [M+H]. This feature was abundant in *Pst*-inoculated wild type and *cyp71b15* but was not detected in *Pst*-inoculated *cyp71a12/cyp71a13-1* mutants (Figure 10A). Using elemental composition (seven possible molecular formulae within 8 ppm) and abundance patterns in the biosynthesis

mutants, this feature was putatively identified as dihydrocamalexic acid (DHCA; $C_{12}H_{10}N_2O_2S$). DHCA has been shown to accumulate in c*yp71b15*, likely due to non-enzymatic cyclization of accumulating Cys(IAN) to DHCA and the mean relative abundance of this compound between samples was highest in *Pst*-inoculated *cyp71b15* IWFs. To confirm the putative identification of DHCA, synthetic standards were obtained from Dr. Erich Glawischnig (Technische Universität München) and via collaboration with Dr. Jim McNulty (Dept. of Chemistry and Chemical Biology, McMaster University). Based on the retention time and fragmentation of these two independently synthesized DHCA standards, the peak at 7.34 minutes with a nominal mass of 247 was confirmed to be DHCA ($[C_{12}H_{10}N_2O_2S+H]$), with fragmentation producing peaks at *m/z* 201.0520 ($[C_{11}H_8N_2S+H]$, loss of carboxylic acid), and *m/z* 143.0604 ($[C_9H_7N_2+H]$, thiazole ring opening or fragmentation) (Böttcher et al., 2009; Zandalinas et al., 2012; Figure 9).

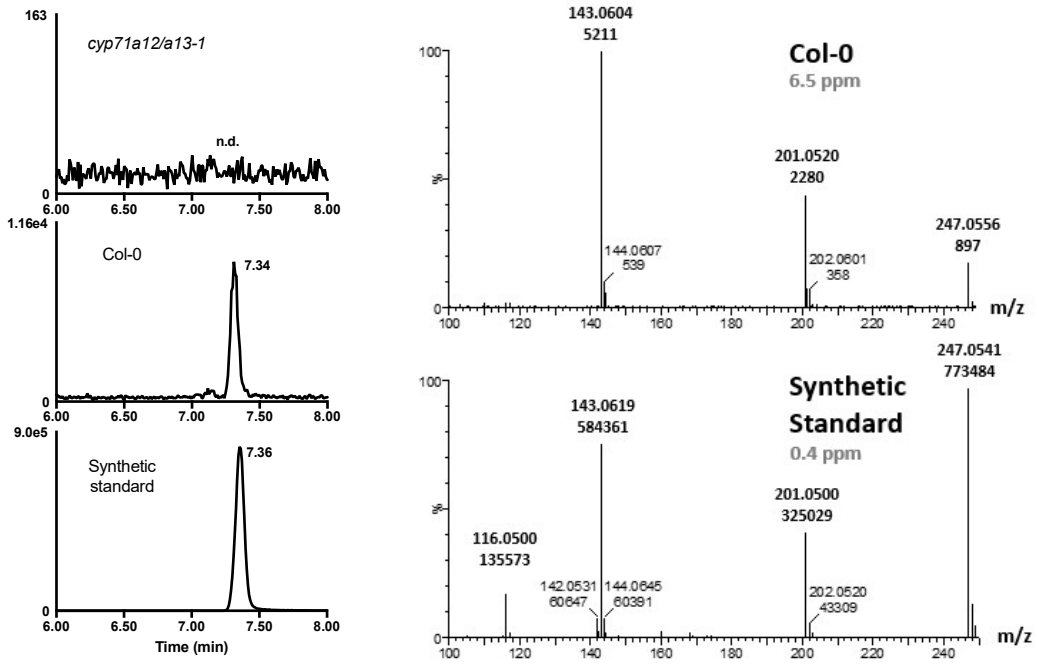

Figure 9. Extracted ion chromatogram and mass spectra for dihydrocamalexic acid (*m/z* 247.0540, [$C_{12}H_{10}N_2O_2S$+H]). Samples were run in positive electrospray ionization mode. The fixed y-axis shows relative intensity for synthetic standard compared to *Pst*-inoculated Col-0 and *cyp71a12/cyp71a13-1*. n.d. indicates compound not detected.

In total, 5 mass spectral features were significantly different between IWF samples in positive ESI mode and 146 mass spectral features were significantly different between IWF samples in negative ESI mode. Of these significantly different features for all treatments, only 5 were significantly different between ARR-defective (*cyp71a12/cyp71a13-1*) and ARR-competent (Col-0 and *cyp71b15*) IWFs and therefore may of biological significance for ARR. Putative identificationsof these features suggest that indolic and sinapic acid derivatives were accumulating differentially in IWFs from these plants (Table 2; Figure S7).

Table 2. Classification of mass spectral features from biochemical profiling of *Arabidopsis* intercellular washing fluids from wild type (Col-0), *cyp71b15* and *cyp71a12/cyp71a13-1* indolic biosynthesis mutants (UPLC-ESI+ or ESI- MS).

Label	Identification	Classification	Elemental Composition	Retention time (min)	Observed *m/z*	Theoretical *m/z*	Mass error (ppm)
A	Dihydrocamalexic acid*	Indolic	$C_{12}H_{11}N_2O_2S$	7.3	247.0554 [M+H]	247.0540 [M+H]	5.7
B	Sinapic acid derivative	Phenylpropanoid	---	5.0	399.0932 [M+H]	---	---
C	1-*O*-sinapoyl-beta-D-glucose	Phenylpropanoid glucoside	$C_{17}H_{21}O_{10}$	6.2	385.1140 [M-H]	385.1135 [M-H]	1.3
D	Indole-3-carboxylic acid derivative	Indolic glucoside	---	7.0	322.0931 [M-H]	322.0927 [M-H]	1.2
E	Unidentified	---	---	16.6	732.3930 [M-H]	---	---

Asterisk (*) indicates identification confirmed by synthetic standard retention time and fragmentation, mass error < 8 ppm. [M+H] indicates *m/z* detected in positive ionization mode; [M-H] indicates *m/z* in negative ionization mode. Data normalized to all compounds in Progenesis QI. One-way ANOVA (False discovery rate-adjusted p-value threshold 0.05, Tukey's HSD).

DHCA and the putatively identified derivative of indole carboxylic acid (compound D) show the greatest differences between *cyp71a12/cyp71a13-1* and the ARR-competent genotypes (Figure 10A, D). The indole-3-carboxylic acid derivative is accumulating in wild type and *cyp71b15* in response to *Pst* and is present but significantly lower in all mock-inoculated IWFs and *cyp71a12/cyp71a13-1*. The unidentified mass feature at *m/z* 732 (compound E) shows an inverse accumulation pattern, with mock-inoculated wild type and *Pst*-inoulated *cyp71a12/cyp71a13-1* IWFs having significantly higher abundance, and *Pst*-inoculated ARR-competent plants having significantly lower accumulation (Figure 10E).

Putatively identified 1-*O*-sinapoyl-beta-D-glucose is lowest in all mock-inoculated IWFs and *Pst*-inoculated *cyp71a12/cyp71a13-1* IWFs (Figure 10C). Although the abundance plot for this sinapic acid glucoside shows accumulation in *Pst*-inoculated ARR-competent IWFs, the difference is not significant because of high variation in accumulation for wild-type IWFs. Compound B appears to be a sinapic acid derivative as one of the fragments associated with the peak at *m/z* 399 has an exact mass similar to that of sinapic acid, but it isn't clear what it is conjugated to or what modifications exist on this molecule if it is related to sinapic acid (Figure S7B). Regardless, compound B is significantly higher in *Pst*-inoculated *cyp71a12/cyp71a13-1* IWFs compared to wild type (Figure 10B). However, ARR-competent *cyp71b15* also accumulates significantly higher levels of compound B in *Pst*-inoculated IWFs compared to wild type (and levels are not significantly different from *cyp71a12/cyp71a13-1* IWFs). Compound B is therefore probably not contributing to ARR, and rather the differences in accumulation between genotypes are reflective of perturbations of indolic biosynthesis in cytochrome P450 mutants. The potential role of sinapic acid and indolic derivatives in defense and ARR is further explored in the Discussion (Chapter 4).

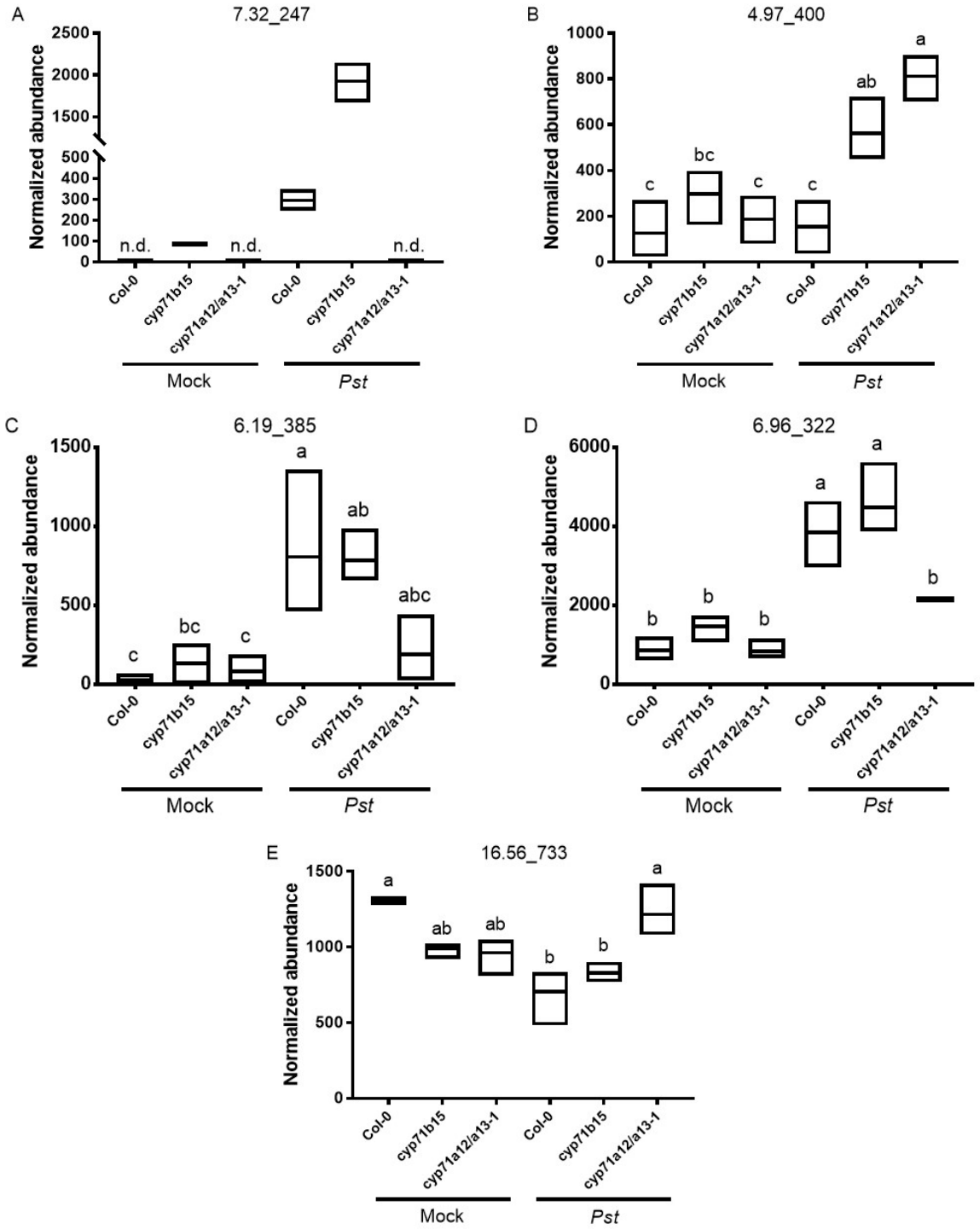

Figure 10. Normalized abundance values for significantly different features detected in intercellular washing fluids (listed in Table 2). Y-axis represents relative peak integration area (normalized to all compounds using Progenesis QI – original and normalized concentrations). All significant differences based on ANOVA (p value < 0.05, FDR-adjusted, Tukey's HSD). Boxes represent maximum and minimum values; middle line represents median. Headings show retention time_nominal mass. Each letter is matched to the feature listed in Table 2.

3.5.2 Quantification of DHCA in IWFs during ARR

DHCA accumulates in IWFs from *Pst*-inoculated plants and is not detected in ARR-defective *cyp71a12/cyp71a13-1*. To quantify the amount of DHCA accumulating in IWFs, standard curves were prepared using synthetic DHCA (2 pg to 6000 ng/µl; Figure S8). At 24 hpi with *Pst*, DHCA accumulated at ~370 ng/ml in wild-type IWFs, ~2405 ng/ml in the *cyp71b15* IWFs, and was not detected in *cyp71a12/cyp71a13-1* (Figure 11). Mock-inoculated wild-type plants did not produce detectable levels of intercellular DHCA, and as expected, mock-inoculated *cyp71b15* accumulated DHCA (~90 ng/ml) due to a block in camalexin biosynthesis whereby the Cys(IAN) precursor accumulated and could have non-enzymatically cyclized to DHCA. Camalexin was not detected in the IWFs regardless of treatment or genotype (Table S2).

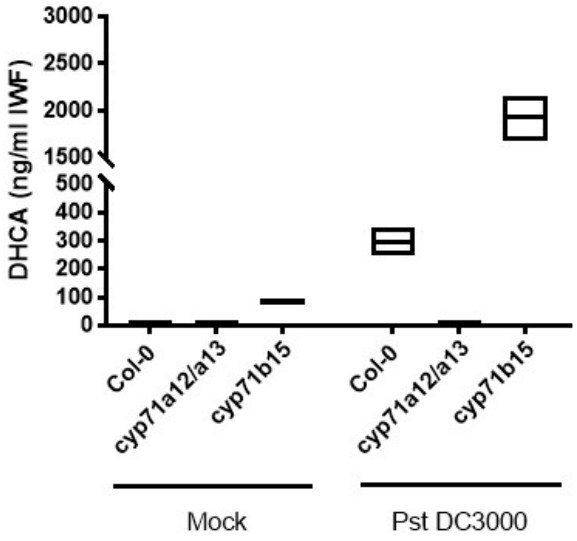

Figure 11. DHCA accumulates in IWFs in response to *Pst.* DHCA levels in the IWFs of Col-0, *cyp71a12/cyp71a13-1,* and *cyp71b15 (pad3-1)* mature plants (7 wpg) 24 hpi with *Pst* DC3000 inoculation or 10 mM $MgCl_2$ (mock) measured by UPLC-MS (ESI+). Boxes represent maximum and minimum values; middle line represents median.

IAN was not expected to accumulate in plants as *Pst* induced expression of genes involved in camalexin biosynthesis, so any IAN produced would likely be used to

produce camalexin and other indolic metabolites. During non-targeted metabolite profiling, IAN was not detected (checked against authentic standard) in IWFs regardless of treatment and genotype (Table S2).

Intercellular SA accumulation is required for ARR and can therefore serve as an metabolic indicator of ARR. SA levels in IWFs were quantified using a commercially available standard and confirmed by retention time, exact mass (< 5 ppm mass error) and fragmentation (Figure S8). At 24 hpi with *Pst,* SA accumulated in IWFs at ~4 to 5 µg/ml for all genotypes at (Figure 12). These results agree with unpublished work by Dr. Marissa Isaacs showing *cyp71a12/cyp71a13-1* accumulated wild-type levels of SA in response to *Pst.*

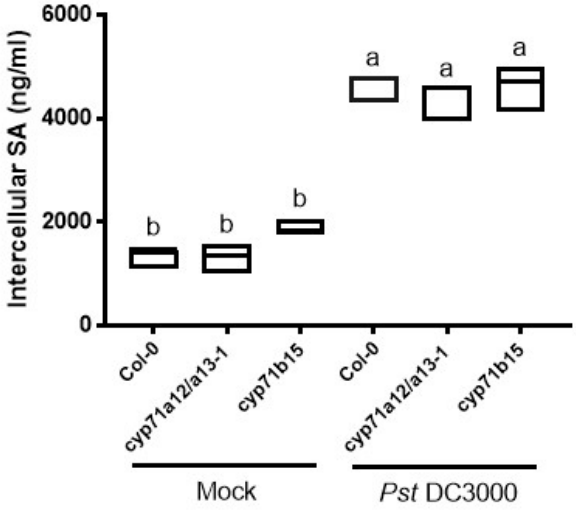

Figure 12. Salicylic acid accumulation in the intercellular space 24 hpi with *Pst.* SA levels in IWFs of Col-0, *cyp71a12/cyp71a13-1,* and *cyp71b15 (pad3-1)* mature plants (7 wpg) 24 hpi with *Pst* DC3000 inoculation or 10 mM $MgCl_2$ (mock) measured by UPLC-MS (ESI+). Boxes represent maximum and minimum values; middle line represents median.

3.6 Testing the contribution of DHCA to ARR

3.6.1 Accumulation of intercellular DHCA in young and mature plants

If DHCA is contributing to ARR against *Pst* then it may accumulate differentially between young and mature in intercellular spaces. Since young plants support higher bacterial density compared to mature plants, IWFs collected from young plants should contain less DHCA than mature IWFs. To examine DHCA accumulation in young plants compared to mature, IWFs were collected for UPLC-MS analysis from young and mature wild-type Col-0 leaves at 24 hpi with *Pst*. In 2 independently grown and collected experiments an ARR response was observed, with young plants supporting 12-fold (Figure 13A) and 15-fold (Figure 13B) higher bacterial density compared to mature plants.

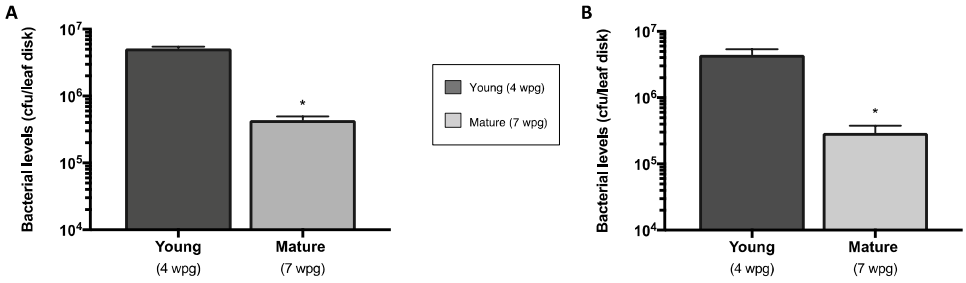

Figure 13. Bacterial quantification of young and mature Col-0 (wild type) from experiments collected for intercellular washing fluids metabolomics analysis. ARR assays were performed by quantifying bacterial density of *Pst* (72 hpi) in young (4 wpg) and mature (7 wpg) wild type (Col-0). Experiment A was completed June 2017 (A) and experiment B was completed July 2017 (B). Values represent the mean +/- standard deviation of three sample replicates. Asterisk (*) indicate statistically significant differences (t-test, $p < 0.05$, n=9 plants / treatment).

Intercellular DHCA was significantly lower in young *Pst*-inoculated IWFs (~91 ng/ml) compared to mature IWFs (~154 ng/ml) from experiment B (Figure 14B). In experiment A, the levels of DHCA between young (~123 ng/ml) and mature (~ 187 ng/ml) IWFs did

not differ significantly (Figure 14A). DHCA was not detected in mock-inoculated plants of either age.

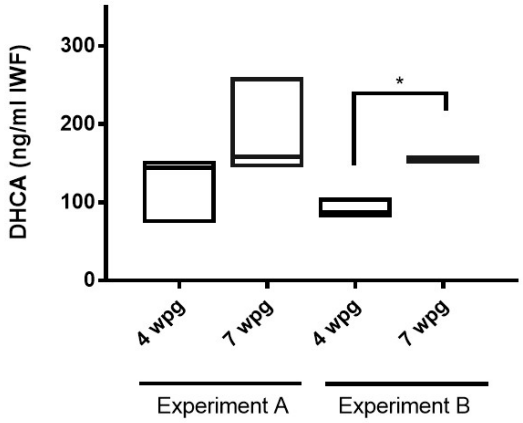

Figure 14. Quantification of DHCA in intercellular washing fluids from young and mature Col-0 (wild type) in response to *Pst.* DHCA levels in IWFs of young (4 wpg) and mature (7 wpg) wild type Col-0 24 hpi with *Pst* measured by UPLC-MS (ESI+). Asterisk (*) indicate statistically significant differences (t-test, $p < 0.05$, n=9 plants / treatment). Boxes represent maximum and minimum values; middle line represents median.

As previously mentioned, intercellular SA accumulation is required for ARR, so SA was quantified in IWFs as an additional assessment of ARR. Unexpectedly, SA levels in young IWFs was not significantly different from SA levels in mature IWFs in both experiment A and B (Figure 15). SA levels were 464 to 4025 ng/ml in young IWFs and mature IWFs had 2677 to 3815 ng/ml SA. In this experiment SA accumulation at 24 hpi between young and mature *Pst*-inoculated IWFs was not significantly different, in contrasts to data from Cameron and Zaton (2004), where intercellular SA was significantly lower in young *Pst*-inoculated plants (75 ± 45 ng/ml SA in young and 461 ± 257 ng/ml SA in mature). SA in mock-inoculated IWFs in these experiments range from 404 to 907 ng/ml, while in previous research, SA accumulated to 50 to 150 ng/ml in mock-inoculated IWFs (Cameron and Zaton 2004, Carivel et al. 2009; Wilson et al.,

2017). The high accumulation of SA in IWFs from young plants may indicate defense priming so DHCA accumulation in young plants may reflect levels after priming. However, the overall trend is that intercellular DHCA levels were lower in young plants compared to mature for these experiments (Figure 14). Potential defense priming of these experiments due to SA accumulation in young IWFs is addressed in the Discussion (Chapter 4).

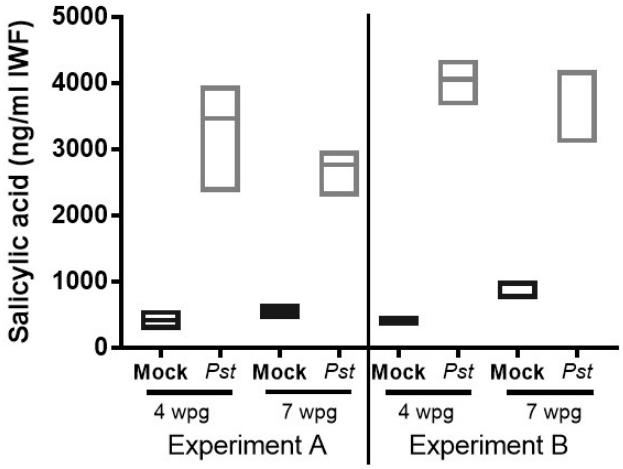

Figure 15. Quantification of SA in intercellular washing fluids from young and mature Col-0 (wild type) in response to *Pst.* SA levels in IWFs of young (4 wpg) and mature (7 wpg) wild type Col-0 24 hpi with *Pst* DC3000 measured by UPLC-MS (ESI+). Boxes represent maximum and minimum values; middle line represents median.

3.6.2 Antigrowth activity of DHCA against *P. syringae in vitro*?

The *cyp71a12/a13-1* mutant was defective for accumulation of DHCA in IWFs in response to *Pst*, and was partially ARR-defective, suggesting that DHCA plays a role in ARR. These data plus the fact that SA-deficient mutants occasionally exhibit a modest ARR response, led to the hypothesis that like SA, DHCA may act as an intercellular antimicrobial compound to inhibit bacterial growth or biofilm-like aggregation during ARR in mature plants. To examine the growth inhibitory activity of DHCA, bacteria were

incubated with concentrations of 50 ng/ml to 1 mg/ml DHCA for ~72 hours at room temperature and bacterial growth was measured. Virulence genes (e.g., *Hrp* genes for pilus assembly that deliver effectors into plant cell) may not be expressed in nutrient-rich media like LB and KB and these media are not representative of the conditions that bacteria experience in the intercellular space (Kim et al., 2009; Wilson et al., 2017). Therefore, *Hrp*-inducing minimal medium (HIM) was used for all *in vitro* assays because this media provides a nutrient availability and pH similar to the intercellular space and induces virulence genes in *P. syringae* (Huynh et al., 1989; Rahme et al., 1992; Kim et al. 2009).

DHCA displayed low growth inhibitory activity against *Pst,* with a minimal inhibitory concentration (MIC; bacteria are alive but little to no growth measured) between 500 µg/ml and 1 mg/ml (Figure 16). The minimal bactericidal (lethal) concentration of DHCA was ~1 mg/ml (Figure 16A). In contrast, SA inhibited *Pst* growth at 250 µg/ml and was bactericidal at 500 µg/ml (Figure 16B).

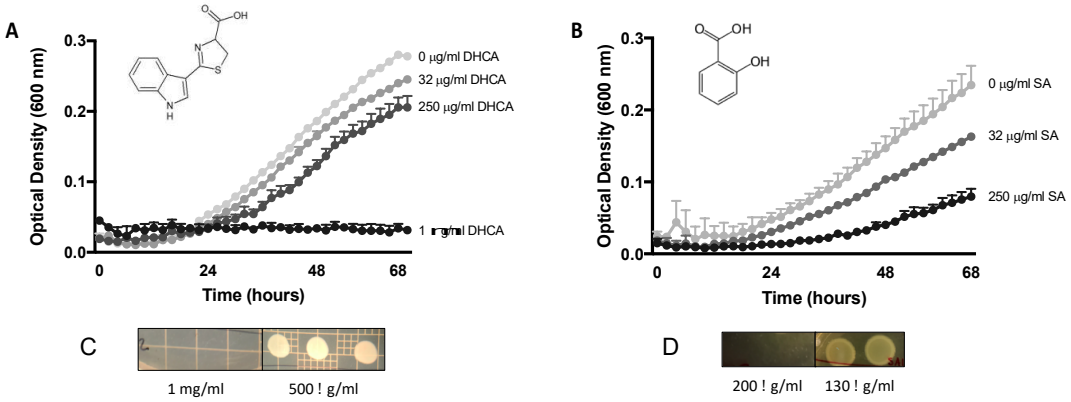

Figure 16. Growth of *Pst* in the presence of DHCA or SA. Dose-dependent effect of dihydrocamalexic acid (A) and salicylic acid (B) on *Pst* growth in Hrp-inducing minimal media as measured by turbidity (OD_{600}) after incubation for 68 hours at room temperature (24 to 26 °C). Each data point is the mean ± SD of three wells per concentration from a 96-well non-tissue-culture-treated plate. C and D. To test for bactericidal activity, wells with cultures displaying little to no growth after 68 hours were spun down and the bacterial pellet was resuspended in 10 mM $MgCl_2$ and plated on non-selective KB media.

3.6.3 Ability of *P. syringae* to utilize DHCA as a nutrient source

Plant metabolites can be utilized by bacteria as a nutrient source and some of these metabolites are antimicrobial only when they are present at sufficiently high concentrations that they cannot be metabolized quickly enough by bacteria (e.g., GABA) (O'Leary et al., 2014). Wilson et al. (2017) showed that *Pst* is unable to grow with SA as a sole carbon source, suggesting that *Pst* is unable to metabolize SA. Howden et al. (2009) tested the ability of *P. syringae* to metabolize IAN and found that *Pst* was unable to hydrolyze IAN for use as a nitrogen source; however, IAN did not accumulate in the intercellular space regardless of treatment in this study (Table S2). As DHCA may be used as a carbon, nitrogen, or sulfur source, the ability of *Pst* to grow with DHCA (32 µg/ml to 1µg/ml) as the sole carbon source or as the sole nitrogen and sulfur source in minimal media was investigated. These concentrations were chosen because they showed little to no growth inhibition relative to the 0 µg/ml controls, so any growth inhibition of

bacteria was likely to result from the lack of nutrient source rather than the bioactivity of DHCA. In minimal media with DHCA as the carbon source (in place of fructose) or as the sole nitrogen and sulfur source (in place of ammonium sulfate), *Pst* did not grow (Figure 17). In both scenarios bacteria survived, but no growth was observed, similar to controls with bacteria incubated in HIM media without fructose or without ammonium sulfate (Figure 17). These results suggest that DHCA is not a significant source of carbon, or nitrogen and sulfur, and that *Pst* is unable to utilize DHCA as a source of nutrients.

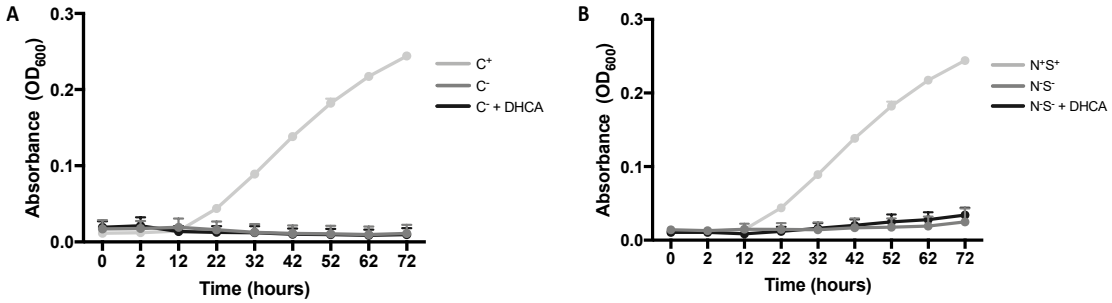

Figure 17. DHCA is not a significant source of carbon or nitrogen and sulfur for *Pst*. Growth assays of *Pst* incubated in Hrp-inducing minimal media without a carbon source (A), or without a nitrogen and sulfur source (B) and DHCA (1 μg/ml). *Pst* growth was measured by turbidity (OD_{600}) over 72 hours of incubation with shaking at room temperature (24 to 26 °C). Each data point is the mean ± SD of three wells per concentration from a 96-well non-tissue-culture-treated plate. To test for bactericidal activity, wells with cultures displaying little to no growth after 72 hours were spun down and the bacterial pellet was resuspended in 10 mM $MgCl_2$ and plated on non-selective KB media.

3.6.4 Examining structure-activity relationships with DHCA analogues

The McNulty group (McMaster University, Chem. and Chem. Bio. Dept) synthesized DHCA and four additional dihydrothiazole carboxylic acids for use in these studies. These compounds are synthetic analogues of DHCA in which the indole ring is replaced by a phenyl group (derived from phenylalanine) or a phenol group (derived from tyrosine). These compounds and camalexin were assayed for growth inhibitory effects against *Pst* to examine how the structure of DHCA relates to its antimicrobial activity.

Using these compounds, modifications to the indole ring and the thiazole ring of DHCA and their affects antimicrobial activity were compared providing information on whether these structural components contribute to antimicrobial activity of DHCA

Of all compounds tested, camalexin and the *S*-enantiomer of the phenyl DHCA analogue were the only compounds that inhibited growth of *Pst*. The *S*-phenyl DHCA analogue was more effective at inhibiting growth of *Pst* compared to DHCA, with an MIC of ~250 µg/ml (Figure 18B) compared to ~500 to 1000 µg/ml for DHCA (Figure 18A). Interestingly, the *S*-phenyl DHCA analogue was less bactericidal than DHCA, as 1 mg/ml (the MBC of DHCA; Figure 18A) completely inhibited *Pst* growth but was not lethal (Figure 18B).

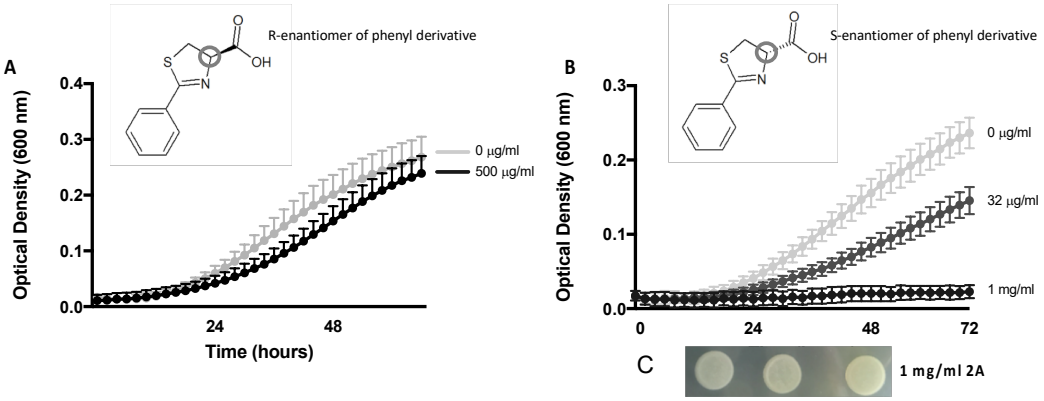

Figure 18. R- and S-enantiomers of phenylalanine-derived dihydrothiazole carboxylic acids have different bioactivity against growth of *Pst*. Dose-dependent effect of R-enantiomer (A) and S-enantiomer (B) on *Pst* growth in Hrp-inducing minimal media as measured by turbidity (OD_{600}) after incubation 68 to 72 hours at room temperature (24 to 26 °C). Each data point is the mean ± SD of three wells per concentration from a 96-well non-tissue-culture-treated plate. (C) To test for bactericidal activity, wells with cultures displaying little to no growth after 72 hours were spun down and the bacterial pellet was resuspended in 10 mM $MgCl_2$ and plated on non-selective KB media.

Camalexin structurally differs from DHCA in that it lacks a carboxylic acid functional group on carbon 4 of the thiazole ring. The antimicrobial activity of DHCA is similar to

that reported for camalexin incubated with *P. syringae* pv. *maculicola* in rich media or in camalexin-spiked IWFs (MIC of ~ 500µg/ml; Rogers et al. 1996) and as shown in this work when camalexin was incubated with *Pst* in HIM media (MIC ~500 µg/ml; Figure 19). Although both DHCA and camalexin have an MIC of ~500 µg/ml, camalexin showed more potent growth inhibitory effects against *Pst* at 250 µg/ml compared to DHCA (Figure 16A). Both camalexin and DHCA are natural products produced by *Arabidopsis* in response to *P. syringae*, however camalexin was not detected in IWFs regardless of genotype and treatment (Table S2).

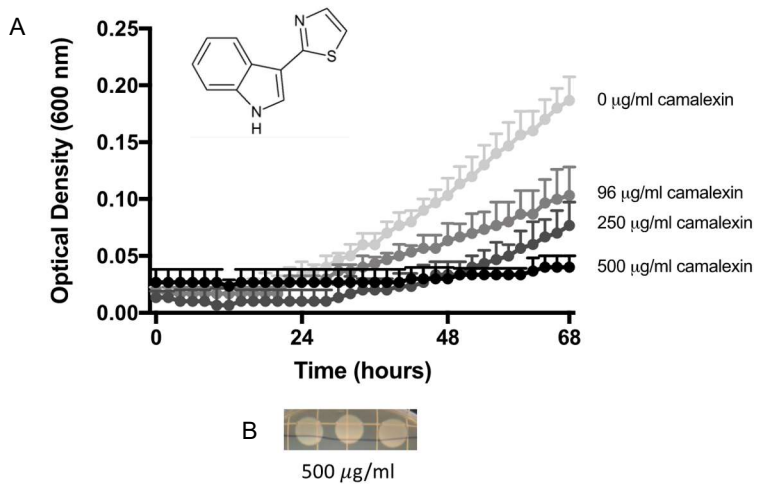

Figure 19. Growth of *Pst* DC3000 in the presence of camalexin. (A) Dose-dependent effect of camalexin on *Pst* growth in Hrp-inducing minimal media as measured by turbidity (OD_{600}) after incubation with shaking for 68 hours at room temperature (24 to 26 °C). Each data point is the mean ± SD of three wells per concentration from a 96-well non-tissue-culture-treated plate. (B) To test for bactericidal activity, wells with cultures displaying little to no growth after 68 hours were spun down and the bacterial pellet was resuspended in 10 mM $MgCl_2$ and plated on non-selective KB media.

There was a complete loss of growth inhibitory activity for the *R*- and *S*- enantiomers of the phenol-derived DHCA analogues (Figure 20) and the *R*-enantiomer of the phenyl-derived DHCA analogue (Figure 18A). At 500 µg/ml *Pst* growth matched that of controls incubated without compounds. These results indicate that the indolic ring contributes to

inhibition of *Pst* growth, and replacement with a phenol moiety causes a loss of antimicrobial activity regardless of stereochemistry. Interestingly, with the phenyl-derived analogue of DHCA, stereochemistry had a marked effect on antimicrobial activity, as the *S*-enantiomer inhibited *Pst* growth (Figure 18B) but the *R*-enantiomer lacked antimicrobial activity (as measured by growth) against *Pst* (Figure 18A).

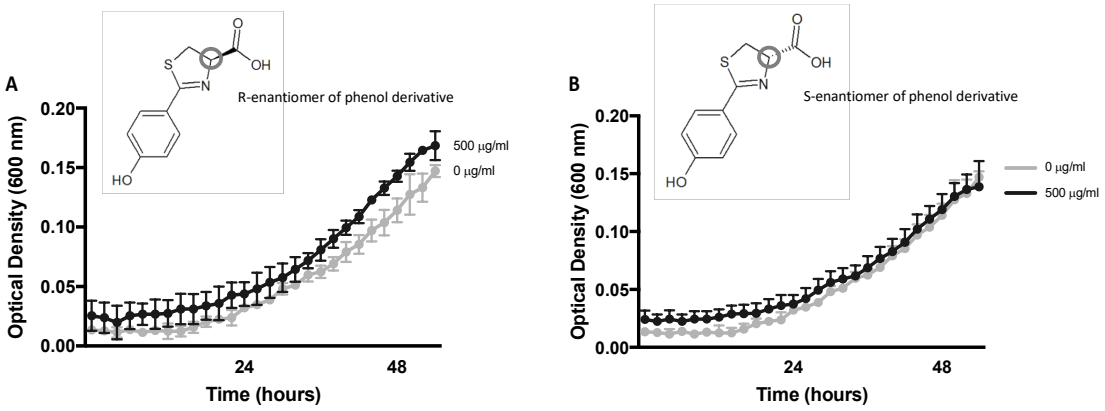

Figure 20. R- and S-enantiomers of phenol (tyrosine)-derived dihydrothiazole carboxylic acids have no effect on growth of *Pst*. Dose-dependent effect of R-enantiomer (A) and S-enantiomer (B) on *Pst* growth in Hrp-inducing minimal media as measured by turbidity (OD_{600}) after incubation 52 hours at room temperature (24 to 26 °C). Each data point is the mean ± SD of three wells per concentration from a 96-well non-tissue-culture-treated plate.

3.6.5 Antibiofilm activity of DHCA against *P. syringae in vitro*?

Biofilms are composed of adherent bacterial cells embedded in a matrix of polysaccharides, DNA, and proteins that provides a protective environment for microbes along surfaces. The formation of biofilm involves bacterial response to environmental cues and bacteria in biofilms have different metabolic and gene expression profiles compared to free-swimming planktonic bacteria (De Kievit et al., 1999; Masák et al., 2014). Biofilm-like aggregation has been reported for *P. syringae* pv. *actinidiae* and pv. *phaseolicola* in the intercellular space of kiwifruit and beans (Ghods et al., 2015; Manoharan et al., 2015) and for *Pst* in the intercellular space of *Arabidopsis* leaves using

GFP-expressing bacteria (Wilson et al., 2017). Wilson et al. (2017) also showed that SA inhibited biofilm formation of *Pst in vitro* at concentrations as low as 2 uM (~270 ng/ml), which is within the range of SA detected in IWFs of ARR-competent plants responding to *Pst* (Cameron and Zaton, 2004; Carviel et al., 2009). DHCA does not inhibit *Pst* growth *in vitro*, therefore it may instead act to inhibit biofilm-like aggregation of *Pst* during ARR. To test for the ability of DHCA to interfere with biofilm formation, a spectrophotometric 96-well plate biofilm assay was used (see Materials and Methods; O'Toole G., 2011). Concentrations of DHCA that do not reduce bacterial growth were chosen (18 μg/ml to 300 ng/ml) based on the results of *Pst* growth inhibition assays and the amount quantified in IWFs (Figure 11, 16A) to ensure that these tests would reflect reduced biofilm formation rather than inhibition of growth. These assays do not support the hypothesis that DHCA inhibits biofilm-like aggregates of *Pst* in mature ARR-competent plants. SA inhibited biofilm formation starting at 48 hours (Figure 21B); however, DHCA had no significant effect on biofilm formation at any concentrations or time points tested (Figure 21A). Similar results were observed in another experiment (Figure S9). Overall, these results suggest that DHCA does not inhibit biofilm formation of *Pst in vitro*.

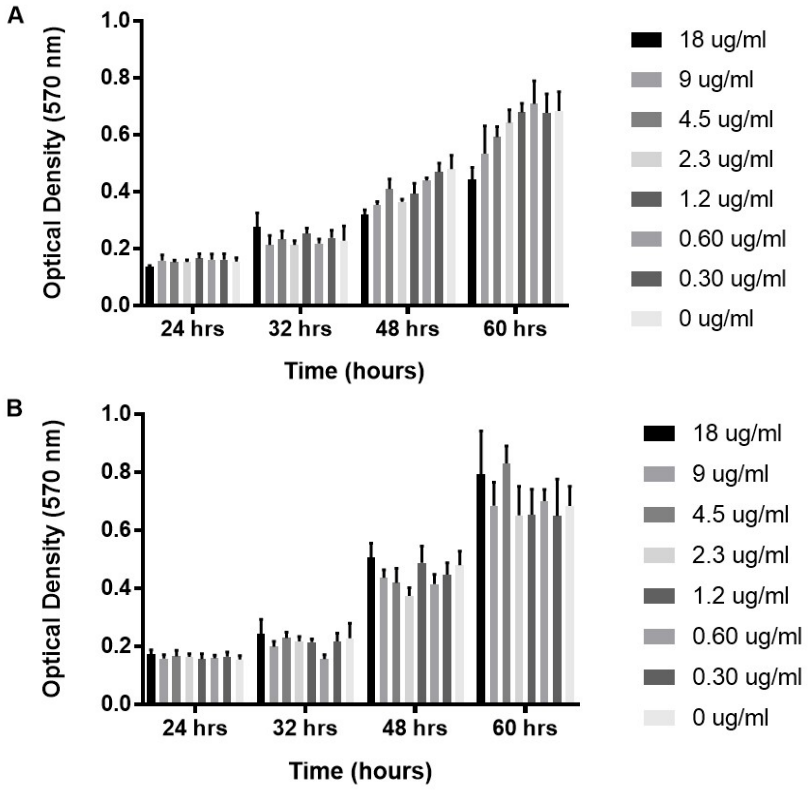

Figure 21. DHCA does not inhibit biofilm formation of *Pst in vitro.* Dose-dependent effect of (A) SA and (B) DHCA on *Pst* biofilm formation *in vitro* in HIM media as measured by crystal violet staining of surface-adherent cells and destaining in acetic acid (OD_{570}) after incubation on stationary bench for 24 to 60 hours at room temperature (~26 °C). Each data point is the mean ± SD of five wells per concentration from a 96-well non-tissue-culture-treated plate.

3.6.6 Assaying additive or synergistic interactions between DHCA and SA in inhibit growth of *P. syringae*

SA is required for ARR and has antimicrobial activity against *Pst*, however, the SA biosynthesis mutant *sid2-2* occasionally displays a residual ARR-like response (Figure S3). The combined effect of several compounds with mechanisms of action that are similar or complementary may enhance antimicrobial activity, resulting in additive or synergistic activity (Lewis and Ausubel, 2006; Bednarek P., 2012). It was hypothesized that the ARR-like response observed in *sid2-2* may be due to the activity of other

intercellular antimicrobial compounds during ARR. In this work, metabolomics studies revealed a potential role for intercellular DHCA in ARR, as it does not accumulate in IWFs of ARR-defective *cyp71a12/cyp71a13-1*. DHCA alone did not exhibit strong growth inhibitory activity against *Pst* (> 500 µg/ml MIC) and accumulated at 200 – 400 ng/ml in IWFs from ARR-competent wild-type plants. However, if DHCA is involved in synergistic or additive interactions with SA, then *in vitro* studies of DHCA alone do not capture this activity. To test for synergistic or additive effects of DHCA and SA against *Pst*, a 96-well plate *in vitro* assay was used with each well containing a different concentration of DHCA and SA ranging from 32 µg/ml to 1 µg/ml (1:1 combined) along with DHCA or SA alone at the same concentrations to assess synergistic, additive, or antagonistic activity for inhibition of *Pst* growth (Doern C., 2014).

SA enhanced the antimicrobial activity of DHCA, but not more than SA alone at the same concentration (32 µg/ml) (Figure 22). At 16 µg/ml of SA or DHCA alone compared to in combination, there was similar growth inhibitory activity against *Pst*. Overall, at 32 µg/ml DHCA and SA may have additive effects against growth of *Pst,* but synergistic activity was not observed.

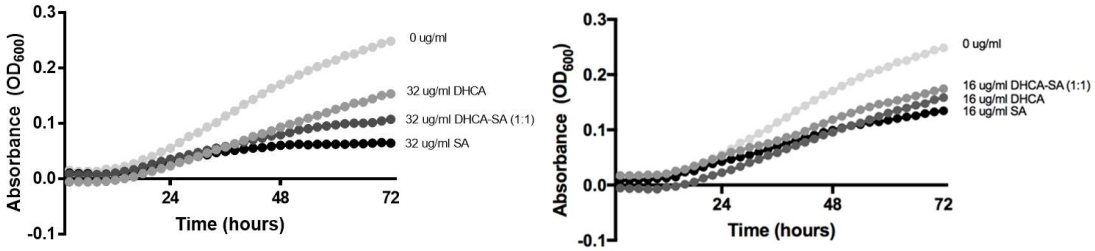

Figure 22. DHCA and SA do not display synergistic antimicrobial activity against growth of *Pst*. Tested DHCA and SA individually and in combination to inhibit *Pst* growth in Hrp-inducing minimal media as measured by turbidity (OD_{600}) after incubation 72 hours at room temperature (24 to 26 °C). Each data point is the mean ± SD of three wells per concentration from a 96-well non-tissue-culture-treated plate.

3.6.7 Exogenous application of DHCA restored ARR to *cyp71a12/cyp71a13-1*

Results from ARR assays (bacterial quantification *in planta*) and metabolomics demonstrated that *cyp71a12/cyp71a13-1* was partially ARR-defective and was defective for accumulation of intercellular DHCA. If DHCA contributes to ARR, then the addition of DHCA to the intercellular space of *cyp71a12/cyp71a13-1* is expected to enhance resistance in this mutant potentially restoring ARR.

DHCA (70 ng/ml) was pressure-infiltrated into the intercellular space of rosette leaves of mature plants (7 wpg) 24 hpi with *Pst*. The concentration of 70 ng/ml was used based on limited availability of synthetic DHCA and the levels that accumulated in mature wild-type ARR-competent plants (Figure 11, 14). In one experiment exogenous infiltration of DHCA enhanced the ARR response in *cyp71a12/cyp71a13-1* from 7-fold (mock) to 12-fold (exogenous DHCA) (Figure 23B). In another experiment, a 2-fold reduction in mature *cyp71a12/a13-1* bacterial density (compared to young) was restored to wild-type levels (21-fold compared to young) after exogenous DHCA application.

Interestingly, DHCA infiltration 4 hpi with *Pst* abolished ARR responses in both wild type and *cyp71a12/cyp71a13-1*, causing both genotypes to become more susceptible to *Pst*. Wild-type plants had a 10-fold ARR response, but with DHCA infiltration at 4 hpi ARR was fully negated and the bacterial levels supported by mature plants increased to 1.3-fold higher than young plants (Figure S10). Similarly, *cyp71a12/cyp71a13-1* had a small but significant reduction in bacterial density when mature (2-fold) but a full ARR-defect was observed after DHCA infiltration at 4hpi.

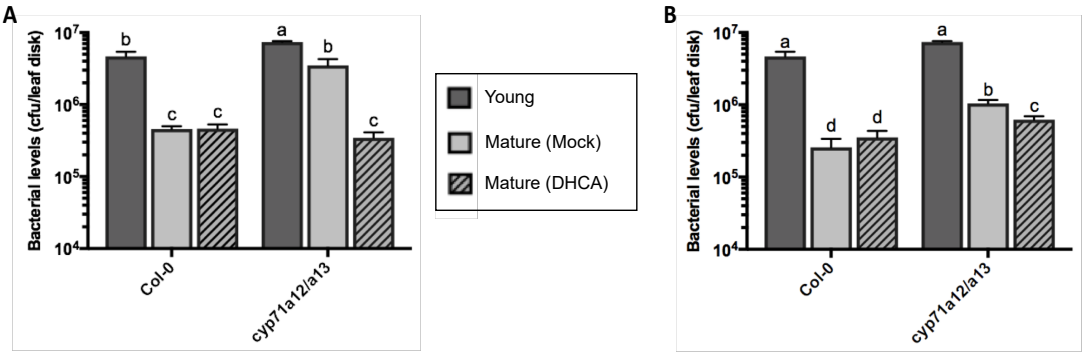

Figure 23. Exogenous application of DHCA enhances resistance in mature ARR-defective *cyp71a12/cyp71a13-1*. Exogenous application of DHCA was applied to Col-0 and *cyp71a12/cyp71a13-1* by pressure infiltration of 70 ng/ml DHCA at 24 hpi with virulent *Pst* or mock treatment (0.06% DMSO in 10 mM $MgCl_2$). Bacterial density was quantified at 3 days post-inoculation in young (3 wpg) and mature (7 wpg) plants for all treatments. Values represent the mean +/- standard deviation of three sample replicates. Different letters indicate statistically significant differences (ANOVA, Tukey's honestly significant difference [HSD], $P < 0.05$).

CHAPTER 4 – DISCUSSION, CONCLUSION AND FUTURE DIRECTIONS

4.1 *CYP71A12* and *CYP71A13* contribute to ARR in *Arabidopsis*

CYP71A13 was initially hypothesized to be involved in ARR because it was upregulated in mature wild-type plants at 12 hpi with *Pst* in comparison to mock-inoculated plants (Carviel et al., 2009). CYP71A12 is 89% identical to CYP71A13 at the amino acid level and can functionally compensate for the loss of *CYP71A13* (Klein et al., 2013; Müller et al., 2015). Functional compensation of CYP71A13 activity by CYP71A12 was demonstrated using *in vitro* and heterologous pathway reconstitution and indolic metabolite profiling of mutants with UPLC-MS (Nafisi et al., 2007; Böttcher et al., 2009; Klein et al., 2013; Müller et al., 2015). *CYP71A12* was upregulated in the Carviel et al. (2009) study in mature *Pst*-inoculated plants; however, at 12 hpi it was not significantly upregulated compared to mock-inoculated plants. The *cyp71a12* and *cyp71a13-1* single mutants were observed to be fully ARR-defective in one out of three experiments and partially ARR-competent in one out of three experiments, while the *cyp71a12/cyp71a13-1* mutant was consistently partially ARR-defective (12 of 12 experiments), providing support that both enzymes contribute to ARR. The ARR response of *cyp71a12/a13-1* is considered partial because these plants were more susceptible to *Pst* when mature compared to wild type, but a significant reduction in bacterial levels was observed in mature *cyp71a12/cyp71a13-1* compared to young plants of the same genotype.

The involvement of *CYP71A12* and *CYP71A13* in camalexin biosynthesis has been well studied (Nafisi et al., 2007; Böttcher et al., 2009; Klein et al., 2013; Møldrup 2013b; Müller et al., 2015; Rajniak et al., 2015). The camalexin pathway begins with CYP79B2

and CYP79B3 which produce IAOx, followed by CYP71A12 and CYP71A13-mediated conversion of IAOx to IAN (Zhao et al., 2002; Nafisi et al., 2007). IAN is then conjugated to glutathione (GSH(IAN)) and catabolized to a cysteine conjugated form (Cys(IAN)). CYP71B15 catalyzes formation of both DHCA and camalexin from Cys(IAN) through two sequential reaction steps. Mutants for these cytochrome P450 (*cyp79b2/b3, cyp71a12/cyp71a13-1, cyp71b15*) all produce trace amounts of camalexin (Zhou et al., 1999; Böttcher et al., 2009; Müller et al., 2015) yet they differ in their ARR phenotypes. As expected, the *cyp79b2/cyp79b3* mutant displayed a similar partial ARR-defective phenotype as *cyp71a12/a13-1*, which supports the hypothesis of a CYP71A12 and CYP71A13 derived compound being involved in ARR, since *cyp79b2/cyp79b3* does not produce the IAOx substrate for *cyp71a12/cyp71a13-1* (Zhao et al., 2002).

Results from this work support a previous study (Kus et al., 2002) suggesting that camalexin is not required for ARR, since *cyp71b15* (*pad3-1*) does not produce camalexin (Zhou et al., 1999) but has a wild-type ARR phenotype. Rajniak et al. (2015) reported that *cyp71b15* (*pad3-1*) exhibited enhanced susceptibility to *Pst* at 4 to 5 wpg compared to wild-type plants. The contrast in results likely stems from differences in inoculation and bacterial quantification methods used by different research groups. Rajniak et al. (2015) spray-inoculated (10^6 CFU/cm^2 leaf area) leaves, which were detached and incubated in 0.8% agar plates for four days prior to extracting bacteria from whole leaves using steel beads. All assays in this work were completed using pressure infiltration (10^6 CFU/ml) of bacteria directly into the intercellular space of attached leaves followed three days later by *in planta* bacterial quantification.

The ARR phenotypes of *cyp79b2/cyp79b3*, *cyp71a12/cyp71a13-1*, and *cyp71b15* suggest a role in ARR for intermediates and enzymes involved downstream of CYP71A12 and CYP71A13 enzyme activity but upstream of CYP71B15-mediated camalexin production. This part of the camalexin pathway is not fully elucidated largely due to functional redundancy in enzyme families and *in vitro* substrate promiscuity of the enzymes hypothesized to produce these intermediates (Geu-Flores et al., 2011; Su et al., 2011; Møldrup et al., 2013a,b; Figure 1).

Another cytochrome P450 homolog, CYP71A18, is 87% identical to CYP71A12 and shares 85% identity with CYP71A13 (at the amino acid level) (Müller et al., 2015). *CYP71A18* expression is weakly induced in response to *Botrytis cinerea, Pst,* and *Phytophtora infestans* (Müller et al., 2015; Rajniak et al. 2015; http://bar.utoronto.ca/efp_arabidopsis/cgi-bin/efpWeb.cgi); however, functional characterization of this enzyme has not been performed. The *CYP71A18* gene was not upregulated in the ARR microarray performed by Carviel et al. (2009), and the *cyp71a18* mutant is not deficient for production of indole-3-carboxylic acid and indole-3-carbonyl nitrile derivatives downstream of CYP71A12 and CYP71A13 activity, so it is not likely to be significantly contributing to DHCA biosynthesis. Importantly, the *cyp71a12/cyp71a13-1* mutant does not produce detectable levels of DHCA, so it is unlikely that CYP71A18 is contributing to biosynthesis of this compound. The *cyp71a12/cyp71a13-1* mutant produces wild-type levels of SA in IWFs when mature, so the partial ARR-defect in this mutant may be due to wild-type accumulation of intercellular SA that inhibits bacterial growth.

4.2 DHCA accumulation in IWFs of *Arabidopsis* during ARR

As previously mentioned, CYP71A12 and CYP71A13 form a metabolic branch point producing IAN that serves as a substrate for camalexin biosynthesis and for other indolic pathway enzymes. Intercellular washing fluids were collected for non-targeted high-resolution metabolite profiling of the intercellular space. These IWF samples are representative of the intercellular space and were used to identify which compounds differentially accumulated in ARR-defective (*cyp71a12/cyp71a13-1*) compared to ARR-competent plants (Col-0 and *cyp71b15*). The *cyp71b15* mutant was included as it is defective for camalexin biosynthesis downstream of CYP71A12 and CYP71A13 but is ARR-competent. Since indolic metabolism is disrupted in *cyp71a12/cyp71a13-1,* non-targeted metabolic datasets from *cyp71b15* were helpful to elucidate compounds important for ARR rather than focusing on differentially accumulating compounds that are changing due to blocks in indolic biosynthesis. DHCA was identified as accumulating in IWFs collected from plants during ARR (wild-type and *cyp71b15)* but was not observed in the *cyp71a12/cyp71a13-1* ARR-defective mutant. The accumulation pattern of DHCA during ARR suggests that it may be a candidate phytoalexin since it was not present in IWFs from mock-inoculated plants. It's absence in IWFs collected from *cyp71a12/cyp71a13-1* inoculated with *Pst* also suggests that DHCA in IWFs is not of bacterial origin. DHCA accumulated to ~ 300 ng/ml and ~2400 ng/ml in IWFs from ARR responding wild-type and *cyp71b15* plants, respectively). DHCA accumulates in *cyp71b15* whole leaves (~5-fold greater DHCA in *cyp71b15* than wild type) after $AgNO_3$ treatment or inoculation with fungal pathogens (Bednarek et al., 2005; Böttcher et al.,

2009). Böttcher et al. (2009) hypothesized that the block in camalexin biosynthesis in *cyp71b15* results in accumulation of Cys(IAN), which is converted to DHCA through non-enzymatic thiazole ring closure. DHCA originates from IAN, so loss of *CYP71A12* and *CYP71A13* is expected to perturb DHCA biosynthesis. DHCA does not readily degrade to other products (Böttcher et al., 2009), so in the absence of CYP71B15 in a localized area like the intercellular space, it could accumulate without being converted to camalexin (camalexin was not detected in IWFs from these experiments; Table S2). CYP71A12, CYP71A13, and CYP71B15 are associated with the endoplasmic reticulum, with their catalytic domains facing out towards the cytosol. DHCA may be directly transported to the intercellular space, but for this to happen, release of DHCA from CYP71B15 would have to occur during the sequential conversion of Cys(IAN) to DHCA and then to camalexin (Shuhegger et al., 2006; Figure 24C). It is also possible that Glu(IAN), Cys(IAN), or intermediates formed during catabolism of Glu(IAN) to Cys(IAN) are transported to the intercellular space where they could be converted to DHCA (Figure 24B). Peaks corresponding to IAN and IAN conjugates were not detected in IWFs in these experiments, but these compounds may have been converted to DHCA before IWF samples were collected at 24 hpi. Moreover, if Glu(IAN) is transported to the intercellular space, it may be converted to Cys(IAN) by GGT activity, as some GGTs are localized to the apoplast, followed by non-enzymatic cyclization to DHCA (Figure 24A). In camalexin biosynthesis, γ-glutamyl peptidase 1 (GGP1) and 3 (GGP3) are generally accepted to be the enzymes involved in catabolism of Glu(IAN) to Cys(IAN), but Su et al. (2011) reported that γ-glutamyl transpeptidase 1 (GGT1) and 2 (GGT2) are the

enzymes responsible for catabolism of Glu(IAN) to Cys(IAN). Møldrup et al. (2013) disagreed with the Su et al. (2011) findings because a GGT enzyme inhibitor that may also inhibit GGP activity was used. Moldrup et al (2013) also pointed out that GGTs localize to the apoplast while the Glu(IAN) substrate is present in the cytosol. Despite these shortcomings the work of Su et al (2011) provides evidence that GGTs could contribute to the formation of Cys(IAN), and as apoplastic proteins they may be catabolizing IAN conjugates to Cys(IAN) in the intercellular space during ARR (Figure 24A). Finally, canonical camalexin pathway-independent precursors may be involved in intercellular DHCA biosynthesis. Bednarek et al. (2005) reported that constitutive accumulation of raphanusamic acid in roots may contribute to camalexin biosynthesis via alternative pathways (e.g., raphanusamic conjugation to indolic compound) but later work showed IAN was the intermediate in camalexin biosynthesis. It is possible that intermediates and enzymes not part of canonical DHCA biosynthesis in the cell contribute to the accumulation of DHCA biosynthesis in the intercellular space during ARR.

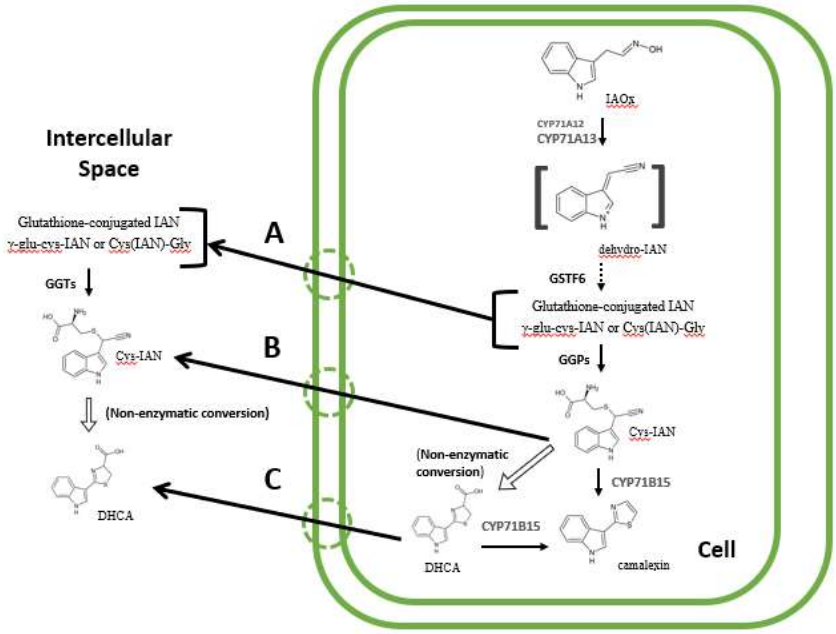

Figure 24. Proposed model of intercellular DHCA accumulation during ARR. Outlined arrows indicate potential non-enzymatic reactions. Solid arrows indicate biosynthetic steps. Dashed arrows indicate multiple reaction steps/simplified for presentation. Green circles with solid arrows indicate transport out of the cell to the intercellular space. Solid arrows indicate enzymatic conversion.IAOx: indole-3-acetaldoxime, IAN: indole-3-acetonitrile, GGP: gamma-glutamyl peptidase, GGT: gamma-glutamyl transpeptidase DHCA: dihydroxamalexic acid

4.3 Intercellular DHCA accumulation in young plants

In two experiments profiling the metabolome of IWFs collected from young and mature wild-type plants, a modest ARR response was observed in two experiments with a 12- and 15-fold reduction in *Pst* levels in mature compared to young plants. A modest increase of DHCA in IWFs of mature plants was observed (1.7-fold statistically significant and 1.5-fold not statistically significant). SA was quantified in IWFs from young and mature plants as a metabolic indicator of a successful ARR response. SA levels were similar in IWFs collected from young and mature plants responding to *Pst*, which contrasts with data from previous work. Cameron and Zaton (2004) showed SA is significantly lower in young *Pst*-inoculated IWFs compared to mature *Pst*-inoculated

IWFs. Mock-inoculated control IWFs contained the expected basal levels of DHCA and SA suggesting that a resistance response was not unintentionally induced prior to *Pst*-inoculation or that the mock solution used was not contaminated with *Pst*. Since the ARR response was not as robust as in other experiments (≥ 50-fold difference), we speculate that high SA levels observed in young IWFs may be due to unintentional exposure of these plants to volatiles from resistance-inducing compounds used in other Cameron lab studies over the course of this work, resulting in enhanced resistance to *Pst* in young plants and accounting for the < 20-fold ARR response observed in both experiments. Therefore, we cannot definitively report that DHCA is lower in young plants using these data since levels quantified here may reflect prior defense priming.

4.4 Exogenous DHCA restores ARR in mature *cyp71a12/cyp71a13-1*

The absence of DHCA in IWFs from *cyp71a12/cyp71a13-1* could have been due to a blockage in the camalexin pathway and not contribute to the ARR-defect in this mutant. *In vitro* assays demonstrated that DHCA displayed weak inhibition of *Pst* growth and did not inhibit biofilm activity against *Pst*. However, *in vitro* studies do not fully replicate the complex metabolic and physiological changes occurring in plants during the ARR response to *Pst* (Bednarek and Osbourn, 2009). Exogenous application of DHCA 24 hpi with *Pst* restored ARR in mature *cyp71a12/cyp71a13-1*, indicating DHCA is involved in ARR. The concentration of 70 ng/ml DHCA for infiltration was chosen to allow several replicates of these experiments to be performed. However, this concentration is lower than the levels observed in IWFs collected from wild-type ARR-competent plants (200-300 ng/ml), therefore full restoration of ARR was not expected to occur in all

experiments. Application of 70 ng/ml DHCA was sufficient to fully restore ARR in *cyp71a12/cyp71a13-1* in one experiment and partially restore ARR in a second experiment.

Unexpectedly, exogenous application of DHCA to the intercellular space at 4 hpi with *Pst* resulted in enhanced susceptibility in mature *cyp71a12/cyp71a13-1* and abolished ARR in wild-type plants. These results may indicate DHCA interacts with another mechanism during ARR that isn't present at 4 hpi or exogenous application of DHCA interferes with host-pathogen interactions in mature plants to enhance susceptibility when infiltrated at 4 hpi. Expression of *CYP71A12*, *CYP71A13*, and *CYP71B15* is induced at ~ 9 hpi with *P. syringae* (Nafisi et al., 2007), so DHCA may not yet be produced and accumulating in the intercellular space at 4 hpi during ARR; therefore, exogenous application at this time point may have negatively affected other defense mechanisms.

4.5 Potential mechanisms of DHCA bioactivity during ARR

4.5.1 Synergistic and additive effects of SA and DHCA

The combined action of two or more antimicrobials can have a greater inhibitory effect on growth or virulence, therefore testing antimicrobial compounds in isolation may not reveal the actual antimicrobial contribution of a compound (Lewis and Ausubel, 2006; Bednarek and Osbourn, 2009). This may explain why DHCA was observed to minimally inhibit *Pst* growth *in vitro*. Moreover, exogenous infiltration of DHCA restored ARR in *cyp71a12/cyp71a13-1*. Taken together, these data suggest that there may be synergistic or additive effects between DHCA and other metabolites accumulating in the intercellular

space of mature plants. Accumulation of intercellular SA and DHCA during ARR may have synergistic or additive antimicrobial activity against *Pst*. However, *in vitro* assays did not reveal synergistic activity between SA and DHCA in term of *Pst* growth inhibition. At higher concentrations, DHCA was less effective at inhibiting *Pst* growth, but more effective if mixed with SA in a 1:1 ratio, yet not as effective as SA alone at the same concentration. Taken together, these data suggest that there may be a weak additive effect between DHCA and SA. This led to the hypothesis that SA and DHCA may interact to inhibit biofilm-like aggregation of *Pst* in *Arabidopsis* during ARR; however, DHCA did not inhibit biofilm formation of *Pst in vitro*.

To test the hypothesis that *CYP71A12* and *CYP71A13* contribute to the small but significant ARR-like response sometimes observed in *sid2* mutants, and that indolic metabolite and SA pathways may have additive effects in plants, *cyp71a12/cyp71a13-1* was crossed with *sid2-2* to produce a triple mutant. Since *sid2-2* was fully ARR-defective in all experiments, it was not possible to evaluate the impact of mutations in *CYP71A12, CYP71A13,* and *ICS1* on the ARR-like response of *sid2*. The ARR-like response in *sid2* was significant but small and not consistently observed. It is possible this response is a result of experimental variation between bacterial levels supported by plants in different assays. Volatile compounds used in neighbouring growth chambers at the time of these experiments may have induced a priming response making it impossible to observe an ARR-like response in *sid2-2.* Additional ARR assays with the triple mutant are needed to determine if SA and DHCA have additive effects during ARR.

4.5.2 Weak antimicrobial activity of DHCA

In vitro assays indicated that DHCA exhibits weak antimicrobial activity with an MIC similar to camalexin (~500 µg/ml; Rogers et al., 1996; this work). *In vitro* studies demonstrated that camalexin rapidly disrupts membrane integrity in *P. syringae* and due to its lipophilic nature, it doesn't dissociate from dying cells such that any surviving bacterial cells continue to grow (Rogers et al., 1996). DHCA has a similar structure to camalexin and may have a similar mode of action. To examine this further, the lipophilic nature of DHCA was compared to camalexin and SA by estimating molecular physical properties such as Log*P* and Log*D*. Log*P* values estimate the solubility of a compound in two immiscible solvents by the partition coefficient of its neutral form (i.e., differential solubility in an organic or aqueous phase). Log*D* (distribution coefficient) factors in pH-dependent changes in solubility. Camalexin has a predicted Log*D* of 2.97 at pH 5.5 while DHCA's predicted Log*D* is -0.67 at pH 5.5. The lipophilicity of DHCA is closer to that of SA (predicted Log*D* of -0.56 at pH 5.5). These values show how the carboxylic acid group of DHCA contributes to the less lipophilic nature of DHCA relative to camalexin. To examine further how structural components of DHCA may affect its antimicrobial activity, enantiomers of phenylalanine and tyrosine derived analogues of DHCA were used in structure-activity relationship studies. These assays examined how the indole ring contributds to growth inhibition against *Pst*. Calculated log*P* values (c Log*P*) are theoretical calculations based on molecular structure that can be used to predict lipophilicity of neutral compounds. The synthetic phenyl and phenol analogues of DHCA have a c Log*P* of 0.91 ± 0.69 and 0.17 ± 0.98 respectively. The c Log*P* for DHCA is 0.84

± 0.98 and camalexin has a c Log*P* of 3.16 ± 0.79. Since DHCA is less lipophilic than camalexin and contains a carboxylic acid functional group, it is less likely to be permanently associated with bacterial membranes; however, lipophilicity estimates do not necessarily correlate with molecular behaviour (e.g., lipophilicity doesn't predict membrane permeability). Both enantiomers of the phenol analogue of DHCA were not observed to inhibit *Pst* growth at the concentrations tested. Interestingly, the *S*-enantiomer of the phenyl DHCA analogue inhibited *Pst* growth but not the *R*-enantiomer. An *R*-enantiomer of DHCA was unavailable for testing, but if it exhibited an inability to inhibit *Pst* growth, this would suggest that stereochemistry is a factor in DHCA bioactivity.

4.5.3 Inhibition of *Pst* virulence gene expression or enzymes during ARR

Anti-virulence compounds can affect bacterial pathogenicity without affecting growth. Targeting virulence factors instead of affecting growth can be advantageous because it is less likely to result in selection for resistance; antigrowth compounds can result in selection pressure for resistant strains that are minimally unaffected, whereas antivirulence compounds reduce pathogenicity of bacteria with fewer affects on bacterial survival (Lee et al., 2011; Totsika M., 2016). It is possible that DHCA or other indolic compounds act as anti-virulence compounds during ARR. This idea is supported by studies that demonstrate that indolic compounds exhibit anti-virulence activity. For example, IAN has been shown to inhibit several anti-virulence activities including biofilm formation, expression of virulence genes for iron acquisition, detoxification enzymes, and motility in human pathogenic E. coli O157:H7 and *P. aeruginosa* (Lee et al., 2011) ICHO

was shown to inhibit biofilm formation of these pathogens as well (Lee et al., 2011). *In vitro* studies with camalexin demonstrated that mycelial growth of *A. brassicicola* and glycolysis and TCA pathway gene expression was inhibited in the presence of camalexin (Pedras et al., 2014). Camalexin has also been shown to inhibit fungal detoxification enzymes involved in detoxification of brassinin and cyclobrassinin produced by canola and brown mustard (examined in fungal isolates) (Pedras et al., 2017). DHCA may interfere with *Pst* virulence genes or proteins during ARR. If this is the case, this may explain why the DHCA concentration that restores ARR in *cyp71a12/cyp71a13-1,* does not inhibit bacterial growth *in vitro*. *In vitro Pst* biofilm formation was not affected by DHCA. Therefore, DHCA may be affecting *Ps*t pathogenicity via other mechanisms (e.g., by inhibiting enzyme activity).

4.5.4 DHCA and other defense mechanisms

Receptors involved in defense may be differentially regulated during plant development, resulting in different disease outcomes for young and mature plants. Developmentally regulated PR proteins are thought to contribute to ARR against fungal pathogens in tomato (Panter et al., 2002), rice (Cao et al., 2007; Zhao et al., 2009), and cucumber (Mansfield et al., 2017). In *Arabidopsis*, *npr1* mutants display ARR despite lower expression of *PR-1*, *PR-2*, and *PR-5* compared to wild-type plants (Cao eta al., 1994) and mature plants have lower *PR* gene expression compared to young plants, suggesting *PR* gene expression is not involved in *Arabidopsis* ARR (Kus et al., 2002). Nonetheless, DHCA may interact with other receptors or proteins not yet known for their role in ARR

to directly or indirectly affect plant-pathogen interactions in mature plants. One could speculate that if intercellular DHCA levels do not differ between young and mature plants, it is because DHCA interacts with proteins or other compounds that are expressed or present in mature plants. In this scenario, young plants remain susceptible to *Pst* despite accumulating intercellular DHCA. Results from exogenous rescue assays with DHCA may support a role for DHCA in interacting with other defense mechanisms in plants or against bacteria, since DHCA infiltration wasn't sufficient for restoration of ARR at 4 hpi but was sufficient for ARR restoration at 24 hpi.

4.5 Non-targeted metabolomics of IWFs during ARR

Non-targeted metabolomics identified indolic and sinapic acid derivatives as differentially accumulating in IWFs collected from ARR-defective (*cyp71a12/cyp71a13-1*) and ARR-competent (Col-0 or *cyp71b15*). As mentioned earlier, it is important to consider that all identifications (except for DHCA) are putative since they have not been confirmed with an authentic reference standard. Identification of a sinapic acid derivative (compound B) and an indole-3-carboxylic acid derivative (compound D) were made based on product ions in mass spectral data but the associated parent ion could not be identified, so the identity of the parent molecule is unknown, only putative components of its structure are known, therefore the compound may be something completely different with a similar mass. For instance, SA has a monoisotopic mass of 138.0317 and elemental composition of $C_7H_6O_3$. There are 138 entries in a publicly available chemical database with elemental composition of $C_7H_6O_3$, each with a different structure. If a mass feature is

detected for an *m/z* corresponding to SA, any molecule with an elemental composition within 5 ppm is a potential candidate. Candidate molecule lists can be reduced using mass fragmentation to predict structures and by considering biological and biosynthetic context (i.e., the structure is a possibility as a natural product in plants or bacteria and could be produced via biosynthetic pathways in the organism(s) profiled). Occasionally non-targeted datasets have mass spectral features that are challenging to identify. Compound E in this work is an unknown compound that accumulates to a significantly higher degree in IWFs from *Pst*-inoculated *cyp71a12/cyp71a13-1* compared to wild-type and *cyp71b15* IWFs. The mass spectrum for this unknown compound lacks associated fragment ions, making it difficult to predict its structural components. Molecular formulae calculated using exact mass (m/z 732.3930) within 5 ppm returned 27 potential elemental compositions without matches in natural products databases or literature searches. The difference in normalized abundance of this unknown compound between IWFs collected from *Pst*-inoculated wild type and *cyp71a12/cyp71a13-1* is relatively small (1.8-fold). It is possible this compound is a contaminant (e.g., from plastics or Parafilm used in the IWF collection process) or contains elements (e.g., Br, Cl, formate) not considered in molecular formula calculations for adducts or as natural products from *Arabidopsis* and *Pst*. Importantly, the differentially accumulating compounds (other than DHCA) identified in this work may not have a role in ARR; blocks in biosynthesis of indolic compounds in mutant lines may change metabolic flux without an affect on the ARR response.

4.6.1 Indolic and sinapic acid pathways in ARR

Cross-talk between indolic and phenylpropanoid biosynthesis pathways has previously been reported in *Arabidopsis*. Alterations in IAOx and downstream indolic metabolite levels have been shown to have a negative regulatory effect on early phenylpropanoid bioynthesis (Hagemeier et al., 2000; Tan et al., 2004; Kim et al., 2015). Sinapic acid (3,5-dimethoxy-4-hydroxycinnamic acid) can be esterified to sugars and is a precursor in lignin biosynthesis (Lim et al., 2001). The sinapic acid ester 1-*O*-sinapoyl-beta-D-glucose (compound C) is one of the main sinapic acid derivatives in Brassicaceae (Nićiforović and Abramovič et al., 2014) and was putatively identified in IWFs. It was low in all mock-inoculated samples, and lower in *cyp71a12/cyp71a13-1* compared to Col-0 and *cyp71b15*, but the difference was not significant in these experiments, probably due to large variation in normalized abundance in wild-type IWFs. Nevertheless, it is possible that sinapic acid derivatives contribute to ARR based on *in vitro* studies demonstrating that free sinapic acid has antimicrobial activity against *E. coli, Enterobacter aerogens, Salmonella enteritidis,* and *Pseudomonas flurescens* with MICs of 200 to 600 μg/ml (Nowak et al., 1992; Barber et al., 2000; Tesaki et al., 1998; Engels et al., 2012). IWFs from ARR-defective *cyp71a12/cyp71a13-1*differentially accumulated two putative phenylpropanoid compounds and two indolic compounds in comparison to IWFs from ARR-competent plants in response to *Pst* (Col-0 and *cyp71b15*). A putative phenypropanoid that may be related to sinapic acid (compound B) was significantly higher in *cyp71a12/cyp71a13-1* IWFs compared to wild-type IWFs. Since this compound is higher in ARR-competent *cyp71b15* and in ARR-incompetent *cyp71a13/cyp71a13-1*

compared to wild-type IWFs, this compound is probably not required for a successful ARR response.

Changes in sinapic acid derivatives in *cyp71a12/cyp71a13-1* may be caused by blocks in indolic metabolite pathways without producing an effect on ARR, but it may be worth testing the ARR response of mutants in the sinapic acid pathway. Hagemeier et al. (2000) investigated the accumulation of ICOOH and sinapic acid derivatives in resistance to *Pst*. They tested resistance to *Pst* in a mutant for *ferulic acid 5-hydroxylase 1* (*F5H1*, also known as *CYP84A1).* This mutant does not produce sinapoyl malate and other sinapic acid derivatives (Figure 25). The *f5h1-7* mutant displayed a wild-type response to *Pst* and was not defective for other indolic compounds at 5 to 6 wpg, but this study was not examining ARR.

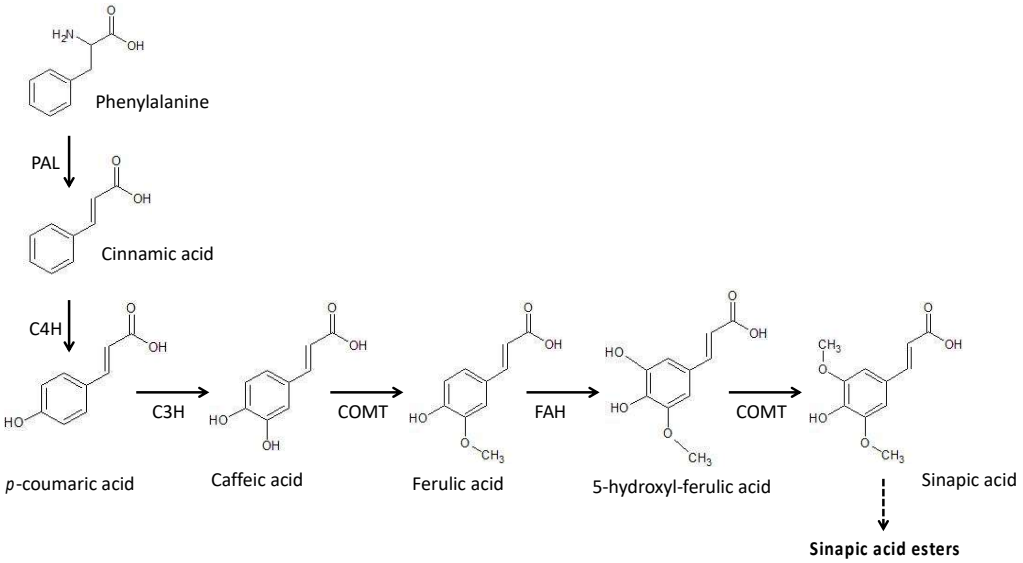

Figure 25. Sinapic acid biosynthesis pathway. Simplified version of sinapic acid biosynthesis. Modified from Humphreys et al. (1999). PAL: phenylalanine ammonia lyase; C4H: cinnamate-4-hydroxylase; C3H: coumarate-3-hydroxylase; COMT: caffeic acid-*O*-methyl transferase; FAH: ferulate-5-hydroxylase.

Compound D has a fragment ion with an exact mass matching the molecular formula for a glucose ester of ICOOH (mass error -3 ppm), but the parent ion couldn't be identified based on fragmentation patterns (see Figure S7D). It is possible that this is an ICOOH derivative that associated with the cell wall and was solubilized during the IWF collection process or it is a glycoside conjugate of ICOOH. It may be involved in ARR as it was elevated in IWFs from ARR-competent plants (Col-0 and *cyp71b15*) compared to IWFs from mock-inoculated ARR-defective *cyp71a12/cyp71a13-1* plants. ICOOH and ICHO have been linked to plant defense as these compounds accumulated after pathogen challenge in cruciferous vegetables (Hagemeier et al., 2001; Bednarek et al., 2005; Iven et al., 2012). ICOOH was esterified to the cell wall in *Arabidopsis* in response to *P. syringae* and has been hypothesized to prevent bacterial aggregation along the cell wall or act as an antimicrobial compound by intercalating into the bacterial membrane (Forcat et al., 2010; Soylu et al., 2005). Assaying the contribution of ICOOH and ICHO pathways in ARR is challenging due to redundancy in these biosynthetic pathways, the complexity of downstream derivatives (e.g., glycosylated and amino acid conjugates, indole-ring hydroxylations), and the fact that the genes involved in producing these compounds are not fully known (Böttcher et al., 2014; Tan et al., 2004). The role of ICOOH derivatives produced from *CYP71A12* and *CYP71A13* was examined using T-DNA insertion mutants in *CYP71B6* and *AAO1*. Results from this work show loss of *CYP71B6* or *AAO1* was not sufficient to disrupt ARR. Although both *cyp71b6* and *aao1* displayed wild-type ARR responses, they also still produced ICOOH and ICHO derivatives (Böttcher et al 2014). Cell wall preparations of *CYP71B6* and *AAO1* T-DNA insertion and overexpression lines

displayed no significant changes in cell wall esterified ICOOH compared to wild type and this may explain why these lines are ARR-competent. Based on metabolic profiling done by Böttcher et al. (2014) *cyp71b6* is defective in producing ICOOGlc and 6-GlcO-ICOOH and *aao1* is defective for 6-GlcO-ICOOGlc after AgNO3 treatment. This may rule out ICOOGlc, 6-GlcO-ICOOH, and 6-GlcO-ICOOGlc as contributing to ARR. Compound D may be related to ICOOH and was higher in IWFs from ARR-competent plants, but it may also be a degradation product of compounds derived from indole carbonylnitrile products. These ICN compounds are unstable and rapidly degrade to ICOOH during extraction in aqueous solutions like IWFs (Rajniak et al., 2015; see Figure 1), therefore it is possible that the ICN pathway contributes to the ARR response.

4.7 Future Directions

ARR assays: The contribution of *CYP71A18* to ARR could be examined by obtaining a *cyp71a18* mutant from TAIR and creating a triple mutant (*cyp71a12/cyp71a13-1/cyp71a18*) and its ARR phenotype compared to *cyp71a12/cyp71a13-1.* If it is involved, it may exhibit a more extreme ARR-defect than the double mutant. To assess the role of GGTs, GGP1, and GGP3 in ARR, mutants could be obtained and the ARR phenotype examined. Double or quadruple mutants may need to be created because GGPs and GGTs exhibit substrate promiscuity and redundancy (Møldrup et al., 2013). Metabolomics results from this work suggest sinapic acid derivatives are differentially accumulating in *cyp71a12/cyp71a13-1*, so an *f5h1* mutant and mutants for other genes in sinapic acid biosynthesis could be tested for ARR-defects. To assess the role of the ICN pathway in

ARR (and given that compound D could be an ICN degradation product), the ARR phenotypes of *cyp82c2* and *fox1* (see Figure 1) could be examined. Two T-DNA insertion lines for *fox1* and *cyp82c2* have already been obtained from TAIR. T-DNA homozygosity should be confirmed before testing the contribution of this pathway to ARR. Additional ARR assays with *cyp71a12/cyp71a13-1/sid2-2* should be performed to test the hypothesis that *CYP71A12* and *CYP71A13* contribute to the ARR-like response in *sid2-2*. If mutants for ICOOH cell wall esterification genes could be identified, these would be ideal candidates for additional ARR studies.

Metabolite-profiling: Understanding how DHCA accumulates in the intercellular space or the fate of exogenously added DHCA may shed light on DHCA's role in ARR. Exogenous DHCA experiments to measure intercellular and intracellular DHCA and camalexin (since *CYP71B15* expression in cells may convert DHCA to camalexin) may clarify the effects of exogenous DHCA application and tell us how ARR is restored after exogenous DHCA application.

Examining the effect of DHCA on *Pst* virulence gene expression and metabolites may provide evidence that DHCA has anti-virulence activity that is important for ARR. Non-targeted metabolite profiling is a powerful approach for testing and generating new hypotheses, but polar metabolites, lipids, or proteins may be contributing to ARR and will not be detected with chromatography methods used to profile semi polar compounds in this work. Polar metabolites change in IWFs in response to *P. syringae* may be involved in ARR. O'Leary et al. (2016) reported widespread changes to polar metabolites like GABA, citrate, and β-L-cyanoalanine in IWFs collected from virulent and avirulent *Psp*-

inoculated bean (*Phaseolus vulgaris*) leaves. This work examined changes to specialized metabolites in intercellular space-enriched IWFs; future 'omics' experiments could examine metabolic changes in whole leaf tissue to capture changes in the cell and intercellular space during ARR.

Antimicrobial mechanisms: To form hypotheses about the antimicrobial mechanisms of DHCA, UPLC-MS analyses of bacterial pellets and media supernatant during growth assays of DHCA and analogues could be examined to test where DHCA accumulates (associated with bacterial cells vs remains soluble in media). Results obtained from these types of experiments may provide ideas about the mechanism of DHCA antimicrobial activity by revealing both where these compounds are associating and if they are being metabolized to other forms by *Pst*.

Synergy testing: Future work could include replicating *in vitro* synergy assays using higher concentrations of DHCA and SA to better test for weak additive effects. The fractional inhibitory concentration index (FIC) is used in pharmacodynamics to quantify positive and negative interactions between drugs and antibiotics in combination therapy (Hall et al., 1983; Meletiadis et al., 2010). Compounds are tested at concentrations spanning their MIC and in different ratios using a 96-well plate checkerboard method (Balouri et al., 2016). The MICs of compounds incubated together vs individually are assessed based on bioactivity (e.g. growth inhibition, reduction in biofilm formation) and a number between 0.5 and 4 is mathematically generated. These numbers correspond to antagonistic, indifferent, additive, or synergistic effects. Given the limited availability of DHCA and its high MIC for *Pst* growth inhibition ($\geq$ 500 μg/ml), concentrations of

DHCA and SA that are above the range of biologically relevant concentrations would need to be used to confirm weak additive effects *in vitr*, therefore these assays were not completed in this work.

DHCA mode of action during ARR: More replicates of DHCA rescue assays are required to confirm that DHCA abolishes ARR at 4 hpi with *Pst*, since it was only tested once in this work. A transcriptomics study of young vs mature wild-type plants (mock- and *Pst*-inoculated) paired with ARR metabolomics data from this work would be valuable to elucidate genes involved in ARR and reveal putative interactions with specialized metabolism.

4.8 Conclusion

My work suggests a novel role for DHCA in ARR against bacterial pathogens and serves as a reminder of the importance of knowing about the localization of key metabolites in defense. Taken together, the data in this thesis provides compelling evidence that *CYP71A12* and *CYP71A13* contribute to ARR via DHCA accumulation in intercellular space. Exogenous infiltration of DHCA into the intercellular space restored ARR in *cyp71a12/cyp71a13-1* at 24 hpi. DHCA did not exhibit antibiofilm activity *in vitro* and DHCA was shown to be weakly antimicrobial against *Pst* growth *in vitro*, suggesting the mechanism for DHCA during ARR is not through direct antimicrobial activity. DHCA has not been previously studied in ARR and accumulation of DHCA in IWFs is a novel finding. Moreover, finding DHCA in the IWFs suggests that transportation of DHCA or precursors to the intercellular space is important for ARR. DHCA and camalexin are not

common to all Brassicaceae species so reconstitution of DHCA and camalexin biosynthesis in other cruciferous vegetables and crop systems may offer protection against fungal and bacterial pathogens. Overall, research into the mechanisms of ARR is an important but often overlooked component of plant disease outcomes. Understanding how mature plants become resistant to pathogens they were susceptible to when younger could allow us to fine-tune broad-spectrum resistance to protect agricultural crops and protect young, susceptible plants from pathogens.

REFERENCES

Abedon, B.G. and Tracy, W.F., 1996. Corngrass 1 of Maize (Zea mays L.) delays development of adult plant resistance to common rust (Puccinia sorghi Schw.) and European corn borer (Ostrinia nubilalis Hubner). *Journal of heredity*, *87*(3), pp.219-223.

Agerbirk, N., De Vos, M., Kim, J.H. and Jander, G., 2009. Indole glucosinolate breakdown and its biological effects. *Phytochemistry Reviews*, *8*(1), p.101.

Agrawal, G.K., Jwa, N.S., Lebrun, M.H., Job, D. and Rakwal, R., 2010. Plant secretome: unlocking secrets of the secreted proteins. *Proteomics*, *10*(4), pp.799-827.

Ahuja, I., Kissen, R. and Bones, A.M., 2012. Phytoalexins in defense against pathogens. *Trends in plant science*, *17*(2), pp.73-90.

Albrecht, T., & Argueso, C. T., 2016. Should I fight or should I grow now? The role of cytokinins in plant growth and immunity and in the growth–defense trade-off. *Annals of botany*, *119*(5), 725-735.

Alonso-Blanco, C. and Koornneef, M., 2000. Naturally occurring variation in Arabidopsis: an underexploited resource for plant genetics. *Trends in plant science*, *5*(1), pp.22-29.

Ando, K., Hammar, S. and Grumet, R., 2009. Age-related resistance of diverse cucurbit fruit to infection by Phytophthora capsici. *Journal of the American Society for Horticultural Science*, *134*(2), pp.176-182.

Andréasson, E., Jørgensen, L.B., Höglund, A.S., Rask, L. and Meijer, J., 2001. Different myrosinase and idioblast distribution in Arabidopsis and Brassica napus. *Plant Physiology*, *127*(4), pp.1750-1763.

Arabidopsis Genome Initiative, 2000. Analysis of the genome sequence of the flowering plant Arabidopsis thaliana. *nature*, *408*(6814), p.796.

Argueso, C.T., Ferreira, F.J., Epple, P., To, J.P., Hutchison, C.E., Schaller, G.E., Dangl, J.L. and Kieber, J.J., 2012. Two-component elements mediate interactions between cytokinin and salicylic acid in plant immunity. *PLoS genetics*, *8*(1), p.e1002448.

Asalf, B., Gadoury, D.M., Tronsmo, A.M., Seem, R.C., Dobson, A., Peres, N.A. and Stensvand, A., 2014. Ontogenic resistance of leaves and fruit, and how leaf folding influences the distribution of powdery mildew on strawberry plants colonized by Podosphaera aphanis. *Phytopathology*, *104*(9), pp.954-963.

Asalf, B., Gadoury, D.M., Tronsmo, A.M., Seem, R.C. and Stensvand, A., 2016. Effects of development of ontogenic resistance in strawberry leaves upon pre-and postgermination growth and sporulation of Podosphaera aphanis. *Plant Disease*, *100*(1), pp.72-78.

Aslam, S.N., Newman, M.A., Erbs, G., Morrissey, K.L., Chinchilla, D., Boller, T., Jensen, T.T., De Castro, C., Ierano, T., Molinaro, A. and Jackson, R.W., 2008. Bacterial polysaccharides suppress induced innate immunity by calcium chelation. *Current Biology*, *18*(14), pp.1078-1083.

Aslam, S.N., Erbs, G., Morrissey, K.L., Newman, M.A., Chinchilla, D., Boller, T., Molinaro, A., Jackson, R.W. and Cooper, R.M., 2009. Microbe-associated molecular pattern (MAMP) signatures, synergy, size and charge: influences on perception or mobility and host defense responses. *Molecular plant pathology*, *10*(3), pp.375-387.

Bak, S., Tax, F.E., Feldmann, K.A., Galbraith, D.W. and Feyereisen, R., 2001. CYP83B1, a cytochrome P450 at the metabolic branch point in auxin and indole glucosinolate biosynthesis in Arabidopsis. *The Plant Cell*, *13*(1), pp.101-111.

Balouiri, M., Sadiki, M. and Ibnsouda, S.K., 2016. Methods for in vitro evaluating antimicrobial activity: A review. *Journal of Pharmaceutical Analysis*, *6*(2), pp.71-79.

Barber, M.S., McConnell, V.S. and DeCaux, B.S., 2000. Antimicrobial intermediates of the general phenylpropanoid and lignin specific pathways. *Phytochemistry*, *54*(1), pp.53-56.

Bednarek, P., Schneider, B., Svatoš, A., Oldham, N.J. and Hahlbrock, K., 2005. Structural complexity, differential response to infection, and tissue specificity of indolic and phenylpropanoid secondary metabolism in Arabidopsis roots. *Plant Physiology*, *138*(2), pp.1058-1070.

Bednarek, P. and Osbourn, A., 2009. Plant-microbe interactions: chemical diversity in plant defense. *Science*, *324*(5928), pp.746-748.

Bednarek, P., Piślewska-Bednarek, M., Ver Loren van Themaat, E., Maddula, R.K., Svatoš, A. and Schulze-Lefert, P., 2011. Conservation and clade-specific diversification of pathogen-inducible tryptophan and indole glucosinolate metabolism in Arabidopsis thaliana relatives. *New Phytologist*, *192*(3), pp.713-726.

Bednarek, P., 2012. Chemical warfare or modulators of defense responses–the function of secondary metabolites in plant immunity. *Current opinion in plant biology*, *15*(4), pp.407-414.

Beets, C.A., Huang, J.C., Madala, N.E. and Dubery, I., 2012. Activation of camalexin biosynthesis in Arabidopsis thaliana in response to perception of bacterial lipopolysaccharides: a gene-to-metabolite study. *Planta*, *236*(1), pp.261-272.

Bi, G. and Zhou, J.M., 2017. MAP kinase signaling pathways: a hub of plant-microbe interactions. *Cell host & microbe*, *21*(3), pp.270-273.

Birkenbihl, R.P., Liu, S. and Somssich, I.E., 2017. Transcriptional events defining plant immune responses. *Current opinion in plant biology*, *38*, pp.1-9.

Boller, T. and He, S.Y., 2009. Innate immunity in plants: an arms race between pattern recognition receptors in plants and effectors in microbial pathogens. *Science*, *324*(5928), pp.742-744.

Böttcher, C., Westphal, L., Schmotz, C., Prade, E., Scheel, D. and Glawischnig, E., 2009. The multifunctional enzyme CYP71B15 (PHYTOALEXIN DEFICIENT3) converts cysteine-indole-3-acetonitrile to camalexin in the indole-3-acetonitrile metabolic network of Arabidopsis thaliana. *The Plant Cell*, *21*(6), pp.1830-1845.

Boureau, T., Routtu, J., Roine, E., Taira, S. and Romantschuk, M., 2002. Localization of hrpA-induced Pseudomonas syringae pv. tomato DC3000 in infected tomato leaves. *Molecular Plant Pathology*, *3*(6), pp.451-460.

Bowling, S.A., Guo, A., Cao, H., Gordon, A.S., Klessig, D.F. and Dong, X., 1994. A mutation in Arabidopsis that leads to constitutive expression of systemic acquired resistance. *The Plant Cell*, *6*(12), pp.1845-1857.

Bowling, S.A., Clarke, J.D., Liu, Y., Klessig, D.F. and Dong, X., 1997. The cpr5 mutant of Arabidopsis expresses both NPR1-dependent and NPR1-independent resistance. *The plant cell*, *9*(9), pp.1573-1584.

Buell, C.R., Joardar, V., Lindeberg, M., Selengut, J., Paulsen, I.T., Gwinn, M.L., Dodson, R.J., Deboy, R.T., Durkin, A.S., Kolonay, J.F. and Madupu, R., 2003. The complete genome sequence of the Arabidopsis and tomato pathogen Pseudomonas syringae pv. tomato DC3000. *Proceedings of the National Academy of Sciences*, *100*(18), pp.10181-10186.

Büttner, D. and He, S.Y., 2009. Type III protein secretion in plant pathogenic bacteria. *Plant physiology*, *150*(4), pp.1656-1664.

Cameron, R.K., Dixon, R.A. and Lamb, C.J., 1994. Biologically induced systemic acquired resistance in Arabidopsis thaliana. *The Plant Journal*, *5*(5), pp.715-725.

Cameron, R.K. and Zaton, K., 2004. Intercellular salicylic acid accumulation is important for age-related resistance in Arabidopsis to Pseudomonas syringae. *Physiological and molecular plant pathology*, *65*(4), pp.197-209.

Cao, H., Bowling, S.A., Gordon, A.S. and Dong, X., 1994. Characterization of an Arabidopsis mutant that is nonresponsive to inducers of systemic acquired resistance. *The Plant Cell*, *6*(11), pp.1583-1592.

Cao, Y., Ding, X., Cai, M., Zhao, J., Lin, Y., Li, X., Xu, C. and Wang, S., 2007. The expression pattern of a rice disease resistance gene Xa3/Xa26 is differentially regulated by the genetic backgrounds and developmental stages that influence its function. *Genetics*, *177*(1), pp.523-533.

Carella, P., Wilson, D.C. and Cameron, R.K., 2015. Some things get better with age: differences in salicylic acid accumulation and defense signaling in young and mature Arabidopsis. *Frontiers in plant science*, *5*, p.775.

Carella, P., Kempthorne, C.J., Wilson, D.C., Isaacs, M. and Cameron, R.K., 2017. Exploring the role of DIR1, DIR1-like and other lipid transfer proteins during systemic immunity in Arabidopsis. *Physiological and molecular plant pathology*, *97*, pp.49-57.

Carisse, O. and Bouchard, J., 2010. Age-related susceptibility of strawberry leaves and berries to infection by Podosphaera aphanis. *Crop Protection*, *29*(9), pp.969-978.

Carviel, J.L., AL-DAOUD, F.A.D.I., Neumann, M., Mohammad, A., Provart, N.J., Moeder, W., Yoshioka, K. and Cameron, R.K., 2009. Forward and reverse genetics to identify genes involved in the age-related resistance response in Arabidopsis thaliana. *Molecular plant pathology*, *10*(5), pp.621-634.

Carviel, J.L., Wilson, D.C., Isaacs, M., Carella, P., Catana, V., Golding, B., Weretilnyk, E.A. and Cameron, R.K., 2014. Investigation of intercellular salicylic acid accumulation during compatible and incompatible Arabidopsis-Pseudomonas syringae interactions using a fast neutron-generated mutant allele of EDS5 identified by genetic mapping and whole-genome sequencing. *PloS one*, *9*(3), p.e88608.

Chandra, S. and Low, P.S., 1997. Measurement of Ca2+ fluxes during elicitation of the oxidative burst in aequorin-transformed tobacco cells. *Journal of Biological Chemistry*, *272*(45), pp.28274-28280.

Chang, W.S., van de Mortel, M., Nielsen, L., de Guzman, G.N., Li, X. and Halverson, L.J., 2007. Alginate production by Pseudomonas putida creates a hydrated microenvironment and contributes to biofilm architecture and stress tolerance under water-limiting conditions. *Journal of bacteriology*, *189*(22), pp.8290-8299.

Cheng, W., Munkvold, K.R., Gao, H., Mathieu, J., Schwizer, S., Wang, S., Yan, Y.B., Wang, J., Martin, G.B. and Chai, J., 2011. Structural analysis of Pseudomonas syringae AvrPtoB bound to host BAK1 reveals two similar kinase-interacting domains in a type III effector. *Cell host & microbe*, *10*(6), pp.616-626.

Choi, H.W. and Klessig, D.F., 2016. DAMPs, MAMPs, and NAMPs in plant innate immunity. *BMC plant biology*, *16*(1), p.232.

Clay, N.K., Adio, A.M., Denoux, C., Jander, G. and Ausubel, F.M., 2009. Glucosinolate metabolites required for an Arabidopsis innate immune response. *Science*, *323*(5910), pp.95-101.

Clauss, M.J., Dietel, S., Schubert, G. and Mitchell-Olds, T., 2006. Glucosinolate and trichome defenses in a natural Arabidopsis lyrata population. *Journal of chemical ecology*, *32*(11), pp.2351-2373.

Chen, Z., Silva, H. and Klessig, D.F., 1993. Active oxygen species in the induction of plant systemic acquired resistance by salicylic acid. *Science*, *262*(5141), pp.1883-1886.

Coelho, P., Bahcevandziev, K., Valerio, L., Monteiro, A., Leckie, D., Astley, D., Crute, I.R. and Boukema, I., 1997, September. The relationship between cotyledon and adult plant resistance to downy mildew (Peronospora parasitica) in Brassica oleracea. In *International Symposium Brassica 97, Xth Crucifer Genetics Workshop 459* (pp. 335-342).

Cramer, G.R. and Jones, R.L., 1996. Osmotic stress and abscisic acid reduce cytosolic calcium activities in roots of Arabidopsis thaliana. *Plant, Cell & Environment*, *19*(11), pp.1291-1298.

Dannel, F., Pfeffer, H. and Marschner, H., 1995. Isolation of apoplasmic fluid from sunflower leaves and its use for studies on influence of nitrogen supply on apoplasmic pH. *Journal of Plant Physiology*, *146*(3), pp.273-278.

Darvill, A.G. and Albersheim, P., 1984. Phytoalexins and their elicitors-a defense against microbial infection in plants. *Annual Review of Plant Physiology*, *35*(1), pp.243-275.

De Kievit, T.R. and Iglewski, B.H., 1999. [8] Quorum sensing, gene expression, and Pseudomonas biofilms. In *Methods in enzymology* (Vol. 310, pp. 117-128). Academic Press.

Delaney, T.P., Uknes, S., Vernooij, B., Friedrich, L., Weymann, K., Negrotto, D., Gaffney, T., Gut-Rella, M., Kessmann, H., Ward, E. and Ryals, J., 1994. A central role of salicylic acid in plant disease resistance. *Science*, *266*(5188), pp.1247-1250.

Delaunois, B., Jeandet, P., Clément, C., Baillieul, F., Dorey, S. and Cordelier, S., 2014. Uncovering plant-pathogen crosstalk through apoplastic proteomic studies. *Frontiers in plant science*, *5*, p.249.

Dempsey, D.M.A., Vlot, A.C., Wildermuth, M.C. and Klessig, D.F., 2011. Salicylic acid biosynthesis and metabolism. *The Arabidopsis Book*, p.e0156.

Denoux, C., Galletti, R., Mammarella, N., Gopalan, S., Werck, D., De Lorenzo, G., Ferrari, S., Ausubel, F.M. and Dewdney, J., 2008. Activation of defense response pathways by OGs and Flg22 elicitors in Arabidopsis seedlings. *Molecular plant*, *1*(3), pp.423-445.

Develey-Rivière, M.P. and Galiana, E., 2007. Resistance to pathogens and host developmental stage: a multifaceted relationship within the plant kingdom. *New Phytologist*, *175*(3), pp.405-416.

Dewdney, J., Reuber, T.L., Wildermuth, M.C., Devoto, A., Cui, J., Stutius, L.M., Drummond, E.P. and Ausubel, F.M., 2000. Three unique mutants of Arabidopsis identify eds loci required for limiting growth of a biotrophic fungal pathogen. *The Plant Journal*, *24*(2), pp.205-218.

Dixon, R.A., 2001. Natural products and plant disease resistance. *Nature*, *411*(6839), p.843.

Dodds, P.N. and Rathjen, J.P., 2010. Plant immunity: towards an integrated view of plant–pathogen interactions. *Nature Reviews Genetics*, *11*(8), p.539.

Doern, C.D., 2014. When does 2 plus 2 equal 5? A review of antimicrobial synergy testing. *Journal of clinical microbiology*, *52*(12), pp.4124-4128.

Engels, C., Schieber, A. and Gänzle, M.G., 2012. Sinapic acid derivatives in defatted Oriental mustard (Brassica juncea L.) seed meal extracts using UHPLC-DAD-ESI-MSn and identification of compounds with antibacterial activity. *European Food Research and Technology*, *234*(3), pp.535-542.

Farinhó, M., Coelho, P., Carlier, J., Svetleva, D., Monteiro, A. and Leitao, J., 2004. Mapping of a locus for adult plant resistance to downy mildew in broccoli (Brassica oleracea convar. italica). *Theoretical and applied genetics*, *109*(7), pp.1392-1398.

Felle, H.H., 1998. The apoplastic pH of the Zea mays root cortex as measured with pH-sensitive microelectrodes: aspects of regulation. *Journal of Experimental Botany*, *49*(323), pp.987-995.

Felle, H.H., Herrmann, A., Hückelhoven, R. and Kogel, K.H., 2005. Root-to-shoot signalling: apoplastic alkalinization, a general stress response and defense factor in barley (Hordeum vulgare). *Protoplasma*, *227*(1), pp.17-24.

Felle, H.H., 2006. Apoplastic pH during low-oxygen stress in barley. *Annals of botany*, *98*(5), pp.1085-1093.

Fett, W.F. and Dunn, M.F., 1989. Exopolysaccharides produced by phytopathogenic Pseudomonas syringae pathovars in infected leaves of susceptible hosts. *Plant physiology*, *89*(1), pp.5-9.

Fiehn, O., Robertson, D., Griffin, J., van der Werf, M., Nikolau, B., Morrison, N., Sumner, L.W., Goodacre, R., Hardy, N.W., Taylor, C. and Fostel, J., 2007. The metabolomics standards initiative (MSI). *Metabolomics*, *3*(3), pp.175-178.

Fiehn, O., Wohlgemuth, G., Scholz, M., Kind, T., Lee, D.Y., Lu, Y., Moon, S. and Nikolau, B., 2008. Quality control for plant metabolomics: reporting MSI-compliant studies. *The Plant Journal*, *53*(4), pp.691-704.

Forcat, S., Bennett, M., Grant, M. and Mansfield, J.W., 2010. Rapid linkage of indole carboxylic acid to the plant cell wall identified as a component of basal defense in Arabidopsis against hrp mutant bacteria. *Phytochemistry*, *71*(8-9), pp.870-876.

Fragnière, C., Serrano, M., Abou-Mansour, E., Métraux, J.P. and L'haridon, F., 2011. Salicylic acid and its location in response to biotic and abiotic stress. *FEBS letters*, *585*(12), pp.1847-1852.

Francl, L.J., 2001. The disease triangle: a plant pathological paradigm revisited. *Plant Health Instructor DOI*, *10*.

Franceschi, V.R. and Nakata, P.A., 2005. Calcium oxalate in plants: formation and function. *Annu. Rev. Plant Biol.*, *56*, pp.41-71.

Frerigmann, H., Glawischnig, E. and Gigolashvili, T., 2015. The role of MYB34, MYB51 and MYB122 in the regulation of camalexin biosynthesis in Arabidopsis thaliana. *Frontiers in plant science*, *6*, p.654.

Gadoury, D.M., Seem, R.C., Ficke, A. and Wilcox, W.F., 2003. Ontogenic resistance to powdery mildew in grape berries. *Phytopathology*, *93*(5), pp.547-555.

Geu-Flores, F., Møldrup, M.E., Böttcher, C., Olsen, C.E., Scheel, D. and Halkier, B.A., 2011. Cytosolic γ-glutamyl peptidases process glutathione conjugates in the biosynthesis of glucosinolates and camalexin in Arabidopsis. *The Plant Cell*, *23*(6), pp.2456-2469.

Ghanmi, D., McNally, D.J., Benhamou, N., Menzies, J.G. and Bélanger, R.R., 2004. Powdery mildew of Arabidopsis thaliana: a pathosystem for exploring the role of silicon in plant–microbe interactions. *Physiological and Molecular Plant Pathology*, *64*(4), pp.189-199.
Ghods, S., Sims, I.M., Moradali, M.F. and Rehm, B.H., 2015. Plant pathogen Pseudomonas syringae pv. actinidiae forms biofilms composed of a novel exopolysaccharide: Growth control by bactericidal compounds. *Applied and Environmental Microbiology*, pp.AEM-00194.

Glawischnig, E., Hansen, B.G., Olsen, C.E. and Halkier, B.A., 2004. Camalexin is synthesized from indole-3-acetaldoxime, a key branching point between primary and secondary metabolism in Arabidopsis. *Proceedings of the National Academy of Sciences of the United States of America*, *101*(21), pp.8245-8250.

Glazebrook, J. and Ausubel, F.M., 1994. Isolation of phytoalexin-deficient mutants of Arabidopsis thaliana and characterization of their interactions with bacterial pathogens. *Proceedings of the National Academy of Sciences*, *91*(19), pp.8955-8959.

Glazebrook, J., Chen, W., Estes, B., Chang, H.S., Nawrath, C., Métraux, J.P., Zhu, T. and Katagiri, F., 2003. Topology of the network integrating salicylate and jasmonate signal transduction derived from global expression phenotyping. *The Plant Journal*, *34*(2), pp.217-228.

Glazebrook, J., 2005. Contrasting mechanisms of defense against biotrophic and necrotrophic pathogens. *Annu. Rev. Phytopathol.*, *43*, pp.205-227.

Gómez-Gómez, L. and Boller, T., 2000. FLS2: an LRR receptor–like kinase involved in the perception of the bacterial elicitor flagellin in Arabidopsis. *Molecular cell*, *5*(6), pp.1003-1011.

Gust, A.A., Biswas, R., Lenz, H.D., Rauhut, T., Ranf, S., Kemmerling, B., Götz, F., Glawischnig, E., Lee, J., Felix, G. and Nürnberger, T., 2007. Bacteria-derived peptidoglycans constitute pathogen-associated molecular patterns triggering innate immunity in Arabidopsis. *Journal of Biological Chemistry*, *282*(44), pp.32338-32348.

Gutknecht, J. and Tosteson, D.C., 1973. Diffusion of weak acids across lipid bilayer membranes: effects of chemical reactions in the unstirred layers. *Science*, *182*(4118), pp.1258-1261.

Häffner, E., Konietzki, S. and Diederichsen, E., 2015. Keeping control: The role of senescence and development in plant pathogenesis and defense. *Plants*, *4*(3), pp.449-488.

Hagemeier, J., Schneider, B., Oldham, N.J. and Hahlbrock, K., 2001. Accumulation of soluble and wall-bound indolic metabolites in Arabidopsis thaliana leaves infected with virulent or avirulent Pseudomonas syringae pathovar tomato strains. *Proceedings of the National Academy of Sciences*, *98*(2), pp.753-758.

Hall, M.J., Middleton, R.F. and Westmacott, D., 1983. The fractional inhibitory concentration (FIC) index as a measure of synergy. *Journal of Antimicrobial Chemotherapy*, *11*(5), pp.427-433.

Hansen, C.H., Du, L., Naur, P., Olsen, C.E., Axelsen, K.B., Hick, A.J., Pickett, J.A. and Halkier, B.A., 2001. CYP83B1 is the oxime-metabolizing enzyme in the glucosinolate pathway in Arabidopsis. *Journal of Biological Chemistry*, *276*(27), pp.24790-24796.

Hatzfeld, Y., Maruyama, A., Schmidt, A., Noji, M., Ishizawa, K. and Saito, K., 2000. β-Cyanoalanine synthase is a mitochondrial cysteine synthase-like protein in spinach and Arabidopsis. *Plant Physiology*, *123*(3), pp.1163-1172.

Hatsugai, N., Igarashi, D., Mase, K., Lu, Y., Tsuda, Y., Chakravarthy, S., Wei, H.L., Foley, J.W., Collmer, A., Glazebrook, J. and Katagiri, F., 2017. A plant effector-triggered immunity signaling sector is inhibited by pattern-triggered immunity. *The EMBO Journal*, *36*(18), pp.2758-2769.

Heil, M. and Baldwin, I.T., 2002. Fitness costs of induced resistance: emerging experimental support for a slippery concept. *Trends in plant science*, *7*(2), pp.61-67.

Hématy, K., Cherk, C. and Somerville, S., 2009. Host–pathogen warfare at the plant cell wall. *Current opinion in plant biology*, *12*(4), pp.406-413.

Hirano, S.S. and Upper, C.D., 2000. Bacteria in the Leaf Ecosystem with Emphasis on Pseudomonas syringae—a Pathogen, Ice Nucleus, and Epiphyte. *Microbiology and molecular biology reviews*, *64*(3), pp.624-653.

Hoffman, L.E., Wilcox, W.F., Gadoury, D.M. and Seem, R.C., 2002. Influence of grape berry age on susceptibility to Guignardia bidwellii and its incubation period length. *Phytopathology*, *92*(10), pp.1068-1076.

Hugot, K., Aimé, S., Conrod, S., Poupet, A. and Galiana, E., 1999. Developmental regulated mechanisms affect the ability of a fungal pathogen to infect and colonize tobacco leaves. *The Plant Journal*, *20*(2), pp.163-170.

Humphreys, J.M., Hemm, M.R. and Chapple, C., 1999. New routes for lignin biosynthesis defined by biochemical characterization of recombinant ferulate 5-hydroxylase, a multifunctional cytochrome P450-dependent monooxygenase. *Proceedings of the National Academy of Sciences*, *96*(18), pp.10045-10050.

Huot, B., Yao, J., Montgomery, B.L. and He, S.Y., 2014. Growth–defense tradeoffs in plants: a balancing act to optimize fitness. *Molecular plant*, *7*(8), pp.1267-1287.

Husted, S. and Schjoerring, J.K., 1995. Apoplastic pH and ammonium concentration in leaves of Brassica napus L. *Plant Physiology*, *109*(4), pp.1453-1460.

Huynh, T.V., Dahlbeck, D. and Staskawicz, B.J., 1989. Bacterial blight of soybean: regulation of a pathogen gene determining host cultivar specificity. *Science*, *245*(4924), pp.1374-1377.

Im Kim, J., Dolan, W.L., Anderson, N.A. and Chapple, C., 2015. Indole glucosinolate biosynthesis limits phenylpropanoid accumulation in Arabidopsis thaliana. *The Plant Cell*, *27*(5), pp.1529-1546.

Iven, T., König, S., Singh, S., Braus-Stromeyer, S.A., Bischoff, M., Tietze, L.F., Braus, G.H., Lipka, V., Feussner, I. and Dröge-Laser, W., 2012. Transcriptional activation and production of tryptophan-derived secondary metabolites in Arabidopsis roots contributes to the defense against the fungal vascular pathogen Verticillium longisporum. *Molecular plant*, *5*(6), pp.1389-1402.

Jeworutzki, E., Roelfsema, M.R.G., Anschütz, U., Krol, E., Elzenga, J.T.M., Felix, G., Boller, T., Hedrich, R. and Becker, D., 2010. Early signaling through the Arabidopsis pattern recognition receptors FLS2 and EFR involves Ca2+-associated opening of plasma membrane anion channels. *The Plant Journal*, *62*(3), pp.367-378.

Jia, W. and Davies, W.J., 2007. Modification of leaf apoplastic pH in relation to stomatal sensitivity to root-sourced abscisic acid signals. *Plant Physiology*, *143*(1), pp.68-77.

Jeun, Y.C. and Hwang, B.K., 1991. Carbohydrate, Amino acid, Phenolic and Mineral Nutrient Contents of Pepper Plants in Relation to Age-Related Resistance to Phytophthora capsici. *Journal of Phytopathology*, *131*(1), pp.40-52.

Kakkar, A., Nizampatnam, N.R., Kondreddy, A., Pradhan, B.B. and Chatterjee, S., 2015. Xanthomonas campestris cell–cell signalling molecule DSF (diffusible signal factor) elicits innate immunity in plants and is suppressed by the exopolysaccharide xanthan. *Journal of experimental botany*, *66*(21), pp.6697-6714.

Kariñho-Betancourt, E., Agrawal, A.A., Halitschke, R. and Núñez-Farfán, J., 2015. Phylogenetic correlations among chemical and physical plant defenses change with ontogeny. *New Phytologist*, *206*(2), pp.796-806.

Katagiri, F., Thilmony, R. and He, S.Y., 2002. The Arabidopsis thaliana-Pseudomonas syringae interaction. *The Arabidopsis Book*, p.e0039.

Khan, M., Subramaniam, R. and Desveaux, D., 2016. Of guards, decoys, baits and traps: pathogen perception in plants by type III effector sensors. *Current opinion in microbiology*, *29*, pp.49-55.

Kim, B.J., Park, J.H., Park, T.H., Bronstein, P.A., Schneider, D.J., Cartinhour, S.W. and Shuler, M.L., 2009. Effect of iron concentration on the growth rate of Pseudomonas syringae and the expression of virulence factors in hrp-inducing minimal medium. *Applied and environmental microbiology*, *75*(9), pp.2720-2726.

Klessig, D.F., 2017. How does the multifaceted plant hormone salicylic acid combat disease in plants and are similar mechanisms utilized in humans?. *BMC biology*, *15*(1), p.23.

Kloek, A.P., Verbsky, M.L., Sharma, S.B., Schoelz, J.E., Vogel, J., Klessig, D.F. and Kunkel, B.N., 2001. Resistance to Pseudomonas syringae conferred by an Arabidopsis thaliana coronatine-insensitive (coi1) mutation occurs through two distinct mechanisms. *The Plant Journal*, *26*(5), pp.509-522.

Koch, M.F., 1991. Effect of plant age and leaf maturity on the quantitative resistance of rice cultivars to Xanthomonas campestris pv. oryzae. *Plant disease, 75*, pp.901-904.

Kus, J.V., Zaton, K., Sarkar, R. and Cameron, R.K., 2002. Age-related resistance in Arabidopsis is a developmentally regulated defense response to Pseudomonas syringae. *The Plant Cell*, *14*(2), pp.479-490.

Kutz, A., Müller, A., Hennig, P., Kaiser, W.M., Piotrowski, M. and Weiler, E.W., 2002. A role for nitrilase 3 in the regulation of root morphology in sulphur-starving Arabidopsis thaliana. *The Plant Journal*, *30*(1), pp.95-106.

Laluk, K. and Mengiste, T., 2010. Necrotroph attacks on plants: wanton destruction or covert extortion?. *The Arabidopsis Book*, p.e0136.

Lazarovits, G., Stössel, R. and Ward, E.W.B., 1981. Age-related changes in specificity and glyceollin production in the hypocotyl reaction of soybeans to Phytophthora megasperma var. sojae. *Phytopathology*, *71*, pp.94-97.

Lee, J.H., Cho, M.H. and Lee, J., 2011. 3-Indolylacetonitrile Decreases Escherichia coli O157: H7 Biofilm Formation and Pseudomonas aeruginosa Virulence. *Environmental microbiology*, *13*(1), pp.62-73.

Lewis, K. and Ausubel, F.M., 2006. Prospects for plant-derived antibacterials. *Nature biotechnology*, *24*(12), p.1504.

Li, B. and Xu, X., 2002. Infection and development of apple scab (Venturia inaequalis) on old leaves. *Journal of Phytopathology*, *150*(11-12), pp.687-691.

Lim, E.K., Li, Y., Parr, A., Jackson, R., Ashford, D.A. and Bowles, D.J., 2001. Identification of glucosyltransferase genes involved in sinapate metabolism and lignin synthesis in Arabidopsis. *Journal of Biological Chemistry*, *276*(6), pp.4344-4349.

Lohaus, G., Pennewiss, K., Sattelmacher, B., Hussmann, M. and Hermann Muehling, K., 2001. Is the infiltration-centrifugation technique appropriate for the isolation of apoplastic fluid? A critical evaluation with different plant species. *Physiologia Plantarum*, *111*(4), pp.457-465.

Macho, A.P. and Zipfel, C., 2015. Targeting of plant pattern recognition receptor-triggered immunity by bacterial type-III secretion system effectors. *Current opinion in microbiology*, *23*, pp.14-22.

Mailloux, R.J., Singh, R., Brewer, G., Auger, C., Lemire, J. and Appanna, V.D., 2009. α-ketoglutarate dehydrogenase and glutamate dehydrogenase work in tandem to modulate the antioxidant α-ketoglutarate during oxidative stress in Pseudomonas fluorescens. *Journal of Bacteriology*, *191*(12), pp.3804-3810.

Malka, S.K. and Cheng, Y., 2017. Possible interactions between the biosynthetic pathways of indole glucosinolate and auxin. *Frontiers in plant science*, *8*, p.2131.

Mann, E.E. and Wozniak, D.J., 2012. Pseudomonas biofilm matrix composition and niche biology. *FEMS microbiology reviews*, *36*(4), pp.893-916.

Manoharan, B., Neale, H.C., Hancock, J.T., Jackson, R.W. and Arnold, D.L., 2015. The identification of genes important in Pseudomonas syringae pv. phaseolicola plant colonisation using in vitro screening of transposon libraries. *PloS one*, *10*(9), p.e0137355.

Mansfield, J., Genin, S., Magori, S., Citovsky, V., Sriariyanum, M., Ronald, P., Dow, M.A.X., Verdier, V., Beer, S.V., Machado, M.A. and Toth, I.A.N., 2012. Top 10 plant pathogenic bacteria in molecular plant pathology. *Molecular plant pathology*, *13*(6), pp.614-629.

Mansfeld, B.N., Colle, M., Kang, Y., Jones, A.D. and Grumet, R., 2017. Transcriptomic and metabolomic analyses of cucumber fruit peels reveal a developmental increase in terpenoid glycosides associated with age-related resistance to Phytophthora capsici. *Horticulture research*, *4*, p.17022.

Masák, J., Čejková, A., Schreiberová, O. and Řezanka, T., 2014. Pseudomonas biofilms: possibilities of their control. *FEMS microbiology ecology*, *89*(1), pp.1-14.

Matsuda, K., Toyoda, H., Yokoyama, K., Wakita, K., Nishio, H., Nishida, T., Dogo, M., Kakutani, K., Hamada, M. and Ouchi, S., 1993. Growth inhibition of Pseudomonas solanacearum by substituted 3-indolepropionic acids and related compounds. *Bioscience, biotechnology, and biochemistry*, *57*(10), pp.1766-1767.

McClerklin, S.A., Lee, S.G., Harper, C.P., Nwumeh, R., Jez, J.M. and Kunkel, B.N., 2018. Indole-3-acetaldehyde dehydrogenase-dependent auxin synthesis contributes to virulence of Pseudomonas syringae strain DC3000. *PLoS pathogens*, *14*(1), p.e1006811.

McDonald, B.A. and Stukenbrock, E.H., 2016. Rapid emergence of pathogens in agro-ecosystems: global threats to agricultural sustainability and food security. *Phil. Trans. R. Soc. B*, *371*(1709), p.20160026.

Meletiadis, J., Pournaras, S., Roilides, E. and Walsh, T.J., 2010. Defining fractional inhibitory concentration index cutoffs for additive interactions based on self-drug additive combinations, Monte Carlo simulation analysis, and in vitro-in vivo correlation data for antifungal drug combinations against Aspergillus fumigatus. *Antimicrobial agents and chemotherapy*, *54*(2), pp.602-609.

Melotto, M., Underwood, W., Koczan, J., Nomura, K. and He, S.Y., 2006. Plant stomata function in innate immunity against bacterial invasion. *Cell*, *126*(5), pp.969-980.

Mittal, S. and Davis, K.R., 1995. Role of the phytotoxin coronatine in the infection of Arabidopsis thaliana by Pseudomonas syringae pv. tomato. *MPMI-Molecular Plant Microbe Interactions*, *8*(1), pp.165-171.

Møldrup, M.E., Geu-Flores, F. and Halkier, B.A., 2013a. Assigning gene function in biosynthetic pathways: camalexin and beyond. *The Plant Cell*, *25*(2), pp.360-367.

Møldrup, M.E., Salomonsen, B., Geu-Flores, F., Olsen, C.E. and Halkier, B.A., 2013b. De novo genetic engineering of the camalexin biosynthetic pathway. *Journal of biotechnology*, *167*(3), pp.296-301.

Moore, R.A., Starratt, A.N., Ma, S.W., Morris, V.L. and Cuppels, D.A., 1989. Identification of a chromosomal region required for biosynthesis of the phytotoxin coronatine by Pseudomonas syringae pv. tomato. *Canadian journal of microbiology*, *35*(10), pp.910-917.
Naseem, M., Kunz, M. and Dandekar, T., 2017. Plant–Pathogen Maneuvering over Apoplastic Sugars. *Trends in plant science*, *22*(9), pp.740-743.

Morris, C.E., Kinkel, L.L., Xiao, K., Prior, P. and Sands, D.C., 2007. Surprising niche for the plant pathogen Pseudomonas syringae. *Infection, Genetics and Evolution*, *7*(1), pp.84-92.

Müller, T.M., Böttcher, C., Morbitzer, R., Götz, C.C., Lehmann, J., Lahaye, T. and Glawischnig, E., 2015. TRANSCRIPTION ACTIVATOR-LIKE EFFECTOR NUCLEASE-mediated generation and metabolic analysis of camalexin-deficient cyp71a12 cyp71a13 double knockout lines. *Plant physiology*, *168*(3), pp.849-858.

Murashige, T. and Skoog, F., 1962. A revised medium for rapid growth and bio assays with tobacco tissue cultures. *Physiologia plantarum*, *15*(3), pp.473-497.

Nafisi, M., Sønderby, I.E., Hansen, B.G., Geu-Flores, F., Nour-Eldin, H.H., Nørholm, M.H., Jensen, N.B., Li, J. and Halkier, B.A., 200. Cytochromes P450 in the biosynthesis of glucosinolates and indole alkaloids. *Phytochemistry reviews*, *5*(2-3), pp.331-346.

Nafisi, M., Goregaoker, S., Botanga, C.J., Glawischnig, E., Olsen, C.E., Halkier, B.A. and Glazebrook, J., 2007. Arabidopsis cytochrome P450 monooxygenase 71A13 catalyzes the conversion of indole-3-acetaldoxime in camalexin synthesis. *The Plant Cell*, *19*(6), pp.2039-2052.

Neilson, E.H., Goodger, J.Q., Woodrow, I.E. and Møller, B.L., 2013. Plant chemical defense: at what cost?. Trends in plant science, 18(5), pp.250-258.

Nićiforović, N. and Abramovič, H., 2014. Sinapic acid and its derivatives: natural sources and bioactivity. *Comprehensive Reviews in Food Science and Food Safety*, *13*(1), pp.34-51.

Norman, C., Howell, K.A., Millar, A.H., Whelan, J.M. and Day, D.A., 2004. Salicylic acid is an uncoupler and inhibitor of mitochondrial electron transport. Plant Physiology, 134(1), pp.492-501.

Normanly, J., Grisafi, P., Fink, G.R. and Bartel, B., 1997. Arabidopsis mutants resistant to the auxin effects of indole-3-acetonitrile are defective in the nitrilase encoded by the NIT1 gene. *The Plant Cell*, *9*(10), pp.1781-1790.

Nowak H, Kujava R, Zadernowski R, Roczniak B, Kozlowska H. 1992. Antioxidative and bactericidal properties of phenolic compounds in rapeseeds. Eur J Lipid Sci Technol 94:149–52.

O'brien, R.D. and Lindow, S.E., 1989. Effect of plant species and environmental conditions on epiphytic population sizes of Pseudomonas syringae and other bacteria. *Phytopathology*, *79*(5), pp.619-627.

O'Brien, J.A., Daudi, A., Butt, V.S. and Bolwell, G.P., 2012. Reactive oxygen species and their role in plant defense and cell wall metabolism. *Planta*, *236*(3), pp.765-779.

O'Leary, B.M., Rico, A., McCraw, S., Fones, H.N. and Preston, G.M., 2014. The infiltration-centrifugation technique for extraction of apoplastic fluid from plant leaves using Phaseolus vulgaris as an example. *Journal of visualized experiments: JoVE*, (94).

O'Leary, B.M., Neale, H.C., Geilfus, C.M., Jackson, R.W., Arnold, D.L. and Preston, G.M., 2016. Early changes in apoplast composition associated with defense and disease in interactions between Phaseolus vulgaris and the halo blight pathogen Pseudomonas syringae pv. phaseolicola. *Plant, cell & environment*, *39*(10), pp.2172-2184.

O'Toole, G.A., 2011. Microtiter dish biofilm formation assay. *Journal of visualized experiments: JoVE*, (47).

Panter, S.N., Hammond-Kosack, K.E., Harrison, K., Jones, J.D. and Jones, D.A., 2002. Developmental control of promoter activity is not responsible for mature onset of Cf-9B-mediated resistance to leaf mold in tomato. *Molecular plant-microbe interactions*, *15*(11), pp.1099-1107.

Park, W.J., Kriechbaumer, V., Müller, A., Piotrowski, M., Meeley, R.B., Gierl, A. and Glawischnig, E., 2003. The nitrilase ZmNIT2 converts indole-3-acetonitrile to indole-3-acetic acid. *Plant physiology*, *133*(2), pp.794-802.

Park, S.W., Kaimoyo, E., Kumar, D., Mosher, S. and Klessig, D.F., 2007. Methyl salicylate is a critical mobile signal for plant systemic acquired resistance. *Science*, *318*(5847), pp.113-116.

Passardi, F., Penel, C. and Dunand, C., 2004. Performing the paradoxical: how plant peroxidases modify the cell wall. *Trends in plant science*, *9*(11), pp.534-540.

Pedras, M.S.C., Yaya, E.E. and Glawischnig, E., 2011. The phytoalexins from cultivated and wild crucifers: chemistry and biology. *Natural product reports*, *28*(8), pp.1381-1405.

Pedras, M.S.C., Minic, Z. and Abdoli, A., 2014. The phytoalexin camalexin induces fundamental changes in the proteome of Alternaria brassicicola different from those caused by brassinin. *Fungal biology*, *118*(1), pp.83-93.

Pedras, M.S.C. and Abdoli, A., 2017. Pathogen inactivation of cruciferous phytoalexins: detoxification reactions, enzymes and inhibitors. *RSC Advances*, *7*(38), pp.23633-23646.

Pieterse, C.M., Leon-Reyes, A., Van der Ent, S. and Van Wees, S.C., 2009. Networking by small-molecule hormones in plant immunity. *Nature chemical biology*, *5*(5), p.308.

Pochon, S., Terrasson, E., Guillemette, T., Iacomi-Vasilescu, B., Georgeault, S., Juchaux, M., Berruyer, R., Debeaujon, I., Simoneau, P. and Campion, C., 2012. The Arabidopsis thaliana-Alternaria brassicicola pathosystem: a model interaction for investigating seed transmission of necrotrophic fungi. *Plant methods*, *8*(1), p.16.

Pretorius, Z.A., Rijkenberg, F.H.J. and Wilcoxson, R.D., 1988. Effects of growth stage, leaf position and temperature on adult-plant resistance of wheat infected by Puccinia recondita f. sp. tritici. *Plant Pathology*, *37*(1), pp.36-44.

Qi, Y., Tsuda, K., Glazebrook, J. and Katagiri, F., 2011. Physical association of pattern-triggered immunity (PTI) and effector-triggered immunity (ETI) immune receptors in Arabidopsis. *Molecular plant pathology*, *12*(7), pp.702-708.

Rahme, L.G., Mindrinos, M.N. and Panopoulos, N.J., 1992. Plant and environmental sensory signals control the expression of hrp genes in Pseudomonas syringae pv. phaseolicola. *Journal of bacteriology*, *174*(11), pp.3499-3507.

Raskin, I., 1992. Role of salicylic acid in plants. *Annual review of plant biology*, *43*(1), pp.439-463.

Renzi, M., Copini, P., Taddei, A.R., Rossetti, A., Gallipoli, L., Mazzaglia, A. and Balestra, G.M., 2012. Bacterial canker on kiwifruit in Italy: anatomical changes in the wood and in the primary infection sites. *Phytopathology*, *102*(9), pp.827-840.

Rogers, D. and Hopfinger, A.J., 1994. Application of genetic function approximation to quantitative structure-activity relationships and quantitative structure-property relationships. *Journal of Chemical Information and Computer Sciences*, *34*(4), pp.854-866.

Rogers, E.E., Glazebrook, J. and Ausubel, F.M., 1996. Mode of action of the Arabidopsis thaliana phytoalexin camalexin and its role in Arabidopsis-pathogen interactions. *Molecular Plant Microbe Interactions*, *9*, pp.748-757.

Rosso, M.G., Li, Y., Strizhov, N., Reiss, B., Dekker, K. and Weisshaar, B., 2003. An Arabidopsis thaliana T-DNA mutagenized population (GABI-Kat) for flanking sequence tag-based reverse genetics. *Plant molecular biology*, *53*(1-2), pp.247-259.

Roux, M., Schwessinger, B., Albrecht, C., Chinchilla, D., Jones, A., Holton, N., Malinovsky, F.G., Tör, M., de Vries, S. and Zipfel, C., 2011. The Arabidopsis leucine-rich repeat receptor–like kinases BAK1/SERK3 and BKK1/SERK4 are required for innate immunity to hemibiotrophic and biotrophic pathogens. *The Plant Cell*, *23*(6), pp.2440-2455.

Rusterucci, C., Zhao, Z., Haines, K., Mellersh, D., Neumann, M. and Cameron, R.K., 2005. Age-related resistance to Pseudomonas syringae pv. tomato is associated with the transition to flowering in Arabidopsis and is effective against Peronospora parasitica. *Physiological and molecular plant pathology*, *66*(6), pp.222-231.

Saga, H., Ogawa, T., Kai, K., Suzuki, H., Ogata, Y., Sakurai, N., Shibata, D. and Ohta, D., 2012. Identification and characterization of ANAC042, a transcription factor family gene involved in the regulation of camalexin biosynthesis in Arabidopsis. *Molecular plant-microbe interactions*, *25*(5), pp.684-696.

Savary, S., Ficke, A., Aubertot, J.N. and Hollier, C., 2012. Crop losses due to diseases and their implications for global food production losses and food security. *Food Security* – The Science, Sociology, and Economics of Food Production and Access to Food. ISSN 1876-4517

Sanchez, L., Courteaux, B., Hubert, J., Kauffmann, S., Renault, J.H., Clément, C., Baillieul, F. and Dorey, S., 2012. Rhamnolipids elicit defense responses and induce disease resistance against biotrophic, hemibiotrophic, and necrotrophic pathogens that require different signaling pathways in Arabidopsis and highlight a central role for salicylic acid. *Plant physiology*, *160*(3), pp.1

Sawada, Y. and Hirai, M.Y., 2013. Integrated LC-MS/MS system for plant metabolomics. *Computational and structural biotechnology journal*, *4*(5), p.e201301011.

Schwa, W.F.S., 1979. Changes in scab susceptibility of apple leaves as influenced by age. *Phytophylactica*, *11*(2), pp.53-56.

Serrano, M., Wang, B., Aryal, B., Garcion, C., Abou-Mansour, E., Heck, S., Geisler, M., Mauch, F., Nawrath, C. and Métraux, J.P., 2013. Export of salicylic acid from the chloroplast requires the multidrug and toxin extrusion-like transporter EDS5. *Plant physiology*, *162*(4), pp.1815-1821.

Shibata, Y., Kawakita, K. and Takemoto, D., 2010. Age-related resistance of Nicotiana benthamiana against hemibiotrophic pathogen Phytophthora infestans requires both ethylene-and salicylic acid–mediated signaling pathways. *Molecular Plant-Microbe Interactions*, *23*(9), pp.1130-1142.

Schuhegger, R., Nafisi, M., Mansourova, M., Petersen, B.L., Olsen, C.E., Svatoš, A., Halkier, B.A. and Glawischnig, E., 2006. CYP71B15 (PAD3) catalyzes the final step in camalexin biosynthesis. *Plant physiology*, *141*(4), pp.1248-1254.

Scholthof, K.B.G., 2007. The disease triangle: pathogens, the environment and society. *Nature Reviews Microbiology*, *5*(2), p.152.

Simon, C., Langlois-Meurinne, M., Bellvert, F., Garmier, M., Didierlaurent, L., Massoud, K., Chaouch, S., Marie, A., Bodo, B., Kauffmann, S. and Noctor, G., 2010. The differential spatial distribution of secondary metabolites in Arabidopsis leaves reacting hypersensitively to Pseudomonas syringae pv. tomato is dependent on the oxidative burst. *Journal of experimental botany*, *61*(12), pp.3355-3370.

Sønderby, I.E., Geu-Flores, F. and Halkier, B.A., 2010. Biosynthesis of glucosinolates–gene discovery and beyond. *Trends in plant science*, *15*(5), pp.283-290.

Soylu, S., Brown, I. and Mansfield, J.W., 2005. Cellular reactions in Arabidopsis following challenge by strains of Pseudomonas syringae: from basal resistance to compatibility. *Physiological and molecular plant pathology*, *66*(6), pp.232-243.

Spaepen, S. and Vanderleyden, J., 2011. Auxin and plant-microbe interactions. *Cold Spring Harbor perspectives in biology*, *3*(4), p.a001438.

Su T, Xu J, Li Y, Lei L, Zhao L, Yang H, Feng J, Liu G, Ren D. Glutathione-indole-3-acetonitrile is required for camalexin biosynthesis in Arabidopsis thaliana. The Plant Cell. 2011 Jan 1;23(1):364-80.

Takikawa, Y. and Takahashi, F., 2014. Bacterial leaf spot and blight of crucifer plants (Brassicaceae) caused by Pseudomonas syringae pv. maculicola and P. cannabina pv. alisalensis. *Journal of general plant pathology*, *80*(6), pp.466-474.

Tan, J., Bednarek, P., Liu, J., Schneider, B., Svatoš, A. and Hahlbrock, K., 2004. Universally occurring phenylpropanoid and species-specific indolic metabolites in infected and uninfected Arabidopsis thaliana roots and leaves. *Phytochemistry*, *65*(6), pp.691-699.

Tesaki, S., Tanabe, S., Ono, H., Fukushi, E., Kawabata, J. and WATANABE, M., 1998. 4-Hydroxy-3-nitrophenylacetic and sinapic acids as antibacterial compounds from mustard seeds. *Bioscience, biotechnology, and biochemistry*, *62*(5), pp.998-1000.

Thomma, B.P., Nürnberger, T. and Joosten, M.H., 2011. Of PAMPs and effectors: the blurred PTI-ETI dichotomy. *The plant cell*, *23*(1), pp.4-15.

Tian, D., Traw, M.B., Chen, J.Q., Kreitman, M. and Bergelson, J., 2003. Fitness costs of R-gene-mediated resistance in Arabidopsis thaliana. *Nature*, *423*(6935), p.74.

Totsika, M., 2016. Benefits and challenges of antivirulence antimicrobials at the dawn of the post-antibiotic era. *Drug Delivery Letters*, *6*(1), pp.30-37.

Tsuda, K. and Katagiri, F., 2010. Comparing signaling mechanisms engaged in pattern-triggered and effector-triggered immunity. *Current opinion in plant biology*, *13*(4), pp.459-465.

Tucker, C. and Avila-Sakar, G., 2010. Ontogenetic changes in tolerance to herbivory in Arabidopsis. *Oecologia*, *164*(4), pp.1005-1015.

Twomey, M.C., Wolfenbarger, S.N., Woods, J.L. and Gent, D.H., 2015. Development of partial ontogenic resistance to powdery mildew in hop cones and its management implications. *PloS one*, *10*(3), p.e0120987.

VanEtten, H.D., Mansfield, J.W., Bailey, J.A. and Farmer, E.E., 1994. Two classes of plant antibiotics: phytoalexins versus" phytoanticipins". *The Plant Cell*, *6*(9), p.1191.

van Loon, L.C., Rep, M. and Pieterse, C.M., 2006. Significance of inducible defense-related proteins in infected plants. *Annu. Rev. Phytopathol.*, *44*, pp.135-162.

Veber, D.F., Johnson, S.R., Cheng, H.Y., Smith, B.R., Ward, K.W. and Kopple, K.D., 2002. Molecular properties that influence the oral bioavailability of drug candidates. *Journal of medicinal chemistry*, *45*(12), pp.2615-2623.

Vorwerk, S., Somerville, S. and Somerville, C., 2004. The role of plant cell wall polysaccharide composition in disease resistance. *Trends in plant science*, *9*(4), pp.203-209.

Wang, K., Senthil-Kumar, M., Ryu, C.M., Kang, L. and Mysore, K.S., 2012. Phytosterols play a key role in plant innate immunity against bacterial pathogens by regulating nutrient efflux into the apoplast. *Plant physiology*, pp.pp-111.

Watanabe, M., Kusano, M., Oikawa, A., Fukushima, A., Noji, M. and Saito, K., 2008. Physiological roles of the β-substituted alanine synthase gene family in Arabidopsis. *Plant physiology*, *146*(1), pp.310-320.

Whalen, M.C., Innes, R.W., Bent, A.F. and Staskawicz, B.J., 1991. Identification of Pseudomonas syringae pathogens of Arabidopsis and a bacterial locus determining avirulence on both Arabidopsis and soybean. *The Plant Cell*, *3*(1), pp.49-59.

Whalen, M.C., 2005. Host defense in a developmental context. *Molecular plant pathology*, *6*(3), pp.347-360.

Whitchurch, C.B., Tolker-Nielsen, T., Ragas, P.C. and Mattick, J.S., 2002. Extracellular DNA required for bacterial biofilm formation. *Science*, *295*(5559), pp.1487-1487.

Wildermuth, M.C., Dewdney, J., Wu, G. and Ausubel, F.M., 2001. Isochorismate synthase is required to synthesize salicylic acid for plant defense. *Nature*, *414*(6863), p.562.

Wilson, D.C., Carella, P., Isaacs, M. and Cameron, R.K., 2013. The floral transition is not the developmental switch that confers competence for the Arabidopsis age-related resistance response to Pseudomonas syringae pv. tomato. *Plant molecular biology*, *83*(3), pp.235-246.

Wittstock, U. and Burow, M., 2010. Glucosinolate breakdown in Arabidopsis: mechanism, regulation and biological significance. *The Arabidopsis Book*, p.e0134.

Xia, J., Sinelnikov, I.V., Han, B. and Wishart, D.S., 2015. MetaboAnalyst 3.0—making metabolomics more meaningful. *Nucleic acids research*, *43*(W1), pp.W251-W257.

Xin, X.F. and He, S.Y., 2013. Pseudomonas syringae pv. tomato DC3000: a model pathogen for probing disease susceptibility and hormone signaling in plants. *Annual review of phytopathology*, *51*, pp.473-498.

Yalpani, N., Shulaev, V. and Raskin, I., 1993. Endogenous salicylic acid levels correlate with accumulation of pathogenesis-related proteins and virus resistance in tobacco. *Phytopathology*, *83*(7), pp.702-708.

Yu, X., Lund, S.P., Scott, R.A., Greenwald, J.W., Records, A.H., Nettleton, D., Lindow, S.E., Gross, D.C. and Beattie, G.A., 2013. Transcriptional responses of Pseudomonas syringae to growth in epiphytic versus apoplastic leaf sites. *Proceedings of the National Academy of Sciences*, *110*(5), pp.E425-E434.

Zandalinas, S.I., Vives-Peris, V., Gómez-Cadenas, A. and Arbona, V., 2012. A fast and precise method to identify indolic glucosinolates and camalexin in plants by combining mass spectrometric and biological information. *Journal of agricultural and food chemistry*, *60*(35), pp.8648-8658.

Zhang, K., Halitschke, R., Yin, C., Liu, C.J. and Gan, S.S., 2013. Salicylic acid 3-hydroxylase regulates Arabidopsis leaf longevity by mediating salicylic acid catabolism. *Proceedings of the National Academy of Sciences*, *110*(36), pp.14807-14812.

Zhao, Y., Hull, A.K., Gupta, N.R., Goss, K.A., Alonso, J., Ecker, J.R., Normanly, J., Chory, J. and Celenza, J.L., 2002. Trp-dependent auxin biosynthesis in Arabidopsis: involvement of cytochrome P450s CYP79B2 and CYP79B3. *Genes & development*, *16*(23), pp.3100-3112.

Zhou, N., Tootle, T.L. and Glazebrook, J., 1999. Arabidopsis PAD3, a gene required for camalexin biosynthesis, encodes a putative cytochrome P450 monooxygenase. *The Plant Cell*, *11*(12), pp.2419-2428.

APPENDIX

Table S1. List of accession and genotypes used in this work

Name	Allele	Source
Columbia (Col-0)	Wild type	
sid2-2	Deletion (~ 68 bp) in exon 9 of *ICS1*[Wildermuth2001]	The *Arabidopsis* Biological Resource Center
cyp79b2 cyp79b3	T-DNA insertion in both genes	Obtained from E. Glawischnig, Technische Universitat München, Freising, Germany
cyp71a13-1	T-DNA insertion in *cyp71a13* SALK 105136	Obtained from J. Glazebrook, University of Minnesota, St. Paul, MN, USA.
cyp71a12/cyp71a13-1	TALEN-mediated insertion in *cyp71a12*[Muller2015] T-DNA insertion in *cyp71a13*	Obtained from E. Glawischnig, Technische Universitat München, Freising, Germany
cyp71b15 (pad3-1)	Deletion (nonsense) in *cyp71b15*[Nafisi2007]	Obtained from J. Glazebrook, University of Minnesota, St. Paul, MN, USA
cyp71a12/cyp71a13-1 sid2-2	(Refer to respective single mutants)	C.J. Kempthorne, D. C. Wilson, R.K. Cameron, McMaster University, Hamilton ON, Canada
aao1	Homozygous T-DNA insertion SALK_126349C	The *Arabidopsis* Biological Resource Center
cyp71a12	Homozygous T-DNA insertion GABI_127H03	The *Arabidopsis* Biological Resource Center
cyp71b6	Homozygous T-DNA insertion SALK_115336C	The *Arabidopsis* Biological Resource Center
cyp82c2	Homozygous T-DNA insertion GABI_261D12	The *Arabidopsis* Biological Resource Center
fox1	Homozygous T-DNA insertion GABI_813E08	The *Arabidopsis* Biological Resource Center

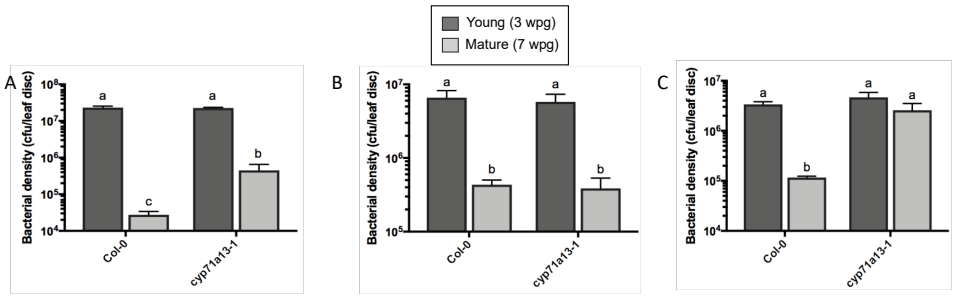

Figure S1. The *cyp71a13-1* single mutant has a variable ARR phenotype. Bacterial quantification assays of young and mature (ARR assays) of Col-0 and *cyp71a13-1.* ARR assays were performed by quantifying bacterial density of virulent *Pst* DC3000 (72 hpi) in young (3 wpg) and mature (7 wpg) plants. Values represent the mean +/- standard deviation of three sample replicates. Different letters indicate statistically significant differences (ANOVA, Tukey's honestly significant difference [HSD], $P < 0.05$, n=9 plants / treatment).

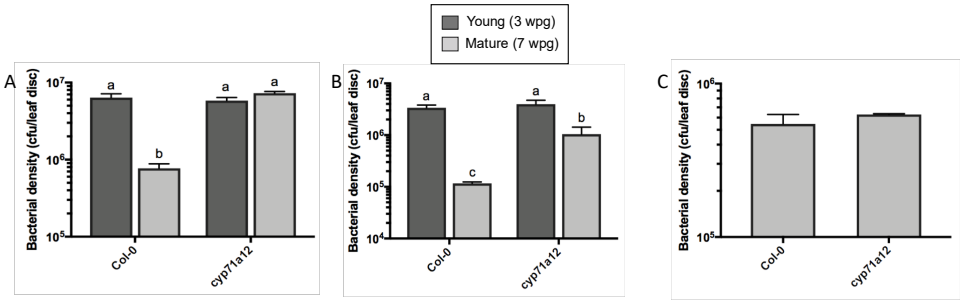

Figure S2. The *cyp71a12* single mutant has a variable ARR phenotype. Bacterial quantification assays of young and mature (ARR assays) of Col-0 and *cyp71a12.* ARR assays were performed by quantifying bacterial density of virulent *Pst* DC3000 (72 hpi) in young (3 wpg) and mature (7 wpg) plants. Values represent the mean +/- standard deviation of three sample replicates. Different letters indicate statistically significant differences (ANOVA, Tukey's honestly significant difference [HSD], $P < 0.05$, n=9 plants / treatment).

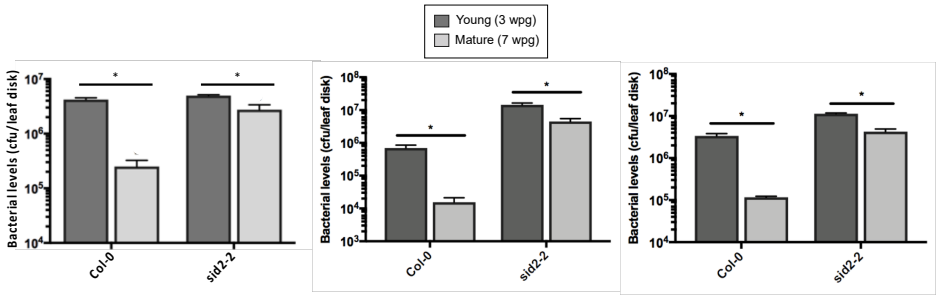

Figure S3. The SA biosynthesis mutant, *sid2-2,* occasionally displays a residual ARR-like response. Bacterial quantification assays of young and mature (ARR assays) of Col-0 and SA biosynthesis mutant *sid2-2.* ARR assays were performed by quantifying bacterial density of virulent *Pst* DC3000 (72 hpi) in young (3 wpg) and mature (7 wpg) plants. Values represent the mean +/- standard deviation of three sample replicates. All experiments were performed at least 3 times with similar results. Asterisks indicate statistically significant differences (T-test $P < 0.05$, n=9 plants / treatment).

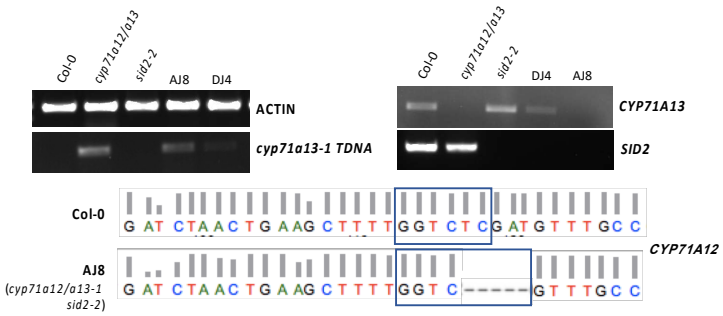

Figure S4 PCR screening and sequencing results for homozygous *cyp71a12/cyp71a13-1 sid2-2*. Primers are listed in Chapter 2 – Materials and Methods. The five base pair TALENs-mediated *CYP71A12* allele was confirmed by sequencing.

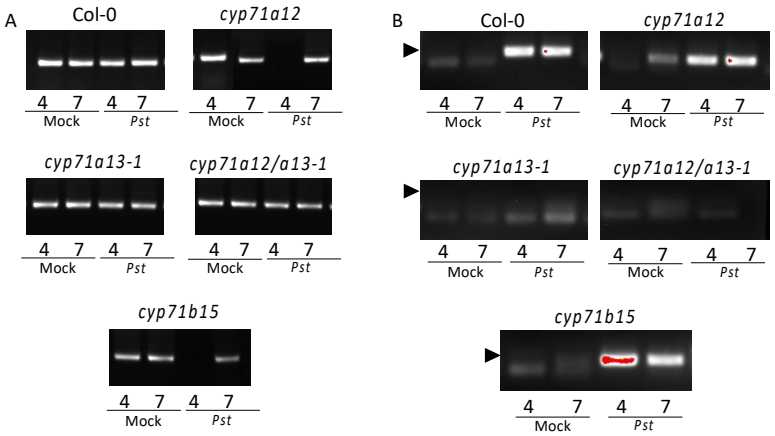

Figure S5. *CYP71A13* is expressed in response to *P. syringae* DC3000 at 24 hpi. RT-PCR of *CYP71A13* (B) in young (4 wpg) and mature (7 wpg) mock and *Pst*-inoculated leaves of indolic biosynthesis mutants. *ACTIN* expression (A) used to confirm cDNA synthesis and reactions and prescence of genomic DNA contamination (indicated by higher weight molecular band in addition to lower weight molecular band for cDNA).

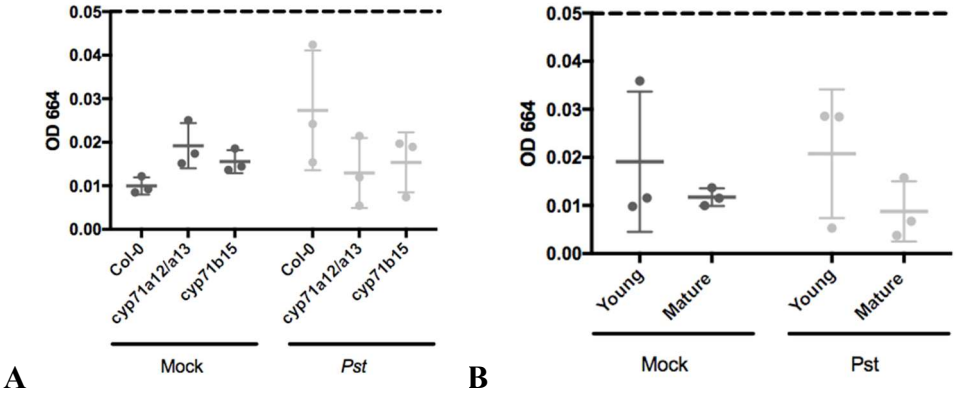

Figure S6. Chlorophyll contamination of intercellular washing fluids as measured by optical density (OD_{664}). IWFs were centrifuged post-collection at 4°C, re-suspended in 1 ml anhydrous ethanol. Each point represents average of 6 wells from 96-well plate for each replicate of IWF collected. (A) shows results from experiments comparing mature Col-0 and the indolic biosynthesis mutant *cyp71a12/cyp71a13-1*. (B) shows results from young and mature wild type Col-0 from ARR experiments. IWFs from both experiments used for UPLC-MS metabolomics studies. Dashed line indicates threshold for intracellular contamination as measured by chlorophyll concentration.

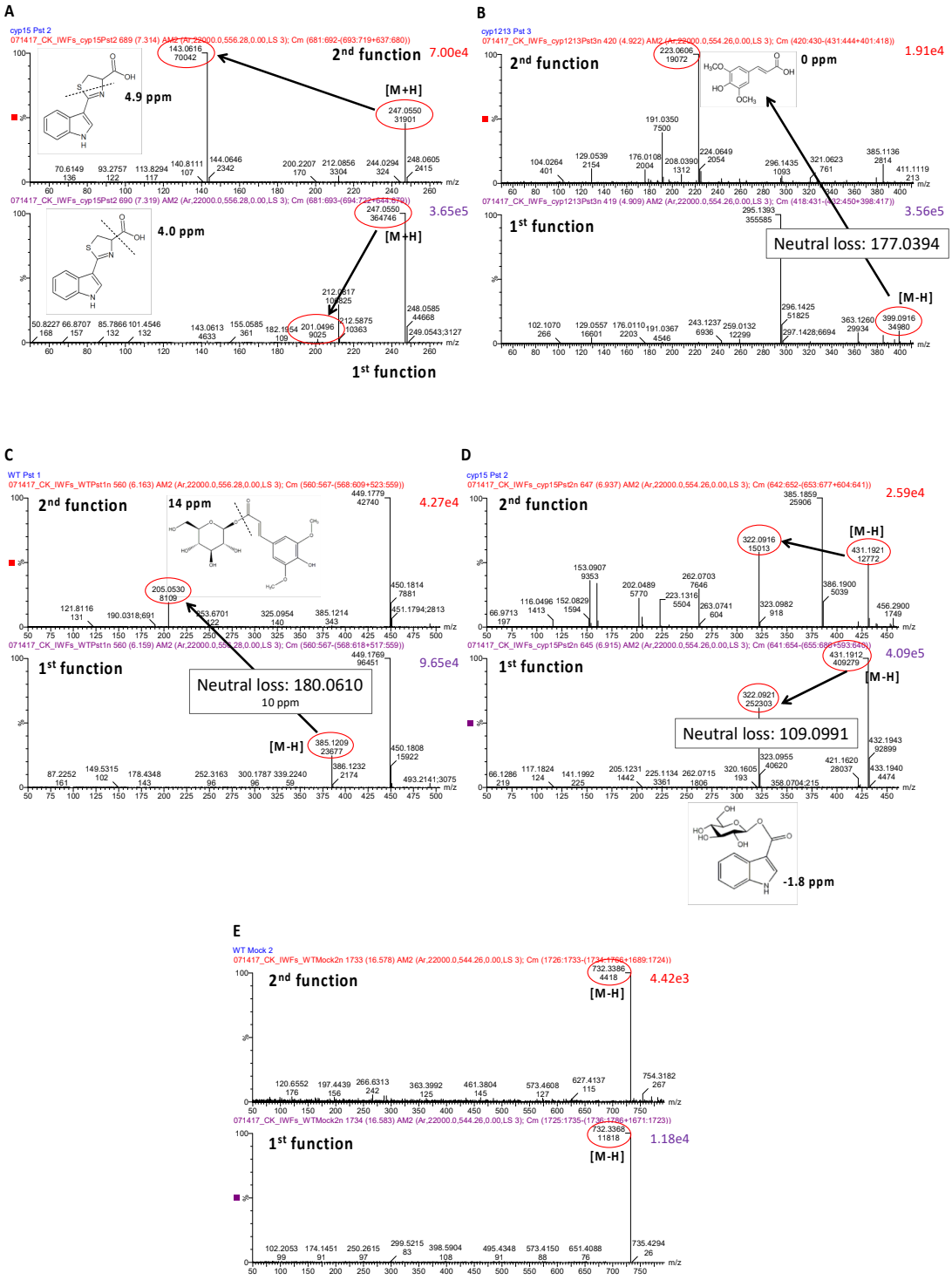
A
cyp15 Pst 2
2nd function
7.00e4
4.9 ppm
[M+H]
247.0550
31901
1st function
3.65e5
4.0 ppm
[M+H]
247.0550
364746
B
cyp1213 Pst 3
2nd function
1.91e4
0 ppm
1st function
3.56e5
Neutral loss: 177.0394
[M-H]
C
WT Pst 1
2nd function
4.27e4
14 ppm
1st function
9.65e5
Neutral loss: 180.0610
10 ppm
[M-H]
D
cyp15 Pst 2
2nd function
2.59e4
[M-H]
1st function
4.09e5
[M-H]
Neutral loss: 109.0991
-1.8 ppm
E
WT Mock 2
2nd function
4.42e3
[M-H]
1st function
1.18e4
[M-H]

Figure S7. Mass spectra and theoretical fragmentation for significantly different features detected in intercellular washing fluids (listed in Table 2). Each letter is matched to the feature listed in Table 2. Theoretical fragmentation for compounds based on calculated elemental compositions from exact mass for parent ions and neutral loss to produce product ions in low energy (function 1) and high energy (function 2) spectra. Lock-mass corrected with leucine enkephalin in Waters MassLynx 4.1

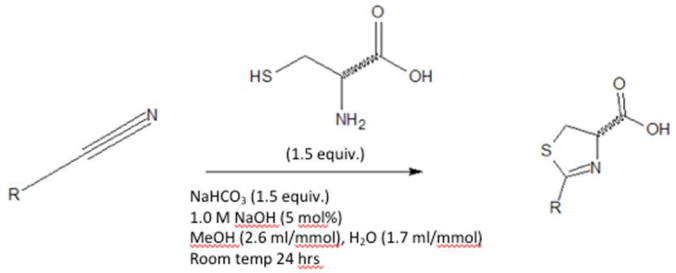

Scheme 1. Synthesis of phenyl enantiomers of 2-aryl-4,5,-dihydrothiazole-4-carboxylic acid

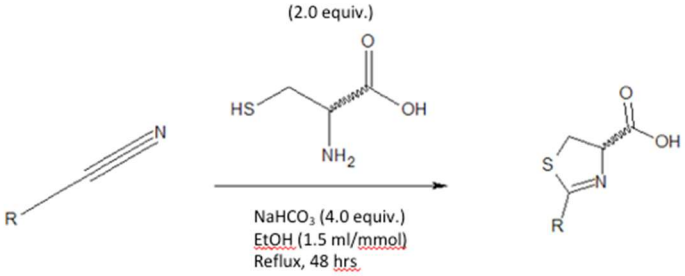

Scheme 2. Synthesis of phenol and indolic enantiomers of 2-aryl-4,5,-dihydrothiazole-4-carboxylic acid

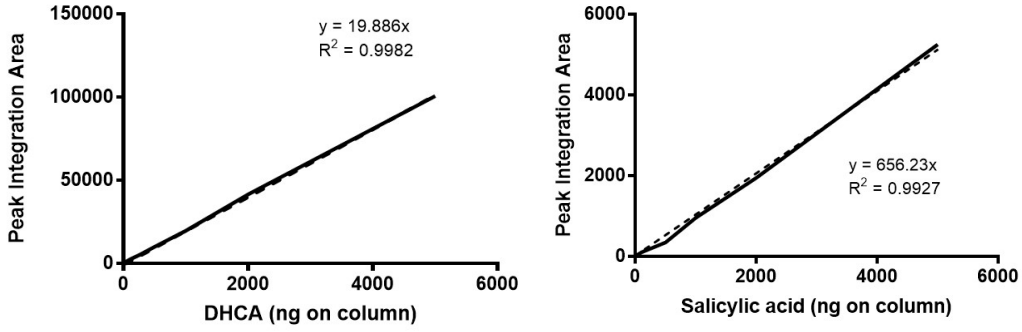

Figure S8. Dihydrocamalexic acid and salicylic acid standard curves. Standard curves of authentic standard at known concentrations for quantification of DHCA (positive ESI mode; xx to xx) and SA (negative ESI mode; 100 to 5000 ng on column).

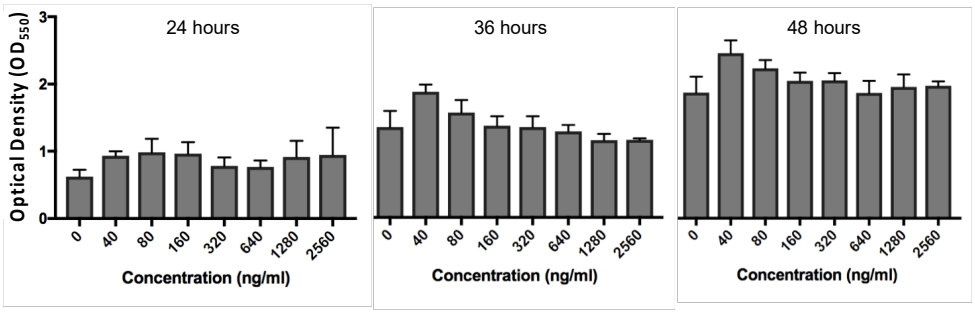

Figure S9. Dihydrocamalexic acid does not inhibit biofilm formation of *Pst* DC3000. Dose-dependent effect of DHCA *Pst* biofilm formation *in vitro* in Hrp-inducing minimal media as measured by crystal violet destaining in acetic acid (OD_{500}) after incubation on stationary bench for 24 to 48 hours at room temperature (~26 °C). Each data point is the mean ± SD of five wells per concentration from a 96-well non-tissue-culture-treated plate. Due to equipment malfunction after staining, these values had to be measured at OD_{500}.

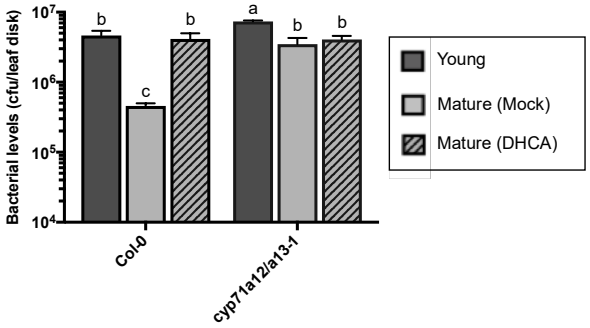

Figure S10. Exogenous application of DHCA at 4 hpi with *Pst* perturbs ARR in mature plants. Exogenous application of DHCA was applied to Col-0 and *cyp71a12/cyp71a13-1* by pressure infiltration of 70 ng/ml DHCA at 4 hpi with virulent *Pst* DC3000 or mock treatment (0.06% DMSO in 10 mM $MgCl_2$). Bacterial density quantified at 3 days post-inoculation in young (3 wpg) and mature (7 wpg) plants for all treatments. Values represent the mean +/- standard deviation of three sample replicates. Different letters indicate statistically significant differences (ANOVA, Tukey's honestly significant difference [HSD], $P < 0.05$).

Table S2. Indolic compounds with peak corresponding to theoretical m/z calculated for [M+H] or [M-H] in mature wild-type IWFs.

Compound	*Pst* IWFs	Mock IWFs	Notes
L-Tryptophan	Confirmed	Confirmed	Confirmed with authentic standard
Indole-3-acetaldoxime	n.d.	n.d.	
Indole-3-acetonitrile	n.d.	n.d.	Confirmed with authentic standard
Indole-3-carbonyl nitrile	n.d.	n.d.	
Indole-3-carboxylic acid	n.d.	n.d.	Confirmed with authentic standard
Indole-3-acetaldehyde	n.d.	n.d.	Confirmed with authentic standard
Indole-3-carboxylic acid glucose conjugate	Putatively detected	Putatively detected	Based on exact mass (≤ 5 ppm), fragmentation, elemental composition
4-OH-indole-3-carboxylic acid	n.d.	n.d.	
4-OH-indole-3-carbonyl nitrile	n.d.	n.d.	
Glutathione IAN	n.d.	n.d.	
Glutathione IAN derivatives	n.d.	n.d.	
Cysteine IAN	n.d.	n.d.	
Dihydrocamalexic acid	Confirmed	n.d.	Confirmed with synthesized standard
Camalexin	n.d.	n.d.	Confirmed with authentic standard
Camalexin hexoside	n.d.	n.d.	
Indole-3-acetic acid	n.d.	n.d.	
1- or 4-methoxy indole-3-methylglucosinolate	n.d.	n.d.	

n.d. indicates not detected.